

# Characterization and fine mapping of a potassium dependent growth QTL in Arabidopsis



PhD thesis  
Aina Prinzenberg  
Cologne 2011

Characterization and fine mapping  
of a potassium dependent growth QTL  
in Arabidopsis

Inaugural-Dissertation  
zur  
Erlangung des Doktorgrades  
der Mathematisch-Naturwissenschaftlichen Fakultät  
der Universität zu Köln  
vorgelegt von

Aina Elisabet Prinzenberg  
aus Köln

Die vorliegende Arbeit wurde am MPI für Pflanzenzüchtungsforschung in Köln- Vogelsang in der Arbeitsgruppe von Dr. Matthieu Reymond und unter der Betreuung von Prof. Dr. Maarten Koornneef durchgeführt.

Berichterstatter (Gutachter): Prof. Dr. Maarten Koornneef  
Prof. Dr. Marcel Bucher

Tag der mündlichen Prüfung: 29.06.2010

**Abstract**

Potassium is an essential macronutrient for plants. Deficiency in potassium leads to a reduction in organ growth and can cause yield loss. Previously, a quantitative trait locus (QTL) analysis was performed with a *Ler/Kas-2* recombinant inbred line (RIL) population of *Arabidopsis thaliana* that was grown using a hydroponic system with contrasted mineral nutrient supplies. QTL for growth related and biochemical traits were detected in each condition. Furthermore, QTL involved in response of these traits to differences in nutrient supply were also detected. The genetic basis of these response QTL could be involved in the adaptation of the plant to the reduction in mineral nutrient supply. One of these QTL was mapped on the bottom of the chromosome five and was involved in the response of rosette weight to lowered potassium supply. In the present study, this response QTL was validated with near isogenic lines (NILs) that had a *Kas-2* introgression only at the QTL position in an otherwise *Ler* genetic background. The NILs retained over 20% more rosette weight than *Ler* in response to the reduced potassium supply. The QTL was further characterized: its effect on growth was present in a wide range of reduced potassium supplies but was abolished in the presence of ammonium. Furthermore, the NILs showed generally higher potassium content in the rosette as well as a higher water loss than *Ler*. There was no difference in stomatal density between the NILs and *Ler* and it is therefore assumed that a differential regulation of stomata opening will cause the water loss difference. The QTL was fine mapped to a ca 3.9 Mbp region and the response phenotype of different recombinant lines suggested that several interacting genes led to the observed effect of the QTL on growth in response to potassium reduction. The selection of candidate genes, underlying the effect of the QTL, is discussed and amongst others the potassium channel *TPK1*. Identification of the genetic and molecular basis of this QTL may shed light on a new regulatory mechanism that influences plant growth in response to potassium starvation and confers higher potassium efficiency to plants.

**Kurzzusammenfassung**

Kalium ist ein essentieller Nährstoff für Pflanzen, eine nicht ausreichende Versorgung kann das Wachstum und folglich auch Ernteerträge beeinträchtigen. Eine „Quantitative Trait Locus“ (QTL) Analyse mit einer Population rekombinanter Inzuchtlinien, aus einer Kreuzung der Ökotypen *Ler* und *Kas-2* von *Arabidopsis thaliana*, wurde in einer Hydrokultur mit unterschiedlichen Nährstoffzufuhren durchgeführt. QTL für wachstumsbezogene Eigenschaften, biochemische Merkmale und QTL für die Reaktion dieser Merkmale auf die verringerte Kaliumzufuhr wurden kartiert. Die genetische Basis letztgenannter QTL kann an Adaptionsmechanismen für Nährstoffmangel beteiligt sein. In der QTL Analyse wurde eine Genregion an der Basis des fünften Chromosoms detektiert, die an der Veränderung des Rosettengewichts in Reaktion auf die Verringerung der Kaliumzufuhr beteiligt war. Die vorliegende Arbeit zeigt die Validierung dieses QTL und seine weitere Charakterisierung und Feinkartierung. Zur Validierung wurden sogenannte „Near Isogenic Lines“ (NILs) gezüchtet, die *Kas-2* Allele in der genomischen Region des QTL in einem ansonsten reinen *Ler*-Genom tragen. Die NILs weisen eine über 20% geringere Gewichtsveränderung in Reaktion auf die reduzierte Kaliumzufuhr auf, als der Ökotyp *Ler*. Damit ist der QTL Effekt validiert worden. Der Effekt dieses QTL auf die Veränderung des Rosettengewichts blieb bestehen, selbst wenn die Kaliumkonzentration des Medium weiter gesenkt wurde. Es konnte jedoch gezeigt werden, dass der QTL Effekt nach Zugabe von Ammonium nicht mehr nachweisbar war. Die Konzentration von Kalium in den Blättern war höher im NIL als in *Ler*, zudem konnte ein erhöhter Wasserverlust des NILs gemessen werden. Da kein Unterschied in der Stomatadichte zwischen *Ler* und dem NIL gezeigt werden konnte wird angenommen, dass der unterschiedliche Wasserverlust durch die Dauer der Stomata Öffnung bestimmt wird. Durch Phänotypisierung von Pflanzen mit Rekombinationsereignissen in der genomischen Region des QTL konnte diese auf ca 3.9 Mbp eingegrenzt werden. Es gibt Indikationen, dass mehrere Gene in dieser Region liegen, die eventuell epistatisch auf einander wirken und zusammen den QTL Effekt bestimmen. Mögliche genetische Ursachen für den QTL Effekt werden diskutiert, unter anderem der mögliche Einfluss des Kanals TPK1. Dieses QTL birgt die Möglichkeit, neue Gene in der Wachstumsregulation für Kaliummangel zu identifizieren, die eine bessere Kaliumeffizienz bei Pflanzen vermitteln.

## Contents

<b>Abstract</b> .....	<b>I</b>
<b>Kurzzusammenfassung</b> .....	<b>II</b>
<b>Contents</b> .....	<b>III</b>
<b>Abbreviations</b> .....	<b>1</b>
<b>List of Figures</b> .....	<b>3</b>
<b>List of Tables</b> .....	<b>5</b>
<b>1. Introduction</b> .....	<b>6</b>
1.1 Potassium availability and plant requirements .....	6
1.2 Functions of potassium in the plant .....	6
1.3 Syndromes and adaptation to potassium deficiency .....	8
1.4 Potassium uptake and transport proteins .....	10
1.5 Potassium sensing and regulation .....	11
1.6 Using natural variation to reveal the genetic basis of a quantitative trait .....	14
1.7 Quantitative trait analysis for plant mineral nutrition .....	16
1.8 The aim of the present study .....	17
<b>2. Material and Methods</b> .....	<b>19</b>
2.1 Growing plants in different nutrient regimes using a hydroponic system .....	19
2.1.1 The mineral nutrient solution .....	19
2.1.2 Seed sterilization .....	21
2.1.3 The setup of the hydroponic system .....	21
2.1.4 Further environmental conditions for the hydroponic growth .....	23
2.2 Selection of the NILs and recombinant lines .....	24
2.2.1 Growth conditions on soil .....	24
2.2.2 Crossing of plants .....	25
2.2.3 Plant material .....	25
2.3 Molecular analysis: genotyping the NILs and recombinant plants .....	25
2.3.1 DNA extraction .....	25
2.3.2 Marker and marker design to reveal polymorphisms between <i>Ler</i> and <i>Kas-2</i> .....	26
2.3.3 PCR reactions .....	28
2.3.4 Digestion of CAPS markers .....	28
2.3.5 Characterization of markers on agarose gel .....	29
2.3.6 Sequencing .....	29
2.3.7 Allelic comparison of the TPK1-gene .....	29
2.4 Trait quantification for validation and the characterization of the QTL .....	30
2.4.1 Quantification of growth related traits .....	30
2.4.2 Quantification of physiological traits: Water loss .....	31
2.4.3 Quantification of Biochemical traits .....	32
2.4.3.1 Total hexose, protein and chlorophyll extraction .....	32
2.4.3.2 Ionic quantification .....	32
2.4.4 Transcription analysis .....	33
2.5 Statistical analysis .....	34
2.5.1 QTL detection .....	34
2.5.2 The Gaussian error propagation .....	34
2.5.3 Significance tests .....	34
2.5.4 Statistical analysis of the microarray data .....	35
<b>3. Results</b> .....	<b>36</b>
3.1 QTL mapping in different nutritional regimes (by Dr. Barbier and Dr. Reymond) ..	36
3.2 Validation of growth response QTL for lowered potassium and phosphate supply .	37

3.3 Characterization of the validated, potassium-responsive QTL on bottom chromosome five .....	42
3.3.1 Different applied growth conditions.....	42
3.3.1.1 Different levels of potassium reduction do not affect the QTL.....	42
3.3.1.2 Growth in different day length does not affect the QTL .....	43
3.3.1.3 The QTL is ammonium sensitive .....	44
3.3.2 Characterization of additional growth related traits observed for the QTL .....	46
3.3.2.1 The response of the rosette dry weight and fresh weight correspond .....	46
3.3.2.2 Root growth effects of the QTL: the root weight response is similar to the rosette weight response.....	47
3.3.2.3 Kas-2 alleles at the QTL are associated with a reduction of water loss .....	49
3.3.2.4 No differences in stomata density coincide with the QTL effects .....	51
3.3.3 Ionic differences between <i>Ler</i> and the NIL3.....	51
3.3.4 Dominance of the <i>Ler</i> allele at the QTL position.....	53
3.4 Fine mapping of the rosette weight response QTL on chromosome five.....	54
3.5 Candidate genes for the potassium dependent rosette weight response QTL .....	59
3.5.1 Genes in the region between the markers CNGC4_11 and m5.17.....	59
3.5.2 Transcriptional differences between <i>Ler</i> and the recombinant line R5.....	61
3.5.3 Polymorphisms between the <i>Ler</i> and Kas-2 alleles of the candidate TPK1 .....	64
<b>4. Discussion .....</b>	<b>66</b>
4.1 The validation of the potassium dependent rosette weight QTL.....	66
4.2 The fine mapping of the potassium dependent rosette weight QTL.....	68
4.3 Characterizing the potassium dependent rosette weight QTL.....	70
4.4 The candidates, what is likely to cause the QTL effect? .....	75
4.5 Conclusion and outlook.....	79
<b>References.....</b>	<b>80</b>
<b>Appendix .....</b>	<b>90</b>
<b>Acknowledgements .....</b>	<b>96</b>
<b>Erklärung .....</b>	<b>97</b>
<b>Lebenslauf .....</b>	<b>98</b>

**Abbreviations**

aa	-	Amino acid
ABA	-	Abscisic acid
AGI code	-	Arabidopsis genome initiative gene annotation code
ANOVA	-	Analysis of variance
<i>A. thaliana</i>	-	<i>Arabidopsis thaliana</i>
ARR6	-	Response regulator 6
bp	-	Base pair
BTB domain	-	Broad complex/tramtrack/bric-a-brac domain
Ca <sup>2+</sup>	-	Calcium ion
CAPS	-	Cleaved amplified polymorphic sequences
CBL	-	Calcineurin B-like
Chr.	-	Chromosome
cM	-	Centi Morgan
CNGC	-	Cyclic nucleotide gated channel
CO <sub>2</sub>	-	Carbon dioxide
DNA	-	Deoxyribonucleic acid
EDTA	-	Ethylendiamin-tetraacetat
EF-hand	-	Helix (“E”)-loop-helix (“F”) structure
ER	-	Endoplasmic reticulum
FIP2	-	FH (formin homology) protein interacting protein
H <sup>+</sup> ATPase	-	ATP driven proton pump
HIF	-	Heterogeneous inbred family
Indel	-	Insertion or deletion
JA	-	Jasmonic acid
K <sup>+</sup>	-	Potassium ion
Kas-2	-	Kashmir 2, natural accession of <i>Arabidopsis thaliana</i> , from Kashmir
<i>Ler</i>	-	Landsberg <i>erecta</i> , natural accession of <i>Arabidopsis thaliana</i> , from Poland
LOD	-	Logarithm of the odds
Mbp	-	Mega base pair
MES	-	2-(N-morpholino)ethanesulfonic acid
min	-	Minute



MQM	-	Multiple QTL model
NIL	-	Near Isogenic Line
OD	-	Optical density
PAM	-	Pulse-amplitude-modulation, fluorometry method
PCR	-	Polymerase chain reaction
pdf	-	Percentage of false prediction
PS II	-	Photosystem II
QTL	-	Quantitative trait locus
RGR	-	Relative growth rate
RIL	-	Recombinant inbred line
ROS	-	Reactive oxygen species
RPD3	-	Reduced potassium dependency 3
rpm	-	Revolutions per minute
RT	-	Room temperature
SDS	-	Sodium dodecyl sulphate
sec	-	Second(s)
SSLP	-	Simple sequence length polymorphism
SNP	-	Single nucleotide polymorphism
SUMO	-	Small ubiquitin-like modifier
TAIR	-	The Arabidopsis information resource ( <a href="http://www.arabidopsis.org">http://www.arabidopsis.org</a> )
TF	-	Transcription factor
TPK1	-	Two-pore K <sup>+</sup> channel (formerly KCO1)
TrisHCl	-	Tris(hydroxymethyl)aminomethane, pH was adjusted using HCl
UTR	-	Untranslated region

**List of Figures**

cover picture:Potassium deprived Arabidopsis grown on hydroponics

Figure I1: Regulation of turgor changes using the example of stomatal closure (adapted from Buchanan et al., 2002).....	7
Figure I2: Proposed signaling mechanism in response to potassium deficiency (adapted from Wang and Wu, 2010) .....	13
Figure I3: General scheme from identification to the cloning of a QTL.....	16
Figure M1: The hydroponic system.....	22
Figure M2: HoBo data logger files showing the environmental conditions measured in the Percival .....	24
Figure R1: Response QTL to reduced potassium and reduced phosphate supply (Dr. Barbier and Dr. Reymond).....	37
Figure R2: RILs tested for response QTL effects.....	39
Figure R3: The responses of <i>Ler</i> , the RIL138 and the selected NILs to reduced potassium supply .....	41
Figure R4: Response of rosette weight to varying levels of potassium supply .....	43
Figure R5: Growth responses of <i>Ler</i> , RIL138 and NIL3 to reduced potassium supply in 14h light.....	44
Figure R6: Rosette weight response of <i>Ler</i> and the NILs without and with ammonium (NH <sub>4</sub> ) in the nutrient media.....	45
Figure R7: Correlation between fresh and dry rosette weight response of <i>Ler</i> and RIL138 .....	47
Figure R8: Root growth responses corresponding to the rosette weight response of <i>Ler</i> and the NIL3 to potassium reduction .....	48
Figure R9: Exemplary pictures of root hairs of <i>Ler</i> and the NIL3 .....	49
Figure R10: Water loss of <i>Ler</i> and the NIL3 in the control and reduced potassium regime .....	50
Figure R11: Ionome of the NIL3 compared to <i>Ler</i> .....	52
Figure R12: Allelic dominance at the QTL position .....	54
Figure R13: Fine mapping I, the recombinant lines R1 to R8.....	55
Figure R14: Fine mapping II, the recombinant lines R9 to R20.....	58

Figure R15: Functional annotations of genes in the region between the markers CNGC4_11 and m5.17 .....	60
Figure R16: Comparison of the predicted protein sequences of TPK1 from <i>Ler</i> , the RIL138 and Col-0 .....	64/65
Figure A1: Sequence alignment of the TPK1-loci of <i>Ler</i> , RIL138 and Col-0 .....	94/95

**List of Tables**

Table M1: Mineral concentrations of the solutions used for the QTL detection .....	20
Table M2: Mineral concentrations of the nutrient solutions with increased potassium reduction .....	20
Table M3: Control and 20-fold reduced potassium media with ammonium .....	21
Table M4: Self designed markers.....	27
Table M5: Primer combinations for sequencing of the TPK1-loci .....	30
Table R1: Expression differences between Ler and the recombinant line R5 .....	63
Table A1: List of all QTL detected by Dr. Barbier and Dr. Reymond.....	90-93

## **1. Introduction**

### **1.1 Potassium availability and plant requirements**

As plants are photoautotrophic organisms, they depend in essence on the supply of water, light and mineral nutrients. Minerals like sulphate, nitrogen or phosphate are major building blocks of organic molecules as nucleic acids or proteins. Others like molybdenum, zinc or magnesium are incorporated into proteins as structural components or as cofactors that are needed in enzymatic reactions. For example potassium and chloride can serve as osmoticum or have electrochemical functions (Marschner, 1995; Buchanan et al., 2002).

Potassium is the most abundant cation in the plant cell. It is usually kept in an order of 100 mM in the cytoplasm (vacuolar concentration can vary considerably between 10 mM and 500 mM) and can make up to 10% of the plants dry weight (Leigh and Jones, 1984; Marschner, 1995). Because of the high need of the plant for potassium it is defined as macronutrient (minerals that constitute between 1000  $\mu\text{g}$  to 15000  $\mu\text{g/g}$  dry weight; Buchanan et al., 2002). Plants are generally able to grow in potassium concentrations ranging from 10  $\mu\text{M}$  to 10 mM (Maathuis and Sanders, 1996; Amtmann et al., 2005); nevertheless, the growth in very low or high potassium concentrations is impaired. Potassium constitutes about 2.6% of the earth crust and is one of the ten most abundant elements (Brinkmann, 1967; Ashley et al., 2006); however, its deficiency for plants occurs frequently and its depletion causes agronomical loss (Pettigrew, 2008; Rengel and Damon, 2008). Only the potassium in the soil solution (with a concentration usually ranging between 0.1 and 6 mM) is available to the plant. The rest of the potassium in the soil is bound to other soil particles and is only partially exchangeable with the soil solution (Ashley et al., 2006; Moody and Bell, 2006). Especial sandy or alkalic soils are prone to cause potassium deficiency in plants (Munson and Nelson, 1963; Rengel and Damon, 2008). Also erosion, low humidity (Liebersbach et al., 2004) and intensive agriculture cause low availability of potassium (Amtmann et al., 2005; Rengel and Damon, 2008).

### **1.2 Functions of potassium in the plant**

Potassium is not incorporated into any higher molecule but constitutes the major osmotic ion of the plant cell and is involved in the regulation of the turgor, pH, plasmamembrane potential and transport (Very and Sentenac, 2003; Pettigrew, 2008). The turgor is the pressure constituted by the water status of the cell on the cell wall and is necessary for the

firmness of herbaceous plants and cell elongation (Fuchs et al., 2006). Potassium transport was further associated with pollen tube elongation (Mouline et al., 2002) and site directed outgrowth of roots in response to seismic factors (Philippar et al., 1999). Turgor changes are also the driving force for cell movements like stomatal opening and closure. At the beginning of the light phase protons are transported in the apoplast and the subsequent hyperpolarization of the membrane causes voltage-dependent potassium channels to open, causing a potassium influx into the cell. Anions like malate and chloride are accumulated in the cell as counter ions. The overall build-up of these ions in the vacuole increases the turgor change and the stomatal opening. The closure of the stomata is induced by ABA and calcium signalling that trigger the release of potassium and anions from the cell (Schroeder and Hedrich, 1989; Blatt, 2000; Roelfsema and Hedrich, 2005; Pandey et al., 2007; Figure 11). Furthermore, potassium is involved in the turgor driven transport of the xylem and

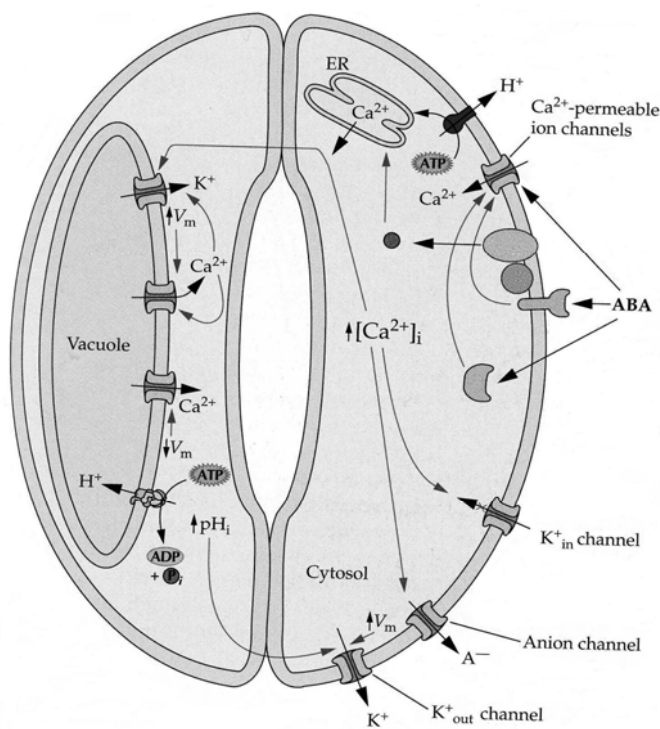


**Figure 11: Regulation of turgor changes using the example of stomatal closure (adapted from Buchanan et al., 2002)**

ABA triggers the increase in cytoplasmic calcium. Vacuolar potassium channels open and the resulting membrane potential change on the vacuole triggers the opening of channels that release further calcium from into the cytoplasm. Thereby, the calcium signal is amplified. The high increase in cytosolic calcium blocks potassium inward rectifying channels at the plasma membrane and activates the anion channels that cause the efflux of anions from the cell. The resulting depolarization (and an increase in stomatal pH) opens potassium outward rectifying channels and the loss in anions and potassium from the cell decreases the turgor and results in stomatal closure.

phloem (Gaymard et al., 1998; Maathuis, 2009). Next to its role in osmotic processes, potassium has electrophysiological roles in the cell. One is the participation in the membrane potential: The potassium concentration is higher in the cytoplasm than in the extracellular space and the resulting outward flux of the positively charged potassium ion creates a negative potential at the inner side of the plasma membrane. This negative charge is further increased by proton pumps ( $H^+$ ATPases) that transport  $H^+$  out of the cell.

Together the potassium and proton efflux give rise to the membrane potential (high H<sup>+</sup> extrusion can be counterbalanced by potassium influx). The membrane potential and the pH gradient across the membrane are the main driving force for membrane transport processes (Maathuis et al., 1997; Buchanan et al., 2002).

### **1.3 Syndromes and adaptation to potassium deficiency**

Potassium is required for the charge balance of negative residues on macromolecules and thereby has a role in proteins stabilisation. Its role as the major counter-ion is thought to have arisen from the fact that it is the major cell osmoticum and the cell tolerates high levels of this ion in the cytoplasm (Lebaudy et al., 2007). At least 60 enzymes were shown to be dependent on potassium for their activity (Amtmann et al., 2005): it is important for the ribosome mediated protein synthesis (Maathuis, 2009) and the activity of pyruvate kinase and starch synthetase (Kachmar and Boyer, 1953; Nitsos and Evans, 1969; Ramírez-Silva et al., 1993). Lower activation of these enzymes and the reduced allocation of sugars through the phloem, are thought to be responsible for an accumulation of free sugars in the leaves and a reduced starch build-up in storage organs of potassium deficient plants (Haeder et al., 1973; Marschner, 1995; Deeken et al., 2002; Pettigrew, 2008). Furthermore, photosynthesis is affected directly by low potassium supply, as ribulose biphosphate carboxylase activity is reduced (Peoples and Koch, 1979), membrane potentials at the thylakoid and mitochondrial membranes are disturbed, photoassimilates accumulate and chlorophyll levels decrease (Tester and Blatt, 1989; Zhao et al., 2001; Basile et al., 2003). All of this causes disturbances in the carbohydrate metabolism in potassium deficient plants. The nitrogen metabolism, specifically the uptake and reduction, can be impaired by low potassium conditions as well (Maathuis, 2009). It could be shown that the nitrate transporter NRT2 was downregulated in response to low potassium supply (Armengaud et al., 2004) that might be a consequence of an increase in glutamine in potassium deficient plants (Amtmann et al., 2005). Glutamine is a product of nitrogen assimilation that acts on the nitrogen transporter in a negative feedback loop (Vidmar et al., 2000; Nazoa et al., 2003). There are indications that also ammonium fluxes are dependent on potassium (Szczerba et al., 2008).

Taken into account all the roles potassium plays in cell regulation and metabolism it is not surprising that the reduced supply of this ion causes major growth reductions. The effect on growth and developmental processes is the first visible effect of potassium starvation to

all plants. A characteristic potassium deficiency syndrome that develops after prolonged deficiency is chlorosis in older leaves. This chlorosis occurs as a result of the allocation of potassium from older leaves to growing tissues (Marschner, 1995; Maathuis and Sanders, 1996; Amtmann et al., 2005). Potassium deficient plants become more susceptible to other biotic and abiotic stresses: Plants with a low potassium status are more susceptible to drought (Imas and Imas, 2007) and cold stress (Larsen, 1976 cited in Marschner, 1995). Sodium stress can lead to potassium deficiency symptoms. However, in early stages of potassium depletion, sodium can complement potassium in its osmotic role and sometimes even activate enzymes that depend on potassium (Clarkson, 1980; Carden et al., 2003; Kronzucker et al., 2008). A higher susceptibility for pathogens in potassium starved plants is thought to be favoured by the increased level of soluble sugars and the reduction in macromolecule formation, such as PR-proteins (due to the disturbed metabolism). Disease susceptibility of potassium deficient plants depends on the plant species as on the infecting agent. In contrast to bacterial or fungal infections, viral attacks have been shown to be rather less infectious to plants with a low potassium status (Amtmann et al., 2008).

As mentioned, visible symptoms, except for growth retardation, only occur at prolonged or very intense potassium deficiency. The high mobility and the capability of plants to store potassium and allocate it to tissues and cell compartments where it is needed is one reason for this. Root architectural changes as shown for nitrogen or phosphate starvation (primary root growth inhibition and the extension of the lateral root system), are not characteristic for potassium. Root responses to potassium deficiency seem to be highly dependent on accompanying environmental factors, plant species and individual variability (Hodge, 2004; Hermans et al., 2006). Also increased root hair growth which is well established as a response to phosphate starvation (Bates and Lynch, 1996; Narang et al., 2000) was only shown in some species and conditions to be a response to potassium starvation (Amtmann et al., 2005; Rengel and Damon, 2008). Also the exudation of organic acids from the plant roots is a possible reaction of the plant to decreasing potassium supply. The resulting acidification of the soil releases more potassium in the soil solution. Efficient potassium uptake of sugar beet and potato varieties that were grown in potassium deficient conditions, was shown to depend on soil acidification by the plants (El-Dessougi et al., 2002; Trehan and Sharma, 2002). In addition, a change in potassium uptake rate occurs if plants grow in environments with low potassium availability.



#### 1.4 Potassium uptake and transport proteins

In a very low external potassium condition (for *A. thaliana* this is starting at external concentrations of potassium of 100/500  $\mu\text{M}$  and below) the uptake rate of potassium increases compared to sufficient potassium supply. The two proposed uptake phases are constituted by a passive low affinity uptake and the high affinity uptake driven by active transport (Epstein et al., 1963; Maathuis and Sanders, 1996; Very and Sentenac, 2003; Britto and Kronzucker, 2008). Passive ion uptake is usually mediated by channels that form hydrophilic pores through which ions can pass along their electrochemical gradient. Active transport is mediated by membrane proteins, transporter, against the electrochemical gradient of the transported ion either by ATP usage, light energy or cotransport of other ions (Lehninger et al., 1993). However, there are some exceptions, also channels (SPIK, AKT1) have been shown to be capable of potassium uptake from an external media that would require high affinity potassium uptake (Spalding et al., 1999; Brownlee, 2002; Mouline et al., 2002). Vice versa, a transporter was shown to be involved in potassium uptake in concentrations in the low affinity potassium uptake range (Fu and Luan, 1998) while this passive uptake is mainly performed by channels. The channel AKT1 and the transporter HAK5 are thought to mediate most of the high affinity potassium uptake in the roots (Rubio et al., 2008; Pyo et al., 2010).

The first cloned potassium transporting protein were the guard cell potassium channel KAT1 (Anderson et al., 1992) and the root uptake channel AKT1 (Sentenac et al., 1992; Ashley et al., 2006). Sequence based prediction has established a large number of potential proteins for potassium transport of which some were functionally characterized by mutant analysis or in heterologous expression systems. For *Arabidopsis thaliana* 71 potassium transporters and channels were annotated so far (Chen et al., 2008). There are three large families of transporters: KUP/HAK/KT, HKT and CPA (Gierth and Maser, 2007) and also three large channel-families, the Shaker, TPK and Kir-like families (Lebaudy et al., 2007). The KUP/HAK/KT-family was identified by homologies with bacterial and fungal potassium transporters. Three of the 13 members in *Arabidopsis* (KUP1, KUP4, HAK5) were shown in planta to function in high affinity potassium uptake. HKTs (high-affinity  $\text{K}^+$  transporters) are topologically related to potassium channels with subunits consisting of two transmembrane domains and one pore domain. However, most of them have shown to be more permeable to sodium than potassium in heterologous expression systems. The cation proton antiporter (CPA) family are thought to work as proton antiporters for sodium

or potassium (reviewed in: Very and Sentenac, 2003; Gierth and Maser, 2007). The channels are all built from so called  $\alpha$ -subunits. These subunits contain either one (Shaker or Kir-like families) or two (TPK-family) pore domains and each functional channel needs to possess four pore domains. Heteromere formation of several subunits was described for the Shaker channel family. The Shaker family channels reside in the plasmalemma and are voltage dependent. If they are activated by hyperpolarization of the membrane they are called inward rectifying channels and function in potassium uptake in the cell, while depolarization activates the outward rectifying channels. Kir-like and TPK family channels (except for TPK4; Voelker et al., 2006) were found to be localized at the tonoplast and seem to be insensitive to membrane voltage changes (reviewed in: Very and Sentenac, 2003; Lebaudy et al., 2007). Apart from those three large channel-families also cation channels with a lower selectivity for potassium were described like the vacuolar channel TPC1 (Peiter et al., 2005) and the cyclic nucleotide gated channels (Köhler et al., 1999).

The uptake of potassium was found to be influenced by the presence of other mineral nutrients in the soil as sodium (Epstein et al., 1963; Rus et al., 2004) or ammonium. The presence of ammonium ( $\text{NH}_4^+$ ) reduced potassium uptake (Rufty et al., 1982; Dean-Drummond and Glass, 1983). Only high affinity transport mechanisms seem to be affected and ammonium sensitive and insensitive uptake pathways were reported (Spalding et al., 1999; Santa-Maria et al., 2000; Szczerba et al., 2006). One proposed mechanism for this ammonium sensitivity is that, due to its similar hydrated ion radius, ammonium competes with the potassium ion for transporter binding sites and maybe for uptake (Vale et al., 1988; Wang et al., 1996; Spalding et al., 1999; ten Hoopen et al., 2010).

### **1.5 Potassium sensing and regulation**

In order to change from a low to a high affinity uptake mechanism, the change in available potassium needs to be perceived and a signalling mechanism needs to be activated that leads to transport protein changes. Recent suggestions about the perception of the reduced supply of potassium in the external medium involve the potassium uptake channel AKT1 in the roots (Wang and Wu, 2010). Potassium ions negatively regulate  $\text{H}^+$ ATPases at the plasma membrane (Buch-Pedersen et al., 2006). Reduced potassium inflow via AKT1 might cause a reduction of potassium ions at the inner membrane site, leading to an increased activity of  $\text{H}^+$ ATPases (Palmgren, 2001). The resulting hyperpolarization in turn may activate inward channels (such as AKT1) which lead together with the acidification of

the soil to an increased potassium uptake (Wang and Wu, 2010; Figure I2). From this local response in the outer root epidermal cells a potassium starvation signal needs to be transmitted to the rest of the plant. In response to potassium starvation, plants have shown to produce increased levels of ethylene (Jung et al., 2009). Furthermore, potassium channels were found to be affected by auxin (Philippar et al., 1999) and cytokinin (Van Steveninck, 1972; Pilot et al., 2003) and transcriptome analysis revealed the upregulation of many transcripts of genes involved in jasmonic acid (JA) synthesis and response (Armengaud et al., 2004). Phytohormones are certainly good candidates for a long range signal, they are usually involved in developmental regulation as well as in abiotic and biotic stress signalling (Buchanan et al., 2002). Yet, also changes in photoassimilate production and translocation from the shoot to the root might act as a systemic signal for potassium starvation. Whether the potassium ion itself contributes to signalling is rather controversial (Amtmann et al., 2005). Low concentrations of potassium in the xylem or phloem could only act as a long range signal in prolonged starvation conditions, when the potassium concentration in the tissues is affected. However, transcriptional responses to potassium deficiency (in the root and the shoot) can already be registered six hours after onset of the stress (Armengaud et al., 2004). Consequently, potassium concentration changes might be perceived as a signal but there need to be another long range signal that acts temporarily before that. The potassium ion homeostasis is thought to be kept constant in the cell over a wide range of external potassium concentrations; therefore, the involvement of potassium as a short range signal is also unlikely. Furthermore, the concentration of potassium in the cell is very high and a perceivable signal would need to cause drastic changes. However, Szczerba et al (2006) suggested that the dogma of potassium homeostasis might not hold true since drastic changes in potassium concentration between 40 mM and 250 mM in plants, grown in sufficient potassium supply, were shown in response to different environmental scenarios. A possible short range signal could be constituted by reactive oxygen species (ROS) and calcium. Reactive oxygen species are a general stress response signals and were also found to be increased in potassium starved roots maybe by an ethylene responsive pathway (Shin and Schachtman, 2004; Jung et al., 2009). Calcium is often a downstream signal of ROS production and there are recent indications for increased calcium levels in the plant (Wang and Wu, 2010) and calcium binding proteins were described to be differentially regulated in response to low potassium supply (Schachtman and Shin, 2007). A presumably ROS and calcium dependent regulation of the channel AKT1 was already described: The calcium binding

proteins CBL1 and CBL9 interact with the kinase CIPK23 that triggered the activation of AKT1 by phosphorylation (Li et al., 2006; Xu et al., 2006). Long and short range signals triggered by potassium deficiency can act on several downstream targets. Transport proteins were shown to be regulated on the one hand by transcriptional activation, for example one of the most important potassium uptake transporter, HAK5, was shown to be upregulated within one day, in response to potassium starvation (Ahn et al., 2004; Gierth et al., 2005). On the other hand transporters and channels are regulated by a multitude of post-transcriptional modifications. These modifications include phosphorylation changes (Li et al., 1998; Lee et al., 2007), heteromerization of different channel subunits (Duby et al., 2008), 14-3-3 proteins (Saalbach et al., 1997; Van den Wijngaard et al., 2001), G-proteins (Walter et al., 1995), cNTPs (Köhler et al., 1999), pH and voltage changes (Very and Sentenac, 2003).

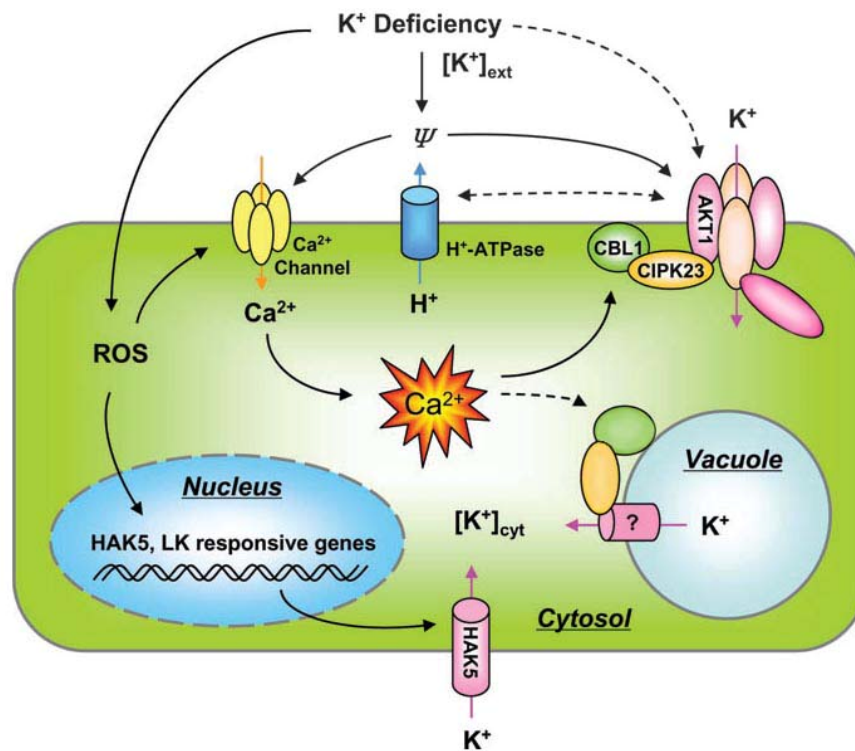


**Figure I2: Proposed signalling mechanism in response to potassium deficiency (adapted from Wang and Wu, 2010)**

The decreased uptake of potassium in deficiency (eg. by AKT1) leads to an activation of H<sup>+</sup>-ATPases that acidifies the apoplast. Overall this leads to a change in the plasma membrane potential ( $\Psi$ ) which in turn activates potassium uptake channels like AKT1 itself but also calcium channels that cause a calcium increase in the cell. The calcium as well as the ROS signals trigger further responses like transcriptional changes (eg. of the uptake transporter HAK5) and the release of potassium from the vacuole.

## 1.6 Using natural variation to reveal the genetic basis of a quantitative trait

Although, several putative and confirmed transport proteins as well as possible signalling factors were described, there is no complete picture of the molecular basis of potassium response effects. So far, mainly reverse genetic approaches were used. In a mutant screen, plants are selected according to an obvious phenotype that is caused by a single mutation. Most phenotypes, or trait variation, in nature arise from the combination of several altered genes. The phenotypes that are caused by multiple genes can vary depending on the different allelic combinations that are possible and can lead to a continuous variation of trait values. To study these quantitative traits, a quantitative trait locus (QTL) mapping can be performed (Alonso-Blanco and Koornneef, 2000). A QTL is a genomic region that is involved in the variation of a quantitative trait. To identify such a locus, genomic markers are tested for their significant association with the variation of the trait values (the probability can be assessed by the LOD-score). To link genomic markers to a phenotype, several genotypes that differ at the tested marker positions need to be analysed for their trait variation. A collection of such genotypes is a mapping population. For the construction of a mapping population, the allelic diversity that is present in natural accessions of a species can be used. This natural variation within a species may result from population history (for instance by genetic divergence) or from the adaptation to the local environment. The first step to develop a mapping population is the cross between at least two natural accessions. The F1 progeny of the cross is heterozygous, consisting of alleles from both parental accessions. The progeny of these hybrids have a mixed allelic genome. Although F2 populations can be used for a QTL mapping, recombinant inbred line (RIL) populations are preferred mostly. They have homozygous genomes (so called immortal mapping population) and are obtained by single seed descendants from individual F2 plants until the F7 - F10 generation. The homozygous lines can be phenotyped in several replicates (and several environments) without the further need to genotype each plant individually. The allelic values at genomic marker positions along the chromosomes are determined for each genotype. If the allelic value at a marker has a significant impact on the trait variation this genomic region is called a QTL. QTL can contribute to varying degrees to the trait variation, those with a high explained variance ( $R^2$ ; percentage of trait variation explained by the single QTL) and/ or high additive effect of the different alleles are called major QTL. A QTL detection bears, like any statistical analysis, the risk of detecting false positives. This is less likely for major QTL than for those of small effect.

However, to finally prove the existence of a QTL it needs to be validated. A certain way to validate the effect, is to derive lines that genetically differ only at the QTL position: Heterogeneous inbred families, for example, have a mixed genetic background of both alleles which is identical between the lines except for the QTL position (HIFs; Tuinstra et al., 1997). Another type of lines for validation are near isogenic lines (NILs) that have a homogenous genetic background of only one allele, with an introgression of a different allelic region at the QTL position (Koornneef et al., 2004; Reymond et al., 2007; Figure I3). The trait difference between those lines should only be caused by the QTL effect, as it is the only genomic region differing between them. If the trait difference between the lines is significant, the QTL is validated. A validated QTL can be fine-mapped to unravel its genetic basis. To do so, lines with recombinant events between the allelic values in the QTL region can be derived. If recombinant plants show the expected allelic effect, the genomic region those lines have in common, is causing the QTL effect. Following this strategy the QTL can be narrowed down to a small number of genes (Figure I3). Alleles from candidate genes can be cloned and transferred into a line with a different allelic value at the QTL position. If the gene is responsible for the QTL effect, the trait value of the transformed line will change accordingly. This complementation test is the final prove for the genetic basis of a QTL (Yano, 2001; Salvi and Tuberosa, 2005).

The benefit of a QTL analysis is that phenotypes which are caused by several genetic factors can be analysed and in some cases even interactions between loci can be detected. This is of interest especially for growth related traits which are usually caused by several genes. Genes with low effect on a trait variation or genes with lethal knock-out mutations can still be detected to be involved in a trait variation. These genes would rarely be detected in a mutant screen for the same trait. Furthermore, most mutants are derived from one accession, Col-0. Genes with non-functional alleles already present in this accession could also go undetected in a mutant screen. The allelic polymorphisms that cause a QTL effect are of functional importance and may allow a more detailed insight into the character of a gene or its regulation (Maloof, 2003; Tonsor et al., 2005). QTL analysis, using natural variation as a basis for the construction of the mapping populations, benefits from the large genetic pool the accessions provide. The allelic difference between accessions may have derived from selection by environmental specificities of the local habitat and a detailed analysis may provide insight into the adaptation of plants to those environments.

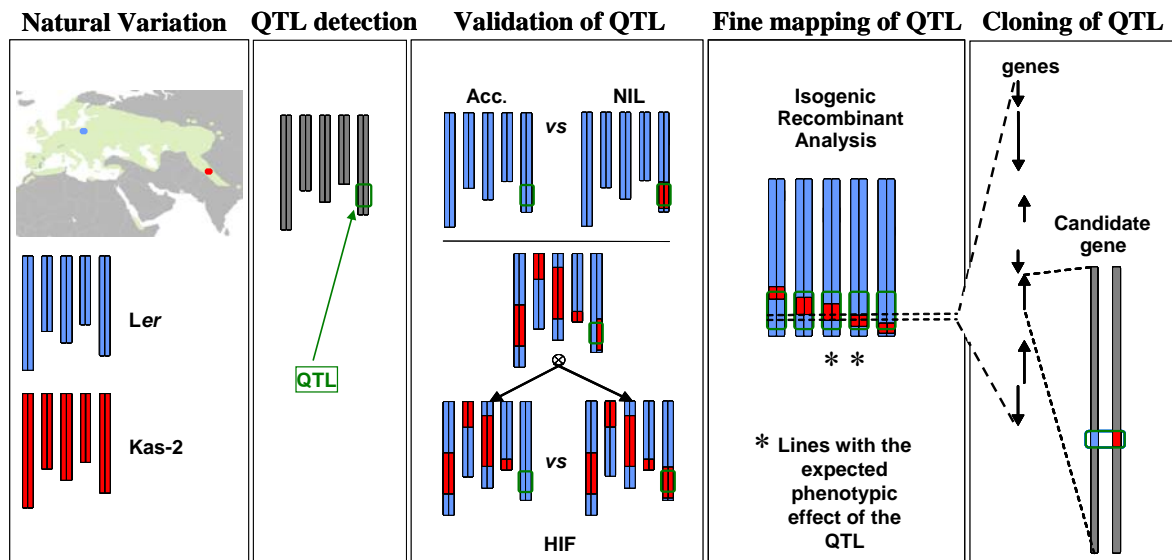


**Figure I3: General scheme from identification to the cloning of a QTL (adapted from Reymond et al., 2007)**

A RIL population from two accessions, like *Ler* from Poland (blue dot) and *Kas-2* from Kashmir (red dot) can be used to detect QTL. To validate the QTL plants that differ only at the QTL position need to be compared in their phenotype, like this the quantitative trait can be “Mendelized”. Those lines are generally near isogenic lines (NILs) or heterogeneous inbred family (HIF) lines. NILs have a genetic background consisting of only one genotype and HIFs have a mixed allelic (but identical) background. To locate the genomic position of a QTL more precisely, lines with recombinant events in the QTL region can be phenotyped. The lines that show the expected effect according to the QTL detection/validation should carry the gene responsible for the QTL effect. This fine mapping is limited at some point by the number of recombinant events that can be selected for in the continuously decreasing QTL region. Among a smaller number of genes, candidates can be cloned and used for a complementation test.

A species with a wide geographic distribution and many accessions is *Arabidopsis thaliana* (L.) Heynh (Alonso-Blanco and Koornneef, 2000). The Brassicaceae species *A. thaliana* is a model organism for higher plants. It has a relative short life cycle, a small genome (130 Mbp, five chromosomes) and a lot of molecular information and methodical protocols are already available for this plant. Several accessions of *A. thaliana* were already used to construct mapping populations for QTL analysis that led to the identification of a number of genes underlying complex traits (Koornneef et al., 2004; El-Lithy et al., 2006; Simon et al., 2008).

### 1.7 Quantitative trait analysis for plant mineral nutrition

A QTL detection with the same mapping population can be performed in different environments and by comparison of the analysis, an environmental effect on the QTL effect can be observed. Constitutive QTL would be present in all conditions which means

they have an overall effect on the trait that is unaltered by the environment. In contrast, QTL can also be present in one condition only or change their effect depending on the conditions. These QTL will further be referred to as response QTL. They may be involved in the adaptation of the plant to the changing condition.

Natural variation bears the potential to identify genotypes with better nutrient uptake or utilization efficiency (Marschner, 1995; Narang et al., 2000; Rengel and Marschner, 2005) and QTL analyses using natural variation already identified genes involved in nutrient deficiency. The multicopper oxidase, LPR1, was identified to cause changes in the primary root growth arrest in response to low phosphate. This oxidase might be involved in the phosphate perception (Reymond et al., 2006; Svistoonoff et al., 2007). Harada et al. (2004) detected QTL for nitrogen content in a *Ler/Cvi* RIL population on chromosome five and suggested an anion channel of the AtCLC family as candidate. A mutant analysis of the proposed gene showed that it affected the nitrogen content. In another study, elemental profiling of several *Arabidopsis thaliana* accessions combined with a microarray-based genotyping approach indicated that the transporter AtHKT1 is involved in sodium content and sensitivity in Arabidopsis. Rus et al. (2006) further confirmed the involvement of AtHKT1 by mutant complementation with the isolated alleles.

The analysis of the ionome of a plant, like the one performed by Rus et al., but also metabolome or proteome analysis is becoming a more and more accessible technology. These “omic” approaches that measure a large number of different substances can be incorporated in the QTL mapping and add information about complex, system wide changes (also in response to changing environmental stimuli). Transcriptome analysis can be used in two ways: On the one hand the global expression data from a RIL population can be used as a “trait” for QTL analysis, giving rise to so called expression QTL (eQTL). These eQTL can be used to unravel regulatory networks, shedding light on pleiotropic effects and trans-regulation of genes (Jansen and Nap, 2001; Keurentjes et al., 2007a). On the other hand, transcriptome analysis can be used in parallel with a fine mapping approach to identify differentially regulated genes as possible candidate genes for a QTL effect.

### **1.8 The aim of the present study**

Dr. Hugues Barbier and Dr. Matthieu Reymond combined a QTL mapping for growth related traits with an ionomic approach. They performed a QTL analysis for several growth related (e.g. rosette weight, RGR, root weight and root length) and biochemical traits in



three different mineral nutritional regimes: a control condition, a reduced potassium supply and a reduced phosphate supply. Furthermore, response QTL of all traits to the change in potassium or phosphate supply were determined (Prinzenberg et al., 2010).

The growth related traits are complex, integrative traits that reflect the impact of many physiological and genetic parameters. The reduction in growth is one of the major impacts potassium as well as phosphate starvation have on plants and the genetic determinism are of agronomical interest. For these reasons the growth related QTL became the major focus of this work, in specific the response QTL that are affected by the mineral nutrition change. Three growth response QTL were detected and one of them a potassium-response QTL for rosette weight was chosen for validation and fine mapping. In addition, this QTL co-located with a response QTL for rosette potassium concentration. In both cases the *Ler* allele increased the response value. This might be an indication for a common genetic cause of these QTL. All of this made this specific QTL region interesting for further analysis. The first aim of this thesis was to validate the potassium response QTL. The QTL was further characterized in different environmental scenarios and for additional phenotypes and the obtained information was used to discuss the possible genetic mechanism underlying the QTL effects. The genetic determinism of the QTL enables the plants to retain a higher fresh weight in potassium deficient conditions, to elucidate this determinism is of interest to understand growth regulation in reduced potassium nutrition.

## **2. Material and Methods**

To determine genes, involved in growth and biochemical reactions of a plant to changing mineral nutrient supply, a QTL mapping had been performed. To control the mineral nutrient supply of the plants, a hydroponic system was used. In this chapter the nutrient solutions, the system itself and the accompanying environmental conditions are described (2.1). The detected QTL were validated with near isogenic lines (NILs) and fine mapped with lines with recombinant events in the genomic region of the QTL. These lines were selected among segregating progeny of a backcross of a recombinant inbred line (RIL) from the mapping population with one of the parental accessions of the population (2.2). The lines were genotyped with molecular markers and the predicted protein sequence of a possible candidate gene for the QTL effects was compared between the genotypes (2.3). The determination of the traits for the QTL detection, the validation and further characterization of the QTL is explained (2.4) as well as the statistical evaluation of those traits (2.5).

### **2.1 Growing plants in different nutrient regimes using a hydroponic system**

#### **2.1.1 The mineral nutrient solution**

The nutrient solutions were derived from the Murashige and Skoog media (Murashige and Skoog, 1962; Tocquin et al., 2003). The control, reduced potassium and reduced phosphate solutions, used for QTL mapping and the first validation steps, are described in table M1. The solutions used for the increased levels of potassium starvation are listed in table M2. Another solution was derived from the control and 20-fold potassium reduced media, to which ammonium was added (Table M3). All solutions were adjusted with 2.39 mM MES to a final pH of optimally 5.8 (between 5.7 and 5.9). To adjust the pH of the buffer, KOH was used for the solution described in table M1 (705  $\mu$ M in the final solution) and NaOH (780  $\mu$ M in the final solution) for the solutions described in the tables M2 and M3.

All chemicals were used in “pro analysis” grade or “tissue culture” grade and purchased from the companies Roth, SIGMA and Merck.

Salts	control	reduced potassium	reduced phosphate
KNO <sub>3</sub>	2000	<b>0</b>	2000
Ca(NO <sub>3</sub> ) <sub>2</sub> 4H <sub>2</sub> O	1000	<b>2000</b>	1000
CaCl <sub>2</sub> 2H <sub>2</sub> O	300	300	300
MgSO <sub>4</sub> 7H <sub>2</sub> O	150	150	150
KH <sub>2</sub> PO <sub>4</sub>	150	150	<b>32</b>
FeSO <sub>4</sub> 7H <sub>2</sub> O	22.4	22.4	22.4
Na <sub>2</sub> EDTA	22.3	22.3	22.3
MnSO <sub>4</sub> H <sub>2</sub> O	15	15	15
H <sub>3</sub> BO <sub>3</sub>	10	10	10
ZnSO <sub>4</sub> 7H <sub>2</sub> O	3	3	3
KI	0.5	0.5	0.5
Na <sub>2</sub> MoO <sub>4</sub> 2H <sub>2</sub> O	0.1	0.1	0.1
CuSO <sub>4</sub> 5H <sub>2</sub> O	0.01	0.01	0.01
CoCl <sub>2</sub> 6H <sub>2</sub> O	0.01	0.01	0.01
KCl	0	0	<b>118</b>

**Table M1: Mineral concentrations of the solutions used for the QTL detection**

The table summarizes the salt concentrations in the three different conditions that were used for the QTL mapping experiment (Figure R1) and for the selection of the RILs for validation (Figure R2). The concentrations are given in  $\mu\text{M}$ . Concentration changes compared to the control solution are highlighted in bold letters.

Salts	control	QTL det.	5-fold	10-fold	13-fold	20-fold	40-fold	100-fold
KNO <sub>3</sub>	2000	<b>705</b>	<b>279.6</b>	<b>64.6</b>	<b>10.8</b>	<b>0</b>	<b>0</b>	<b>0</b>
Ca(NO <sub>3</sub> ) <sub>2</sub> 4H <sub>2</sub> O	1000	<b>1647.5</b>	<b>1860.2</b>	<b>1967.7</b>	<b>1994.6</b>	<b>2000</b>	<b>2000</b>	<b>2000</b>
CaCl <sub>2</sub> 2H <sub>2</sub> O	300	300	300	300	300	300	300	300
MgSO <sub>4</sub> 7H <sub>2</sub> O	150	150	150	150	150	150	150	150
KH <sub>2</sub> PO <sub>4</sub>	150	150	150	150	150	<b>107</b>	<b>53.3</b>	<b>0</b>
FeSO <sub>4</sub> 7H <sub>2</sub> O	22.4	22.4	22.4	22.4	22.4	22.4	22.4	22.4
Na <sub>2</sub> EDTA	22.3	22.3	22.3	22.3	22.3	22.3	22.3	22.3
MnSO <sub>4</sub> H <sub>2</sub> O	15	15	15	15	15	15	15	15
H <sub>3</sub> BO <sub>3</sub>	10	10	10	10	10	10	10	10
ZnSO <sub>4</sub> 7H <sub>2</sub> O	3	3	3	3	3	3	3	3
KI	0.5	0.5	0.5	0.5	0.5	0.5	0.5	0.5
Na <sub>2</sub> MoO <sub>4</sub> 2H <sub>2</sub> O	0.1	0.1	0.1	0.1	0.1	0.1	0.1	0.1
CuSO <sub>4</sub> 5H <sub>2</sub> O	0.01	0.01	0.01	0.01	0.01	0.01	0.01	0.01
CoCl <sub>2</sub> 6H <sub>2</sub> O	0.01	0.01	0.01	0.01	0.01	0.01	0.01	0.01
Ca(H <sub>2</sub> PO <sub>4</sub> ) <sub>2</sub> H <sub>2</sub> O	0	0	0	0	0	<b>21.5</b>	<b>48.4</b>	<b>75</b>

**Table M2: Mineral concentrations of the nutrient solutions with increased potassium reduction**

By using an alternatively buffered solution (see text), the potassium concentration could be decreased further. The concentrations of each salt (in  $\mu\text{M}$ ) in the control and the different media with reduced potassium concentrations are listed, ranging from the concentration used in the QTL detection (QTL det.) to a nearly 100-fold reduction in potassium. Concentration changes to the control solution are highlighted in bold letters.

To test the effect of the potassium response QTL in the presence of ammonium a solution was derived from the control solution (Table M2) in which part of the nitrogen was supplied as ammonium and not solely by nitrate. The presumed optimal ratio of

ammonium in the total nitrogen source is between 1/4 to 1/3 (Marschner, 1995; Lea-Cox et al., 1999), in the solution of the present study it is 1/4 (Table M3).

Salts	control	reduced potassium
KNO <sub>3</sub>	2000	0
NH <sub>4</sub> NO <sub>3</sub>	<b>1000</b>	<b>1000</b>
CaCl <sub>2</sub> 2H <sub>2</sub> O	300	300
MgSO <sub>4</sub> 7H <sub>2</sub> O	150	150
KH <sub>2</sub> PO <sub>4</sub>	150	107
FeSO <sub>4</sub> 7H <sub>2</sub> O	22.4	22.4
Na <sub>2</sub> EDTA	22.3	22.3
MnSO <sub>4</sub> H <sub>2</sub> O	15	15
H <sub>3</sub> BO <sub>3</sub>	10	10
ZnSO <sub>4</sub> 7H <sub>2</sub> O	3	3
KI	0.5	0.5
Na <sub>2</sub> MoO <sub>4</sub> 2H <sub>2</sub> O	0.1	0.1
CuSO <sub>4</sub> 5H <sub>2</sub> O	0.01	0.01
CoCl <sub>2</sub> 6H <sub>2</sub> O	0.01	0.01
Ca(NO <sub>3</sub> ) <sub>2</sub> 4H <sub>2</sub> O	<b>0</b>	<b>1000</b>
Ca(H <sub>2</sub> PO <sub>4</sub> ) <sub>2</sub> H <sub>2</sub> O	0	21.5

**Table M3: Control and 20-fold reduced potassium media with ammonium**

The concentrations are given in  $\mu\text{M}$ . Concentration changes compared to the solution shown in table M2 are highlighted in bold letters.

### 2.1.2 Seed sterilization

Seeds were rinsed in 70% EtOH for 1 min and afterwards kept for 8 min in a hypochloride solution (1.2% NaOCl, 0.1% SDS) under constant agitation (Thermo-shaker, Haep Labor Consult, Borenden). Afterwards they were rinsed three times in autoclaved millipore water and air dried in a sterile laminar flow work bench (Hera safe; Heraeus Instruments; Hanau) on autoclaved filter paper (Macherey-Nagel GmbH & Co. KG, Düren).

### 2.1.3 The setup of the hydroponic system

The hydroponic system is derived from the system of Tocquin et al (2003). *A. thaliana* seeds were sown on tip-cut, agar-filled tubes that hang through holes in a plate into a box with nutrient solution. In one tray of ten litres, 81 plants can be grown (Picture M1).

Before sowing, the seeds were sterilized using a hypochloride solution (2.1.2). Approximately 0.5 cm of the tubes (PP; Sarstedt, Nümbrecht) tip were cut off and filled with agar (0.65% Daishin agar, Duchefa Biochemie, Haarlem, Netherlands). As soon as the agar polymerized the tubes were collected in the tip-wholes of a 1ml-pipette tip case (10x96 slots, TipOne, Starlab, Ahrensburg) which was filled with the respective nutrient

solution. The sterilized seeds are placed on the agar surface. The tip case with the seeds was covered and placed for two to three days in the fridge ( $\sim 4^{\circ}\text{C}$ ) for stratification. After stratification the boxes were transferred to a growth cabinet (2.1.4), the lids of the boxes remaining closed until germination. When the majority of seeds germinated and the first cotyledons were formed (ca. three days after transfer to the growth cabinet) the lid was removed. Subsequently, the evaporated water was refilled each day with Millipore water (QGard1; QuantumEX Ultrapure Organex cartridge, Millipore GmbH, Schwalbach). One week after the transfer the roots of the young plants were about to penetrate through the agar and to reach the nutrient solution. At this point the tubes were transferred from the tip boxes to a 31 cm by 46 cm plastic plates with wholes corresponding to the size of the tubes. The plastic plates were covered with a white foil on the surface and the plants are grown in a distance of 2 cm to 4 cm (Figure M1). From this plate the tubes hung into a tray of 10 l-volume, filled with mineral nutrient solution. Quantification of the traits, mentioned in 2.4, was performed 32 days after the transfer to the growth cabinet. To minimize positional effects, the plates were swapped between replicate boxes and thereby the position of the plants changed within the growth cabinet. Furthermore, each genotype was grown in several replicates (usually between nine to 15 replicates) which were distributed randomly on the plastic plate. The pH of the solutions was monitored and the solutions renewed, if the pH dropped below 5.70.



**Figure M1: The hydroponic system**

*Arabidopsis thaliana* (32 days old in this picture) was grown on agar filled tubes that hang into a tray filled with nutrient solution (see lifted tray on the left). The trays are in a growth cabinet with light bulbs and light tubes illuminating the plants from above.

#### 2.1.4 Further environmental conditions for the hydroponic growth

The plants in the hydroponic system were grown in a growth chamber (AR95L, Percival Scientific Inc., Wertingen) with an 8 hours light and 16 hours dark cycle per day. The chamber was illuminated by light tubes (25W, F25T8/TL741 Alto, Philips, Andover, MA) and bulbs (25W matt, RIVA, WS Walter Schrickel GmbH, Philippsburg) with a total light intensity of approximately 10500 lx ( $\sim 180 \mu\text{mol s}^{-1} \text{m}^{-2}$ ). The bulbs were switched on 15 min before the tubes and went off 15 min after the tubes, increasing the light phase in total by 30 min at 120 lx ( $\sim 5 \mu\text{mol s}^{-1} \text{m}^{-2}$ ). The temperature was set at 22°C during the light phase and at 18°C during the dark phase. The relative humidity was approximately 60% during the light phase and 80% during the dark phase.

For the long day experiment the plants were grown in a different growth chamber (growbanks, CLF Plant Climatics, Emersacker). Light tubes and bulbs were of the same quality but the light phase was shifted to 14 hours (plus two times 15 min bulbs only). The temperature was set to 22°C during the light phase and 18°C during the dark phase with an relative humidity of approximately 50% and 70%, respectively.

The light intensity in  $\mu\text{mol s}^{-1} \text{m}^{-2}$  was determined from averaged values, measured with a light meter (LI-250A, LI-COR Biosciences, Bad Homburg). The temperature, light intensity and relative humidity were monitored by a HoBo U12 data logger (Onset Computer Corporation, Bourne, MA) that recorded these parameters in an interval at every three or five minutes. Figure M2 represents the usual readout of the HoBo probe in the growth chamber for the short day experiments (Percival).

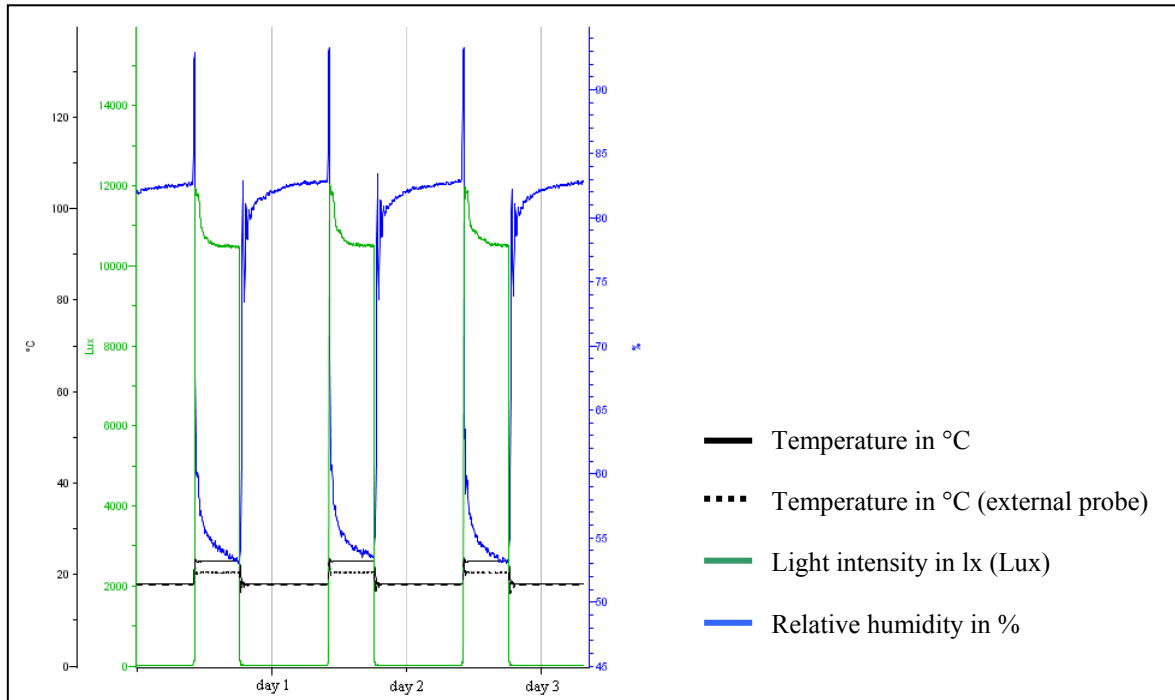


**Figure M2: HoBo data logger files showing the environmental conditions measured in the Percival**

An exemplary time period of three days is shown. The green line indicates the light intensity, the blue line the relative humidity and the black lines the temperature. The temperature was measured in the hobo data logger with all the other environmental parameters (full line) and with an external probe that was glued on the hydroponic tray directly next to the plants.

## 2.2 Selection of the NILs and recombinant lines

### 2.2.1 Growth conditions on soil

The genotypes that were grown in the hydroponic system were mainly homozygous. The selection of those genotypes from heterozygous parents was done on soil, as well as further seed propagation and the cultivation of lines used for crosses. The soil used, was “Mini-Tray” from the company Balster Einheitserdewerk (in Fröndenberg) with 1 kg/m<sup>3</sup> Triabon and 1 kg/m<sup>3</sup> Osmocote fertilizer (Scotts Celaflor GmbH & Co. KG, Mainz). The greenhouse environmental controls were set to a 16 hours light/ 8 hours dark period (with approximately 20°C/18°C). To break dormancy and to synchronize the plant germination, the seeds were stratified in Petri dishes on moist filter paper for at least two days before sowing in the greenhouse.

### **2.2.2 Crossing of plants**

To perform crosses, flowering plants were chosen that only had few if any siliques formed yet. As a mother for the cross, closed flower buds were chosen, ideally which already showed white tips of the first petals. The flower buds were opened with a pair of tweezers (No.5; A. Dumont & Fils, Montignez, Switzerland) and the anthers of the mother were removed, if possible, without removing the sepals and petals. Thereafter, mature anthers were taken from the other genotype for the cross (*Ler*) to pollinate the stigma of the mother plant.

### **2.2.3 Plant material**

The NILs and all recombinant plants were derived from backcrosses of the RIL138 from the *Ler*/Kas-2 RIL population (El-Lithy et al., 2006) and *Ler*. *Ler* was always used as a pollen donator. The NIL1, NIL2 and NIL3 were selected in the F<sub>2</sub>-generation of the backcross of *Ler* and RIL138 (thanks to Dr. Bjorn Pieper for sharing his F<sub>1</sub> seeds of the cross *Ler* x RIL138). The recombinant plants R1 to R8 are the fourth generation of this backcross (derived from six different heterozygous F<sub>3</sub> plants that were selected among the progeny of two F<sub>2</sub> plants). The recombinant lines R13, R15 and R17 were selected in the F<sub>6</sub> generation of the first backcross (which were derived from a common F<sub>3</sub> plant). The recombinant lines R9-R12, R14, R16 and R18-R20 are the third generation of a second backcross (BC2F<sub>3</sub>). They were obtained from a cross between *Ler* and one of the F<sub>3</sub> genotypes (parent of R6) of the first backcross of the RIL138 with *Ler* (the lines were derived from seven different heterozygous BC2F<sub>2</sub> plants selected from four different heterozygous BC2F<sub>1</sub> plants). The markers used for the genotyping of the lines are listed in chapter 2.3.2.

## **2.3 Molecular analysis: genotyping the NILs and recombinant plants**

### **2.3.1 DNA extraction**

Depending on the number of plants that needed to be genotyped, two different extraction methods were used: For the characterization of large segregating populations, the plant material was collected in boxes for 96 samples (collection micro tubes, racked 10x96, Quiagen, Hilden) and extracted with an DNA extraction robot (BioSprint 96, Quiagen) and



the Biosprint plant DNA extraction kit (Quiagen; according to the protocol). If only few samples were analyzed (for instance genotyping the F1 generation of crosses), the plant material was collected in Eppendorf reaction tubes and DNA extraction was performed, using the following protocol: The samples were frozen in liquid nitrogen and tungsten carbide beads (3 mm, Qiagen, Hilden) were added to the reaction tubes. Plant material was then ground by vortexing and dissolved in 400 µl of extraction buffer (0.1 M TrisHCl pH=8; 0.1 M NaCl; 0.05 M EDTA pH=8; 2% SDS) at 37°C. After centrifugation (10 min, 13000 rpm, room temperature - RT) the supernatant was mixed with an equal amount of isopropanol and incubated for at least 10 min at RT. After centrifugation (10 min, 13000 rpm, RT) the pellet was washed with 200 µl of 70% ethanol and air dried. The dry pellet was resuspended in 50 µl of 5 mM TrisHCl (pH=8, containing 10 µg/ml RNaseA).

### **2.3.2 Marker and marker design to reveal polymorphisms between *Ler* and *Kas-2***

Two different kinds of markers were used for the genotyping, simple sequence length polymorphism (SSLP) and Cleaved Amplified Polymorphic Sequences (CAPS) markers. SSLP marker amplified a length polymorphism between the genotypes and CAPS are based on the digestion at the position of a single nucleotide polymorphism between the genotypes. To genotype the plant material, SSLP marker were used that were described and applied for genotyping the mapping population (El-Lithy et al., 2006). Another source of SSLP markers was described in the INRA MSAT database (<http://www.inra.fr/internet/Produits/vast/msat.php>).

To obtain a higher density of molecular markers, especially on the bottom of chromosome five, new markers were designed in this study. Those markers (Table M4) were either based on allelic polymorphism information from the webdatabase Multiple SNP Query Tool (<http://msqt.weigelworld.org>) or from sequencing PCR products from *Ler* and the RIL138, respectively. Mainly intergenic regions and introns at the locus of interest were sequenced, since a higher density of allelic polymorphism is expected in those regions compared to exons. The primers were designed to be usually between 18 bp and 25 bp in length with an GC- content between 40% and 60%, one or two G/C-bp flanking the sequence and no hair pin or dimer formation that would affect the 3' end of the sequence. The program Gene Runner (Version 3.5, Hastings Software Inc., Las Vegas, NV) was used to predict the secondary structure of the primers. To assess the quality of the self-made markers, they were tested with DNA samples from *Ler*, RIL138 and heterozygous DNA

from a cross between those lines. This was necessary as annotated polymorphisms between *Ler* and *Kas-2*, according to the web-sources mentioned above, were not always reproducible in the *Ler/Kas-2* RIL population.

name	position in Mbp (chromosome)	forward primer (5'→3')	reverse primer (5'→3')	annealing temp. (in °C)	enzyme (if CAPS)	used for
lktop1.1	4.99 (1)	CAAATCATCCATATGGCAAAGC	CTAGAGCCTCCCACCATGAC	60		V
lkb05.1	10.1 (5)	GAAGAGAGATTTGTGTGGTG	GTTTGTCAAGGTATTTGGATG	55		V, FM1, FM2
lkb05.2	14.76 (5)	GGAACGGTATTGAGAATGAAC	CGTGGCAAATAATGGAGAG	55		FM1, FM2
lkb05.3	16.6 (5)	GATATCCCTGAAGCGAATG	GTATCGGTAGAAAACAAGCGAG	55		FM1
lkb05.4	17.57 (5)	CTGAGCATGTGTTAGTCCTG	CAAACACCACAACAATTCAC	50		V, FM1
lkb05.17	18.07 (5)	CGTTGCTTCGTTTGTATGGAC	GTTCCAGCAGATGGTTGTGTTT	60	Bsg1	FM1, FM2
lkb05.5	18.37 (5)	GCTGTTGATCCGGTAATCACTTG	CAAACCCTAGCACCGCGAAAG	65		FM1
lkb05.6	18.57 (5)	GAGGGTCTTTTATTATTCGC	CTTACCGACACAACCAGC	50		V, FM1
lkb05.22	19.5 (5)	GCACTCGGGACCTATTTG	CTGAATACAACGAAGAAAAC	50	BstU1	FM1, FM2
lkb05.18	20.02 (5)	GGTTTTACTTGAATGTTGGAG	GGAAATGAGATGTGTAECTAC	55	Mbo2	FM1, FM2
lkb05.16	20.41 (5)	GCAGAAACAACGCAGGAG	CCTTCGATTCCACTTCTC	55		FM1, FM2
lkb05.19	20.92 (5)	CCTTTTGTGTTTCTTTCTCTC	CCACAGAAAAACAAAAGAAGC	55	Mnl1	FM1, FM2
lkb05.15	21.32 (5)	CTCGTTTTCCCGCCATTTT	GCTCCACCGATCAAAATCTC	55	Hinf1	V, FM1, FM2
lkb05.20	21.88 (5)	CTTGAAATCCGTAAGTCTG	CAAAAGGAGAGGATGCAACC	55	Acc1	FM1, FM2
lkb05.21	22.02 (5)	CTGATGTTGGTCTTTGAAATGTGG	GTTTCCGTCTCCTGCGTTTCG	60	Rsa1	FM1, FM2
CNGC4_11	22.03 (5)	GGCCATTGAAAGTACTAACG	GAATGATCCTTCACTTTCCA	55	Rsa1	FM1, FM2
lkb05.8	22.4 (5)	CTCAATCTCGATCCTACACC	CTCTCTCTTCTGCTTATACTG	55		V, FM1, FM2
lkb05.24	22.63 (5)	GGTTGCTAAGAAGGGACG	CTTCCATATCCCGAGTCTG	55	Dde1	FM2
MUL3-1	23.1 (5)*	ACGGATTGTTCAAGAAAGGAG	CCAAAGTTCAAACCGAATAATC	50	Hpy81	V, FM1, FM2
236B	23.6 (5)	CCGAGGAATGAACGTGTATC	GCTTTACGAGGACTAGAGACTAG	55	FnuH1	FM2
mxk3-5	25.99 (5)*	TGTCTTGTCTCACTATTTCTC	TAACAAGGCCATATAACTG	55	Hpy188I	FM1, FM2
MAF34	26.01 (5)*	ATTCATCATTACACTTGCCT	TGACTTATCATTTGTCCGG	55		FM2
K21L13	26.23 (5)*	GAATCTGTTGGTTGCTGAC	CCGATGAAGATGGAACAG	55	Mse1	FM2
lkb05.29	26.44 (5)	GGAAAGAGCACAGATAGCAG	GTTATACTCATCCATGAAGTAGTC	55	Fnu4H1	FM2
lkb05.25	26.44 (5)	GATAGACAAAGGAGGAATGC	CTCCTCAACATCTGATCTGC	55	Fnu4H1	FM2
Rab18A	26.54 (5)	GTTCCACAGTGGACGAGAGG	GCTCGGTACGTATCAAGTG	55	BspE1	FM2

**Table M4: Self designed markers**

The table lists the marker name and position, primer sequence and the annealing temperature of the primers. In the case of a CAPS marker, the respective enzyme used for the digest is listed. In addition, the lines that were genotyped with the respective marker are indicated: The NILs used for the validation (V; Figure R3b), the recombinant lines R1 to R8 form the first fine mapping (FM1; Figure R13b) and the lines R9 to R20 from the second fine mapping experiments (FM2; Figure R14b); \* the marker MUL3-1, mxk3-5, MAF34 and K2113 were designed by Dr. Bjorn Pieper (Pieper, 2009)

The markers used for genotyping the selected lines are presented in Table M4, in addition the following markers were used: For the NILs (see Figure R3b for genotypes): nga59, m1.10, CIW12, nga6, nga76, SO191, nga129, Jv61/62, F15L12, mbk5, K8A10; For the

recombinant lines R1 to R8 (Figure R13b): SO262, m5.22, SO191, nga129, K7B16, MDF20, F15L12, mbk5, m5.17, K8A10; For the recombinant lines R9 to R20 (Figure R14b): nga129, K7B16, MDF20, F15L12, mbk5, m5.17, K8A10.

### 2.3.3 PCR reactions

The PCR reactions were generally performed with 2  $\mu$ l DNA sample and 18  $\mu$ l reaction mix that contained:

12.72 $\mu$ l	water	(LiChrosolv; Merck)
2 $\mu$ l	buffer	(10x Standard buffer; Amplicon)
1.2 $\mu$ l	dNTPs	(1 mM; Roche)
1 $\mu$ l	of each Primer	(10 $\mu$ M; Sigma)
0.08 $\mu$ l	Taq-Polymerase	(5 U/ $\mu$ l; Amplicon)

The PCR reactions were all conducted with a standard program with changing annealing temperatures (xx°C) according to the scheme:

Step one:	3 min	at 93°C
Step two:	15 sec	at 93°C
Step three:	45 sec	at xx°C
Step four:	1.5 min	at 72°C
Step five:	5 min	at 72°C
Step seven:	$\infty$	at 10° C

The steps two to four were repeated 35 times.

The PCR-thermocyclers labcycler (SensoQuest GmbH, Göttingen) and DNA Engine Dyad® Peltier Thermal Cycler (MJ Research, Waltham, MA) were used.

### 2.3.4 Digestion of CAPS markers

If the polymorphism underlying a marker is an SNP the PCR product amplifying this polymorphism needed to be digested with an enzyme with differential cutting sites at the position of the polymorphism. The digestion was done with 10  $\mu$ l PCR-product. 5  $\mu$ l of a digestion mix were added to the PCR-product, vortexed and incubated at the enzyme specific temperature over night. The digestion mix for ten reactions consisted of 35  $\mu$ l water (LiChrosolv, Merck, Darmstadt), 15  $\mu$ l buffer (10 x buffer specific for the enzyme

from Roche, Mannheim or New England Biolabs, Frankfurt am Main) and 0.5 µl enzyme (Roche or New England Biolabs).

### **2.3.5 Characterization of markers on agarose gel**

PCR- and digestion-products were mixed with loading buffer (10x Orange G loading buffer: 0.5% Orange G, 40% Sucrose, 10 mM TrisHCl with pH=8.5 in 10 ml water) and loaded on agarose (Universalagarose, Bio-Budget Technologies GmbH, Krefeld) gels with 0.03% ethidiumbromide (Roth, Karlsruhe) to separate the different PCR amplified fragments. The gels were run in TAE-buffer (40 mM Tris; 0.1% acetic acid; 1 mM EDTA at pH=8). Depending on the fragment size a 1 kb marker (Invitrogen, Darmstadt) or a low range DNA ladder (Gene Ruler, Fermentas, St. Leon-Rot) was used to assess the PCR product size. Pictures were taken on an UV-screen with a digital camera (Gel Photodokumentationsanlage, INTAS, Göttingen) and the software INTAS GDS Windows.

### **2.3.6 Sequencing**

Prior to sequencing, PCR products were loaded on a gel (as described in 2.3.5) to verify that only one amplicon was produced. 80 µl of the PCR products were cleaned according to the protocol of the QIAquick PCR purification kit (Quiagen). The concentration of these samples was determined (Nanodrop, ND-1000 Spectrophotometer, peqlab Biotechnologies GmbH, Erlangen) and adjusted to the requirements for sequencing of the in house service group. DNA sequences were determined by the Max Planck Institute for Plant Breeding Research (MPIZ) DNA core facility on Applied Biosystems (Weiterstadt, Germany) Abi Prism 377, 3100 and 3730 sequencers using BigDye-terminator v3.1 chemistry. Premixed reagents distributed by Applied Biosystems

To compare the sequencing results of the different genotypes, the sequences were aligned with the program Seqman (Lasergene Seqman, version 7.0.0, DNASTar Inc., Madison, WI).

### **2.3.7 Allelic comparison of the TPK1-gene**

The genomic loci of the TPK1-gene of *Ler* and of the RIL138 were sequenced using the four overlapping primer combinations listed in table M5. Each PCR product was sequenced (see 2.3.6) with the forward and the reverse primer. The PCR-reaction and

sequencing of the coding regions was done two times (and both individual replicate revealed the same polymorphisms).

The predicted coding regions (gene model At5g55630.1, TAIR 9) of *Ler* and RIL138 as well as of the Col-0 reference sequence from TAIR were translated and aligned with the software MegAlign (Lasergene Seqman, version 7.0.0, DNASTar Inc.).

PCR product	forward primer	reverse primer	annealing temperature
No. 1	GAATTGGCCAACACTGTGAGAAC	GAAATCTTGAGCCATGGTATC	55°C
No. 2	GCCATTGTTACCCACTGAGA	GCCAACAATGAAGAGGACTACA	55°C
No. 3	GCTCGTTAGGGCTTTCCAT	CGAACTCATCCATTATCCCAG	55°C
No. 4	GAAAGAAATGGGTAAGATTGATG	CGAGAAACGACGACTTCC	55°C

**Table M5: Primer combinations for sequencing of the TPK1-loci**

The primer sequences and annealing temperatures for the four PCR products that were used to sequence the TPK1-gene are listed.

## 2.4 Trait quantification for validation and the characterization of the QTL

### 2.4.1 Quantification of growth related traits

Growth related traits, as rosette weight, root weight and root length were quantified 32 days after the transfer of the seeds to the light, or after 23 days in case of the long day experiment. To measure the weight of the rosettes and roots a computerized balance (Pioneer, OHAUS, Pine Brook, NJ) coupled with OHAUS collect 6.1 software (Labtronics Inc., Ontario) was used. For the quantification of the root length the total length of the root system of individual plants was measured. The roots were dried quickly with tissue paper to remove the surrounding nutrient solution before weighting. After the measurement of 32 days old plants, rosette and root materials were frozen in liquid nitrogen and stored at -80°C for RNA extraction (2.4.5) or freeze dried (Christ, Alpha1-4 LSC). To obtain the dry weight of the plant material, the freeze dried rosettes and roots were weighted.

To determine relative growth rate (RGR) pictures of the plants were taken with a digital camera (Sony Cyber-shot DSC-F828) fixed to a tripod. The projected leaf area was determined at 12, 15, 19, 23 and 26 days after the transfer for the test of the lines RIL135 and *Ler*, for the QTL analysis measurements at day 7, 10, 15, 17, 20, 22 had been performed. To obtain the leaf area in cm<sup>2</sup> the pictures were analysed with the software Image Pro Analyser 6.0 (Mediacybernetics Inc., Bethesda, MD). The growth rate of each plant was calculated as the logarithm of the rosette area over time (in days<sup>-1</sup>). Quantification of nine replicates of one genotype allowed the calculation of a standard error for the RGR.

In the QTL analysis the rosette leaf number had been scored at day 22 and 32.

The response of a growth related trait was calculated as the change of the trait in percent, of plants grown in a reduced nutrient supply media compared to the control media (2.1.1) with the formula:

$$(\text{trait value}_{\text{control}} - \text{trait value}_{\text{reduced mineral supply}}) / \text{trait value}_{\text{control}}$$

To estimate the stomata density, prints of the abaxial side of the first or second leaf were taken by applying a thin layer of nail polish (clear Maybelin NY express finish). Once the polish was dried (1 min), the leaves were pressed on a clear sticky tape (Tesa crystal clear, Hamburg) and the imprint of the abaxial epidermis stripped off and fixed to a microscope object slide (VWR International GmbH, Darmstadt). The pictures were taken under a 200 times magnification with a Leica microscope (Axioplan2, Carl Zeiss MicroImaging GmbH, Köln) and acquired via a digital camera (DFC 490, Leica Mikrosysteme Vertrieb GmbH, Wetzlar) with the software Leica application suite (Version 2.5.0R1, Leica Mikrosysteme Vertrieb GmbH). Per line and condition the stomata density on  $0.04 \text{ mm}^2$  was determined of three leaves from three plants (9 to 10 counts per line and condition).

Root tips of ca 5 cm length of the primary and lateral roots were cut off and placed in nutrient solution on a microscope object slide. Pictures were taken (using the same camera equipment as mentioned above) of the very root tip and the area with the longest root hairs (ca. 2 cm to 3 cm from the tip).

#### **2.4.2 Quantification of physiological traits: Water loss**

To determine the water loss of the plants, the first or second leaf was detached and the weight determined. Each leaf was placed on a filter paper, kept at room temperature and weighted approximately every 10 min. The balance OHAUS Pioneer coupled with the software OHAUS collect (see 2.4.1) allowed obtaining the exact time point of each measurement. For each plant leaf the weight loss, which equates the water loss, was plotted against the time. The water loss in the first 150 min followed a logarithmic pattern. The logarithm of the weight loss (in %) was then plotted against the time and the rate of water loss was expressed as the slope calculated from this relationship. Between three and eight replicates per genotype and condition were used to calculate a water loss and standard error. The averages of four experiments were combined.

### 2.4.3 Quantification of Biochemical traits

#### 2.4.3.1 Total hexose, protein and chlorophyll extraction

For the QTL detection the leaves had been analyzed for hexose-, protein- and chlorophyll-contents. 300 to 500 mg fresh leaf material was ground and the cell debris was washed three times with 500 µl of 80% ethanol, heated at 80°C for 10 min, to extract sugars and chlorophylls. Half of the extracted sample was kept on ice in opaque 2 ml microtubes (Sigma-Aldrich, Taufkirchen) and a colorimetric analysis (at 646 nm, 663 nm and 750 nm) was performed to calculate the amount of chlorophyll a and b (Chl a, b; Porra, 2002):

$$\text{Chl a} = (12.5 * (\text{OD}_{663} - \text{OD}_{750}) - 2.55 * (\text{OD}_{646} - \text{OD}_{750}))$$

$$\text{Chl b} = (20.5 * (\text{OD}_{646} - \text{OD}_{750}) - 4.91 * (\text{OD}_{663} - \text{OD}_{750}))$$

The amount of chlorophyll was divided by the quantity of used fresh weight and the volume of extract used for the colorimetric analysis. The other half of the sample (750 µl) was dried over night in a rotary evaporator. The pellet was dissolved in 500 µl of deionised water and total hexoses were quantified according to Viola and Davies (1992). For the protein extraction 300 to 500 mg crushed, fresh leaf material was washed three times with 300 µl of 0.1M TrisHCl/ 0.1% Triton X100 pH=7 by vortexing it for 10 min. Protein quantification was done in 96 well microtiter plates using Coomassie Plus Protein Assay Reagen (Thermo Scientific Inc., Wermelskirchen).

#### 2.4.3.2 Ionic quantification

The freeze dried samples were crushed with glas beads (425 - 600 µm, acid washed, Sigma-Aldrich) on a mixer mill (MM300, Retsch, Haan). Between 2 to 5 mg of the crushed plant material was sent for the analysis. Ion quantification was performed by Prof. Dr. David E. Salt (Purdue University, West Lafayette, USA). The lyophilized tissue were placed into 100 x 16 mm Pyrex tubes and digested with 700 µl of concentrated HNO<sub>3</sub> (Mallinckrodt, AR Select grade) at 110°C for 4 hours. Each sample was diluted to 6 ml with 18 MΩ water and analyzed on a PerkinElmer Elan DRCe ICP-MS. Indium (EM Science) was used as an internal standard. National Institute of Standards and Technology traceable calibration standards (ULTRAScientific) were used for the calibration.

Plant material from four and two experiments for rosette and root materials, respectively, was used for the ionomic quantification of the NIL3 and *Ler*. Three samples per line and condition were quantified with each sample containing on average the root material of three plants or the rosette material of four plants.

For the QTL analysis three samples per line and condition had been analysed of the root and rosette, respectively. Each sample contained pooled material of in average two or three plants.

#### **2.4.4 Transcription analysis**

The effect of the presence of Kas-2 alleles at the studied QTL on gene expression level on a genome wide scale was analysed using Affymetrix microarrays (Fremont, CA). Three replicates (from independent experiments) per line (*R5*, *Ler*) and per condition (control, reduced potassium) were hybridized on arrays. Equal amounts of leaf material pooled from at least three plants per line and condition were used for each experimental replicate. The plant material was ground in liquid nitrogen with a cordless motor (Kontes, Gerresheimer) and 1.5 ml Pellet Pestles (Kontes, Gerresheimer) in RNase-free 1.5 ml microfuge tubes (Ambion, Darmstadt). Total RNA was extracted using the RNeasy plant mini kit (Quiagen) according to the manual. The RNA quality was controlled on the basis of the 18S/26S rRNA ratio determined with Bio Analyzer (Agilent Technologies). Transcriptomes were analyzed using 1 µg of total RNA as starting material. Targets were prepared with MessageAmpII-Biotin Enhanced Single Round aRNA Amplification Kit (Ambion) and hybridized to ATH1 gene chips (Affymetrix) for 16 hours as recommended by the supplier (Gene expression analysis manual, Affymetrix). Chips were read out with the Gene chip scanner 7G (Affymetrix). RNA quality control and all subsequent steps were performed by Dr. Bruno Hüttl (Affymetrix Service, Max Planck Institute for Plant Breeding Research, Cologne).



## 2.5 Statistical analysis

### 2.5.1 QTL detection

For each trait, the values per RIL were averaged and a QTL analysis was performed with MapQTL 5.0 (Van Ooijen, J.W., 2004 MapQTL®5, Software for the mapping of quantitative trait loci in experimental populations. Kyazma B.V., Wageningen, Netherlands) using the MQM procedure. Incompatible lines (Alcázar et al., 2009) were removed from the QTL analysis in order to avoid confusion of effects on growth-related traits. A permutation test using 1000 permutations of the original data resulted in a genome wide 95% LOD threshold of ~2.4 for every trait. Markers, used as cofactors, have been chosen by backward selection. For each detected QTL, a marker near the QTL was used as a cofactor in the final model.

### 2.5.2 The Gaussian error propagation

A standard error of the response was estimated by using the Gaussian error propagation (Tipler and Mosca, 2004). If a value Y is derived from several values  $X_1$  to  $X_m$ , each with

an error  $\Delta X_i = \sqrt{\left(\frac{1}{n} \sum_{i=1}^n (X_i - \bar{X})\right)}$ , the error for Y is  $\Delta Y = \sqrt{\sum_{j=1}^m \left(\left(\frac{dY}{dX_j}\right) \Delta X_j\right)^2}$ .  $dY/dX_j$  is

the differentiation of the value Y for the value  $X_j$ . For the response the calculation would

be as follows:  $sterr_{response} = \sqrt{\left(\left(\frac{100}{C}\right) dR\right)^2 + \left(\left(\frac{-R \cdot 100}{C^2}\right) dC\right)^2}$ , where C is the trait value

in the control and R the trait value in the reduced nutrient supply. dC and dR are the respective standard errors of the traits in the two conditions.

### 2.5.3 Significance tests

A Student-Newman-Keuls test (SNK) was used to test the significant difference of the responses of *Ler*, RIL138, the NILs or the recombinant lines (using SPSS 13.0 for Windows, SPSS GmbH Software, München).

For the ionic comparison and the water loss between the NIL3 and *Ler* the significance was tested by an ANOVA (univariate linear model; using SPSS 13.0 for Windows).

#### **2.5.4 Statistical analysis of the microarray data**

The data analysis was performed by Dr. Ulrike Göbel (Bioinformatics Service, Max Planck Institute for Plant Breeding Research, Cologne) using an R-script based on the rank product method of Breitling et al (2004). Prior to analysis, the expression values were normalized by the RMA procedure (Irizarry et al., 2003) as implemented in the Affymetrix package (Gautier et al., 2004). The assignment of ATH1 probe IDs to genes was done using the ath1121501.db package (TAIR version April 2009). The chip quality was assessed according to affyQCReport (Parman and Halling 2009, affyQCR Report; [www.bioconductor.org](http://www.bioconductor.org)).

### 3. Results

#### 3.1 QTL mapping in different nutritional regimes (by Dr. Barbier and Dr. Reymond) (Published in Prinzenberg et al., 2010 after thesis submission)

To detect genetic regions that are involved in growth related traits in different nutritional regimes, Dr. Barbier and Dr. Reymond performed a QTL analysis in three environmental conditions: A control medium with a standard level of nutrients for plant cultivation; a medium that was reduced in potassium supply by 3.3-fold and a medium reduced in phosphate supply by 4.1 times. 125 lines from a *Ler/Kas-2* RIL population (El-Lithy et al., 2006) were grown with nine replicates in all three conditions. To apply the different mineral nutrient regimes a hydroponic system was used similar to the one described in Toquin et al. (2003). Growth related traits (rosette weight, relative growth rate, root weight, root length and leaf number) were quantified after 32 days of growth in the respective nutrient regime. In addition, biochemical traits (e.g. total protein and hexose content) and ion contents of several mineral nutrients and trace elements in the rosette and root were quantified for all lines of the mapping population. With these data sets, a QTL analysis was performed for each trait in each condition but also for the response (percentage of change between the trait in the control and in one of the reduced mineral supplies) of each trait to the low potassium or phosphate regime. For all the quantified traits QTL were detected, some were constitutive and some were specific to one or two growth conditions. The QTL analysis (Table A1 in the appendix) revealed the presence of in total 333 QTL for all conditions and 48 QTL for the response of the measured traits to potassium or phosphate (Figure R1). The QTL detected in a single growth condition (control, lowered potassium supply or lowered phosphate supply) usually explained between 2% and 30% of the overall trait value, just four QTL (one for sodium and three for molybdenum content) explained from 38.3% up to 62.1% of the trait variation. The response QTL explained between 6.1% and 22.1% (with the exception for rosette molybdenum content in response to the lowered phosphate supply which explained 40.9%). Response QTL were detected for rosette weight, relative growth rate (RGR), root length and most ion contents. There was no apparent clustering of the response QTL, they were detected all over the genome. The highest amount of co-localizing response QTL was on the bottom of chromosome five with ten response QTL (Figure R1).

Response QTL reflect the answers of a plant to changing environmental conditions. Their allelic values influence a trait differentially in different growing conditions. In the QTL detection these different conditions comprise the three mineral nutrient media. The response QTL should therefore highlight genetic regions that have differential effects on plant growth in control media and in a reduced potassium or phosphate supply and may be involved in adaptation to the changing mineral nutrient supply.

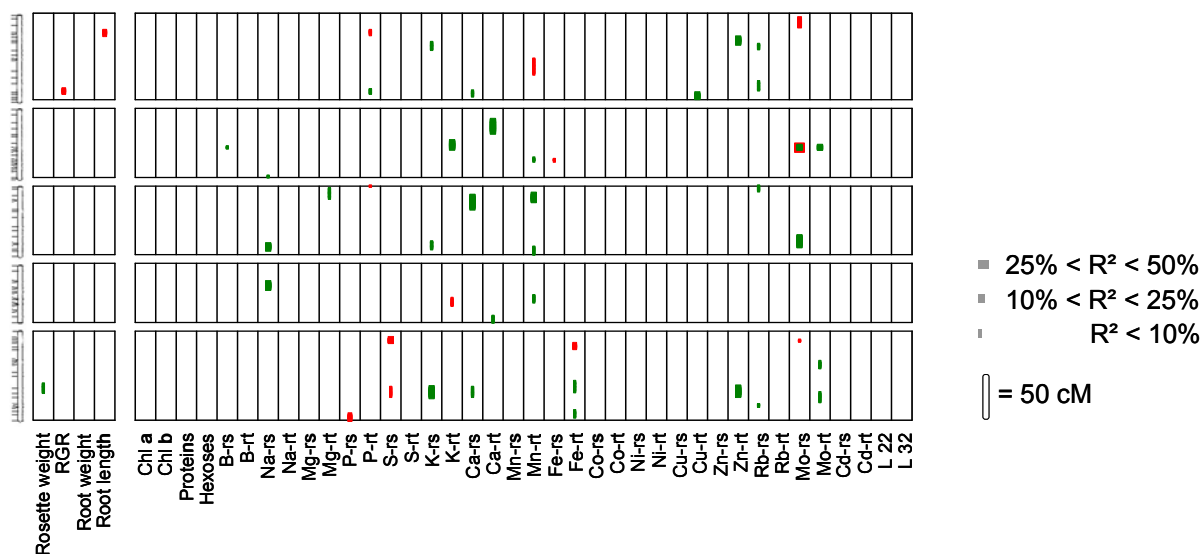


**Figure R1: Response QTL to reduced potassium and reduced phosphate supply (Dr. Barbier and Dr. Reymond)**

The five chromosomes of *Arabidopsis thaliana* (marker are indicated by ticks) are represented as bars (Chr. one to five from the top to the bottom) on the left of the figure. The response QTL for each trait are indicated by colored boxes (red for QTL detected in response to reduced phosphate supply and green for QTL detected in response to reduced potassium supply). The thickness of the boxes indicates the  $R^2$  (see legend). The measured traits are rosette weight, relative growth rate (RGR), root weight, root length, chlorophyll a and b content (Chl a, Chl b), total protein and hexose content, ion contents in the rosette (-rs) and in the root (-rt) and the leaf number at day 22 and day 32 (L22, L32).

### 3.2 Validation of growth response QTL for lowered potassium and phosphate supply

According to the QTL analysis (Figure R1), three response QTL were detected in the *Ler/Kas-2* RIL population that affect the growth related traits: One for rosette weight in response to reduced potassium supply and two in response to reduced phosphate supply, for relative growth rate of the rosette and for root length. A way to validate biologically the effect of a detected QTL is to observe contrasting phenotypes in near isogenic lines (NILs) or heterozygous inbred family (HIF) lines. Therefore, RILs were selected according to their genotype that were appropriate starting material to construct NILs. The selected lines had a mainly *Ler* or *Kas-2* allelic background. At the locus of the QTL they contained

alleles different from the respective allelic background (as well as on some other loci; Figure R2b). If the QTL effect can be validated, these RILs should have a different response compared to *Ler* or Kas-2 (depending on the allelic background of the RIL). To phenotype the RILs and the two parental accessions, the lines were grown in the same hydroponic system which was used for the mapping experiment (3.1). The respective trait value (rosette weight, RGR or root length) was determined for the plants grown in the control condition and in either the lower potassium or the lower phosphate supply, depending on the QTL effect that was under investigation. Further, the response was calculated as the trait change in percent between the control and the lowered nutrient condition. The rosette weight response QTL for lowered potassium supply is located on the bottom of chromosome five (marker snp97, 68.3 cM/ 17.2 Mbp) and it explained 9.3% of the trait variation. According to the QTL detection, the additive effect (that predicts the trait difference between the two allelic values) was 14% and the *Ler* allele conferred the more positive rosette weight response (Table A1). For the rosette weight response QTL, the line RIL138 was selected for confirmation of the QTL effect. RIL138 contains only two Kas-2 introgressions, one on the top of chromosome one and one on the bottom of chromosome five, in an otherwise *Ler* genetic background. Being Kas-2 at the bottom of chromosome five, the RIL138 should therefore have a 14% lower response of rosette weight to the reduced potassium supply than *Ler*. Although, *Ler* and the RIL138 did not show significantly different responses, the RIL138 had a 4.5% lower response than *Ler* (Figure R2). The phosphate response QTL on chromosome one is located at the marker position snp177 (89.5 cM/ 26 Mbp). The QTL explains 14.6% of the variation in RGR response and conferred a 5% higher response for the *Ler* allele (Table A1). The line RIL135 differs from the parental line Kas-2 at the position snp177, which is the location of the RGR response QTL and at few other genetic positions. Therefore, the RIL135 was expected to have a 5% higher response in RGR but its response did not differ from Kas-2 (Figure R2). The last growth related response QTL, for root length in response to lowered phosphate supply, was also located on chromosome one but at the top, at the marker m1-10 (23.1 cM/ 7.3 Mbp). This response QTL explained 15.6% of the root length response and the *Ler* allele conferred a 8% higher response than the Kas-2 allele. RIL85, had an *Ler* allelic introgression on chromosome one in an otherwise mainly Kas-2 background. The *Ler* introgression on chromosome one included the marker M1-10. At this position, the QTL for root length response is located and this QTL should confer the 8% higher response of root length to the RIL85 compared to Kas-2. In contrast to these mapping

predictions, the root length response of the RIL85 was of opposite effect than that of Kas-2. The root length of Kas-2 decreased by 43%, while the root length of RIL85 increased by 3% (Figure R2). The effect of the RGR response QTL could not be established with the RIL135 and its validation was not pursued. The RIL85 showed a significant response difference compared to Kas-2. Nevertheless, the QTL was of minor interest to be pursued,

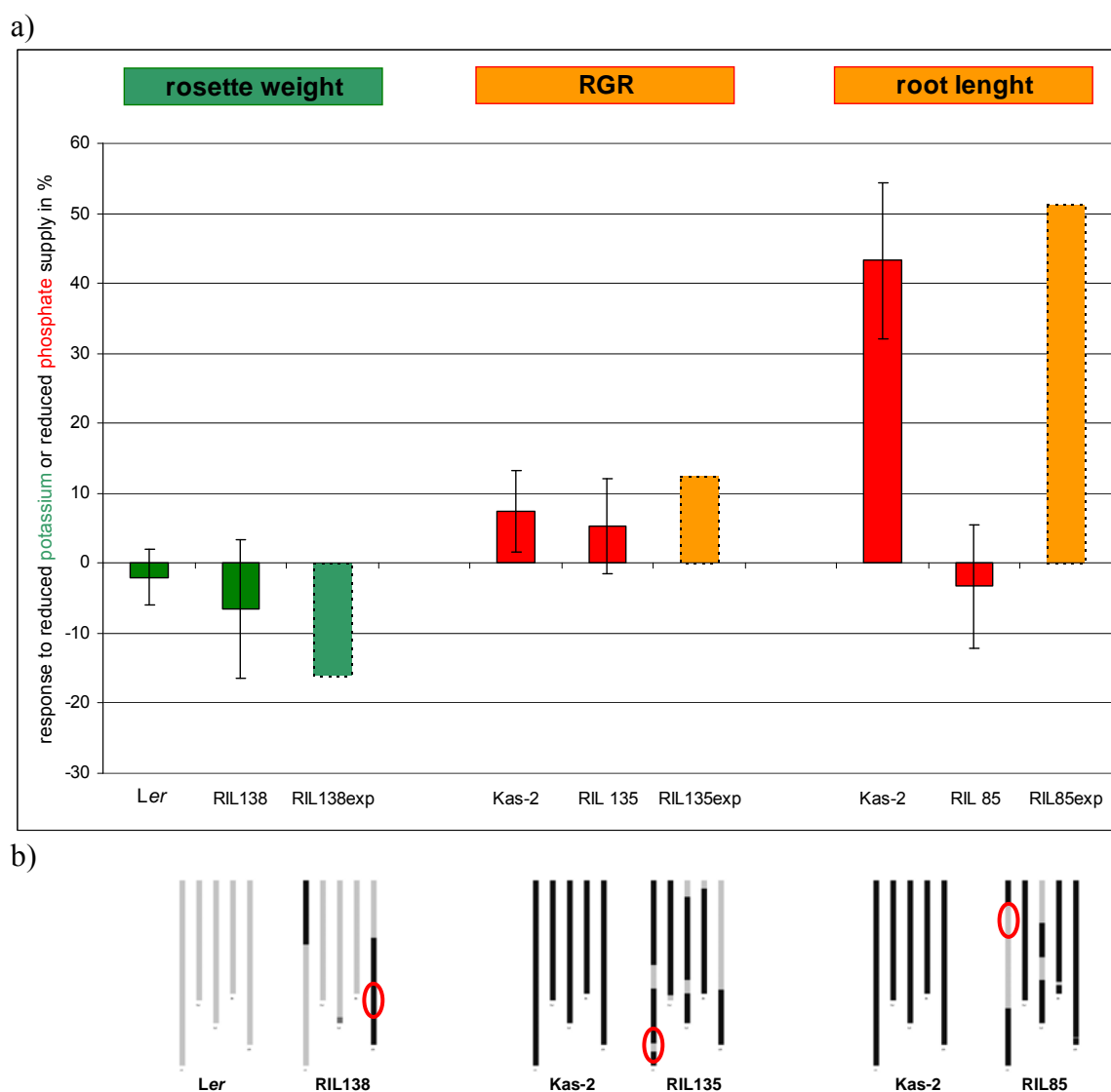
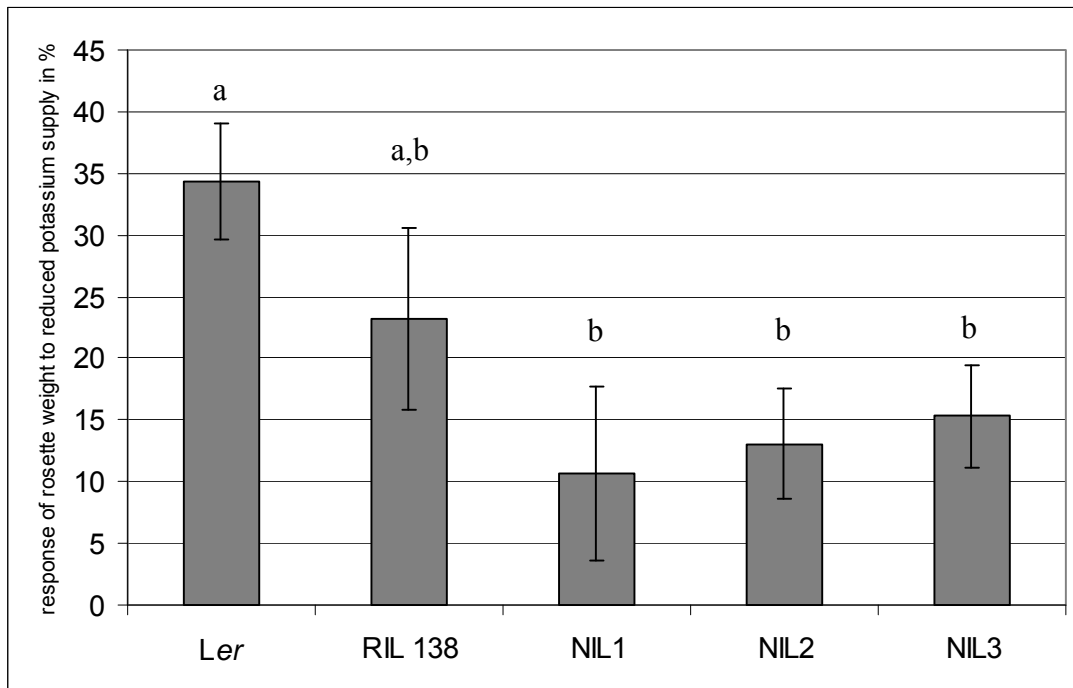


**Figure R2: RILs tested for response QTL effects**

The three RILs (138, 135 and 85) presented here were selected according to their genotype to examine the response QTL effect in comparison to another line with a different allelic value at the QTL position (indicated by a red circle in the schematic presentation of the genotype differences). The bar chart shows the response of the tested lines to reduced potassium (green) and phosphate (red) supply compared to plants of the same genotype grown in a control media (a). The growth related traits tested are rosette weight in response to reduced potassium and relative growth rate (RGR) and root length in response to reduced phosphate. The lighter-colored, dashed bars represent the response value of the RILs that would be expected according to the QTL mapping when compared to the parental line (RIL138exp, RIL135exp and RIL85exp). Beneath the bar chart are the schematic presentations of the genotypes of the compared lines (the red circle highlights the position of the respective QTL).

as its basis is likely to be known already. Svistoonoff et al. (2007) identified the gene LPR1 as the genetic basis for a QTL for primary root growth arrest in response to phosphate starvation that co-localizes with the described root length response QTL. The RIL138 did not differ significantly from *Ler* in its response of rosette weight but there was a convincing tendency for the right effect. Furthermore, the potassium response QTL on bottom chromosome five was not described before. Taken together, the RIL138 was an appropriate line to construct NILs for validation. In order to build NILs, the line RIL138 was backcrossed to *Ler* and NILs were selected in the 2<sup>nd</sup> generation of the backcross (BC1F2). The NILs have a *Ler* genome, except for a Kas-2 introgression that comprises the lower half of the chromosome five (from the marker *lkbot5.1* at 10.1 Mbp to the bottom; Figure R3b). The NILs one and two contain a small heterozygous introgression on top of this region (at the marker *lkbot5.1*). *Ler* and the NILs were grown in the hydroponic system in a control medium and a reduced potassium supply medium. The potassium content of the reduced potassium medium was further decreased compared to the mapping experiment (see 3.3.1.1). The NILs rosette weight responses to the reduced potassium supply were between 10.7%  $\pm$ 7% and 15.3%  $\pm$ 4.1% while *Ler* responds with an effect of 34.3%  $\pm$ 4.8% (Figure R3a). These values are averages of the response of the lines in three independent experiments. The NILs rosette weight responds far less to the applied low potassium regime than *Ler* but also less than the one of RIL138 (23.3%  $\pm$ 7.4%; Figure R3a). According to a Student-Newman-Keuls test the responses of *Ler* and the NILs can be divided into two groups, with a likelihood of 95% (Figure R3a).

a)



b)

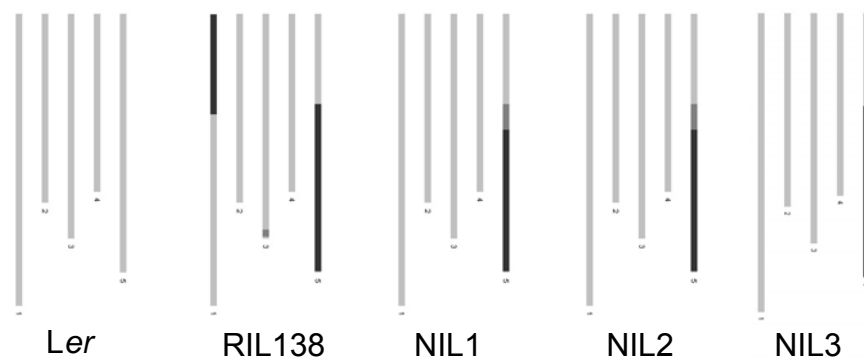


**Figure R3: The responses of *Ler*, the RIL138 and the selected NILs to reduced potassium supply**

*Ler*, the RIL138 and the three NILs that were derived from a cross between *Ler* and the RIL138, were grown in control media and in 20-fold reduced potassium supply. The response of the rosette weight to the two different conditions was calculated as a change in percent (a). The data was derived from an average of three independent experiments and the letters indicate the two different groups (a,b) identified by the Student- Newman-Keuls test (95% confidence interval). The genotypes of the lines are indicated below (b) with *Ler* alleles in light grey, Kas-2 alleles in black and heterozygous alleles in dark grey.



### **3.3 Characterization of the validated, potassium-responsive QTL on bottom chromosome five**

#### **3.3.1 Different applied growth conditions**

##### **3.3.1.1 Different levels of potassium reduction do not affect the QTL**

The initial phenotyping of the RIL138, in the conditions used for QTL mapping, revealed a tendency for a rosette weight response that was in accordance with the response QTL on bottom chromosome five. To validate the QTL and to fine map it, the difference in response between *Ler* and the RIL needed to be increased. One hypothesised possibility to increase that response difference, was to increase the level of potassium reduction in the solution and thereby the stress. This may trigger increased differences between the growth responses of *Ler* and the RIL138.

In the mapping experiment the potassium concentration was 3.3-fold lower in the reduced potassium supply (855.5  $\mu\text{M}$ ) than in the control (2855.5  $\mu\text{M}$ ). The solution was buffered with potassium hydroxide. To increase the potassium concentration, the buffer needed to be replaced by a buffer which pH was adjusted with sodium hydroxide. By these means the solutions potassium concentration could be reduced by 5 times (430.1  $\mu\text{M}$ ), 10 times (215.05  $\mu\text{M}$ ), 13 times (161.3  $\mu\text{M}$ ), 20 times (107.5  $\mu\text{M}$ ) and 40 times (53.8  $\mu\text{M}$ ) compared to the new control solution (2150.5  $\mu\text{M}$ ). In addition, a solution without potassium (0.5  $\mu\text{M}$  remained as counter-ion for iodide which could not be replaced) was used as a negative control. The plants grown in this solution without potassium died in the seedling stage. *Ler* and the RIL138 were grown in the different levels of low potassium supply and the responses were calculated (Figure R4). The data are from single experiments and the error is calculated from the variation of the line within one condition according to the Gaussian error propagation (Tipler and Mosca, 2004; see material and methods). Independent of the reduction in potassium supply, the response of *Ler* was always more positive than the one of RIL138. The response in the 3.3, 20 and 40 times reduced potassium media was clearly different between the lines. The difference in response was largest in the 3.3- and in the 20-fold reduction. The significant difference between the lines could be an experimental effect of this single experiment but the response difference proved to be reproducible for the 20-fold reduction in all subsequent experiments. The rosette weight decreased markedly in the 20-fold reduced potassium supply showing the significant impact of this growth condition on both genotypes. The

weight difference between the lines in each condition (a growth trait that was observed at this time instead of the response) was greater in the 20 times reduced potassium supply than in the 3.3 times. Furthermore, the variation of the fresh weight within one genotype was slightly lower in the 20-fold reduction than in the 3.3-fold reduction over several experiments (data not shown). Altogether, this led to the choice of the 20-fold reduced potassium condition for the further phenotyping of the lines.

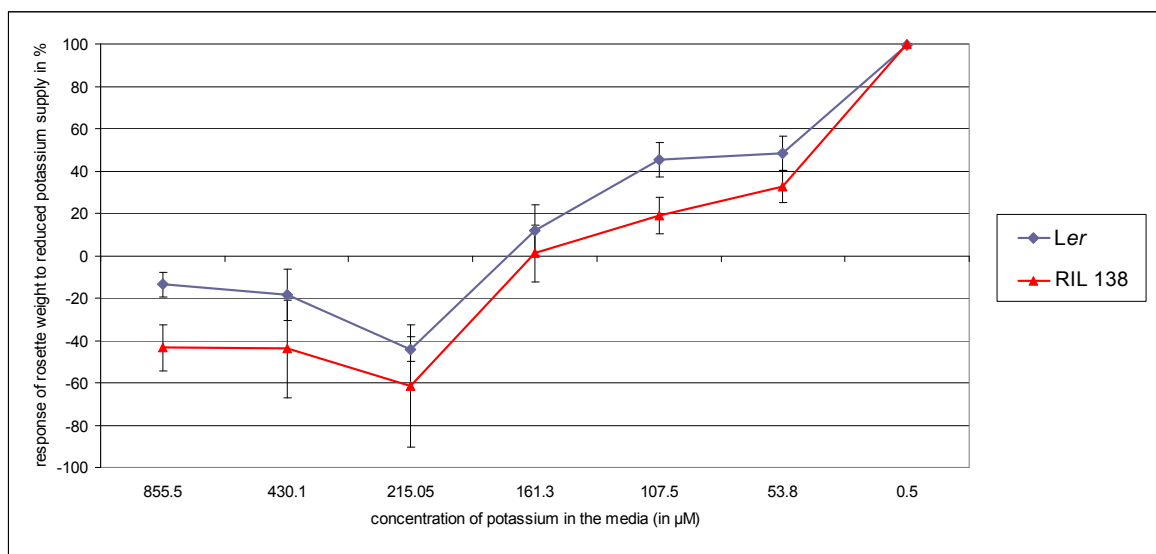


**Figure R4: Response of rosette weight to varying levels of potassium supply**

*Ler* and the RIL138 were grown in a control solution and in different levels of reduced potassium supply. The calculated responses for *Ler* (blue line) and the RIL138 (red line) are plotted against the corresponding potassium concentrations of the growth media. Standard errors are calculated by the Gaussian error propagation from one experiment.

### 3.3.1.2 Growth in different day length does not affect the QTL

The mapping experiment was performed in 8 hours light conditions to allow a maximum time span of vegetative growth and thereby prolong the time span in which the plant is exposed to the reduced potassium media. The onset of flowering time which was shown to interfere with growth related traits (Chen et al., 2009; Mendez-Vigo et al., 2010) was further avoided by the growth in short day. However, *Ler*, the RIL138 and the NIL3 were grown in long day conditions (14 hours light) to evaluate the effect on the rosette weight response. Some potassium transport proteins were shown to be regulated by light and photoassimilate dependent processes (Deeken et al., 2000; Dietrich et al., 2001) and the increased growth rate in the long day conditions (Cookson et al., 2007) might trigger a higher need for potassium. The rosette weight was measured 23 days after the transfer of

the plants to the long day growth cabinet, at this time point the plants started to bolt (the bolting occurred simultaneously for all lines in these conditions, while the NILs were delayed in flowering time on soil). The relative effect on rosette weight response to the 20-fold reduction in potassium concentration was similar in long days as in short days. *Ler* reduced its rosette weight by  $40.8\% \pm 7.6\%$ , while the RIL138 and the NIL3 reduced their rosette weight by  $23.3\% \pm 4.6\%$  and  $8.6\% \pm 8.6\%$ , respectively (Figure R5).

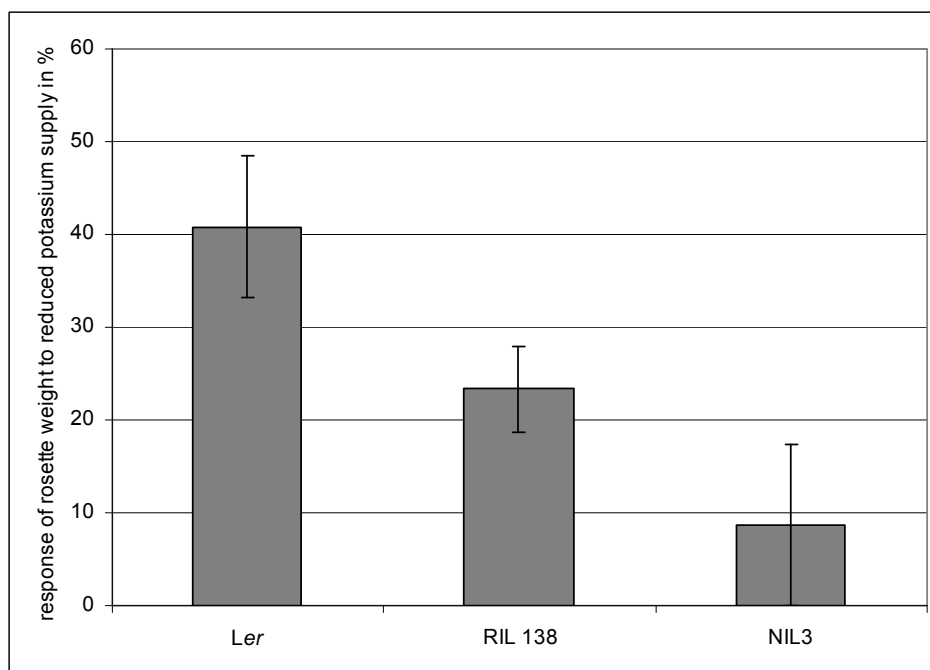


**Figure R5: Growth responses of *Ler*, RIL138 and NIL3 to reduced potassium supply in 14h light**  
The three different genotypes were grown in the control and the 20-fold reduced potassium media in long day conditions with 14 hours light. The response of rosette was calculated and standard errors were determined by the Gaussian error propagation from one experiment.

### 3.3.1.3 The QTL is ammonium sensitive

It was shown that the high affinity potassium uptake mechanism can be sensitive to ammonium (Hirsch et al., 1998; Spalding et al., 1999; Szczerba et al., 2008). Ammonium was absent from the solutions used for the mapping and the validation experiments. To test, if ammonium has an impact on the QTL effect, *Ler* and the three NILs were grown in control and 20-fold reduced potassium media with and without ammonium. One quarter of the nitrogen supply in the growth media was given as ammonium. This ammonium concentration is far from being toxic to the plant (Britto et al., 2001) and the plants looked healthy, in both control solutions (e.g. no signs of chlorosis; Walch-Liu et al., 2000). The rosette weight in the ammonium supplied control media was not negatively affected but

even increased. The NILs grown in the control with ammonium compared to the control without ammonium increased their rosette weight on average by  $39\% \pm 10\%$ , whereas *Ler* had the same rosette weight in the control conditions with and without ammonium. When the growth in the lower potassium supply without and with ammonium is compared, *Ler* had a slightly higher rosette weight ( $19\% \pm 16\%$ ) when ammonium was added to the solution. The NILs did not significantly change their rosette weight when ammonium was added to the reduced potassium supply media.

From those rosette weight measurements, the response to the reduced potassium regime was calculated for the lines grown without additional supply of ammonium (medium used for validation) and with ammonium (Figure R6). The addition of ammonium increased the response of the NILs rosette weight to reduced potassium supply drastically from on average  $6\% \pm 8\%$  to  $36\% \pm 5\%$  while in *Ler* the response decreased in tendency (from  $32\% \pm 9\%$  to  $19\% \pm 10\%$ ). The response QTL is clearly sensitive to ammonium.

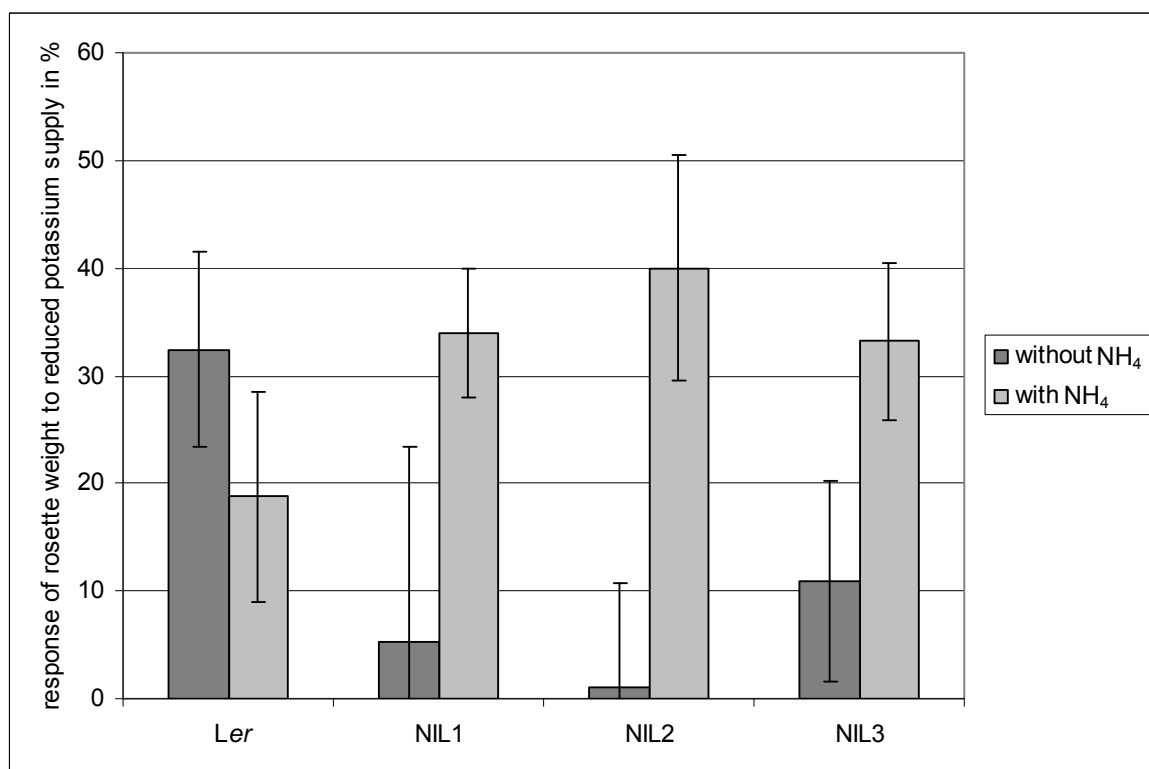


**Figure R6: Rosette weight response of *Ler* and the NILs without and with ammonium (NH<sub>4</sub>) in the nutrient media**

The four lines were grown in parallel experiments in control media and 20-fold reduced potassium media without and with ammonium and the response of the rosette weight was calculated. The data was derived from one experiment with five replicates per line and condition.

### 3.3.2 Characterization of additional growth related traits observed for the QTL

#### 3.3.2.1 The response of the rosette dry weight and fresh weight correspond

The validated QTL on bottom chromosome five affects the response of rosette weight to reduced potassium supply. To see, if this is due to a difference in biomatter or in osmotic pressure and thereby water content, the dry weight of the lines used for validation was calculated. *Ler* showed a higher rosette dry weight response of 27%  $\pm$ 9% than the NIL with 11%  $\pm$ 8%. The dry weight of the RIL138 and *Ler* was also determined for the different levels of potassium reduction that were tested in chapter 3.3.1.1. In all cases, the rosette dry weight response of *Ler* was more negative than the one of RIL138. This is the same trend that was observed for the rosette fresh weight response (3.3.1.1). *Ler* and the RIL138 showed a significant response difference to the 20-fold (40.1%  $\pm$ 8.7% vs. 16.4%  $\pm$ 9.4%) and the 40-fold (32.4%  $\pm$ 9.2% vs. 8.8%  $\pm$ 10.7%) potassium reduction. Furthermore, a correlation plot between the dry and fresh rosette weight response, over all tested potassium reductions, showed a very high correlation between the two traits (Figure R7). The dry weight response and the fresh weight response are highly similar which suggests that the QTL effect is caused by a biomass production rather than a water content change.

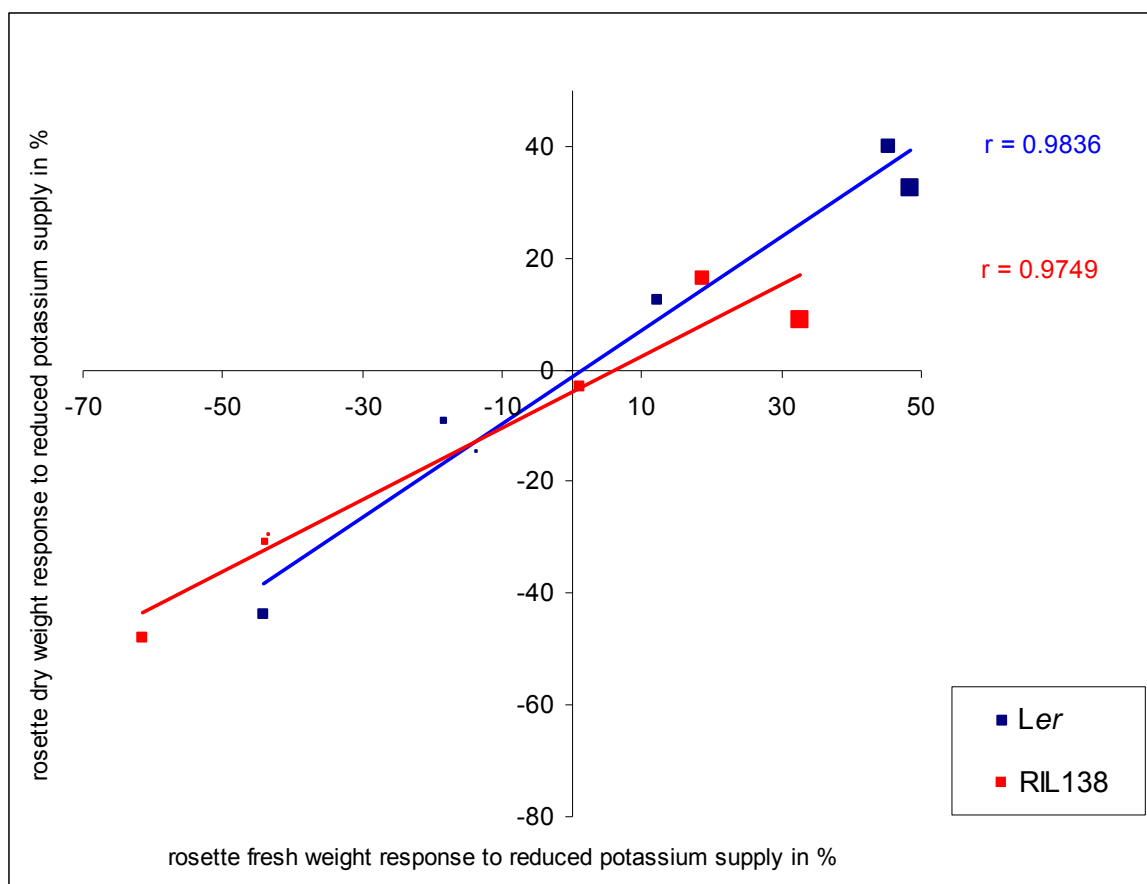


**Figure R7: Correlation between fresh and dry rosette weight response of *Ler* and RIL138**

*Ler* and the RIL138 were grown in a control solution and in different concentrations of potassium (see 3.2.1.1) and the responses of rosette fresh weight and dry weight were calculated. The responses of fresh weight and dry weight were plotted against each other. The level of potassium reduction is indicated by the size of the dots which increases with the increase in potassium reduction (smallest dot represents 3.3-fold and the largest 40-fold of potassium reduction, respectively). The Pearson correlation coefficient for each line is indicated ( $r$ ). Data were derived from one experiment.

### 3.3.2.2 Root growth effects of the QTL: the root weight response is similar to the rosette weight response

The root weight and the root length of *Ler* and the NIL3 were measured at 32 days in both the control and the reduced potassium supply and the responses to reduced potassium supply were determined. The root weight response is identical to the rosette weight response for both genotypes, the NIL3 reduced its root weight less compared to *Ler* (Figure R8). The root length was not significantly affected by the treatment and did not differ between the lines (Figure R8).

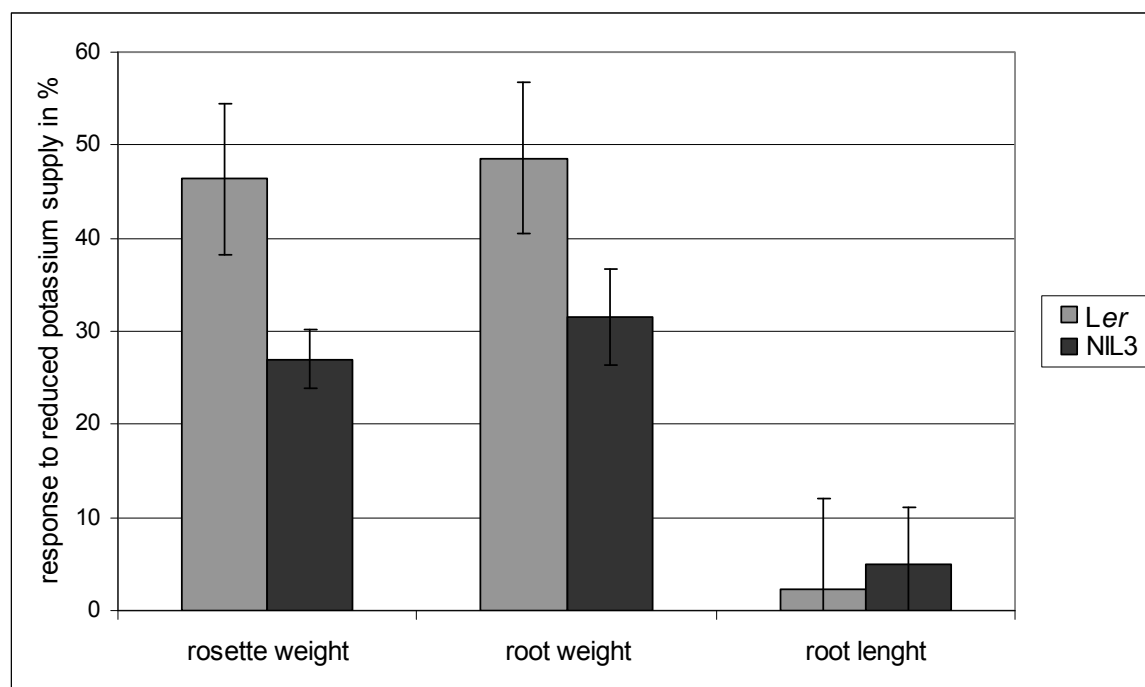


**Figure R8: Root growth responses corresponding to the rosette weight response of *Ler* and the NIL3 to potassium reduction**

The rosette weight and the root weight of *Ler* and the NIL3 was obtained from plants growing in control media and in 20-fold reduced potassium supply and the responses for rosette weight, root weight and root length was calculated. Only plants from which all three traits could be measured were used for the calculation, to be able to compare the responses to each other (reliable root data could not be obtained in all cases, as the roots of several plants can intertangle in the solution). The data was obtained from two independent experiments with three to eight replicates per line in each condition.

Root hairs are important for potassium uptake (Ahn et al., 2004) and some crops were shown to increase root hair length in response to low potassium supply (Rengel and Damon, 2008). For *A. thaliana* a considerable natural variation for root hair density and length was described (Narang et al., 2000) but not correlated with low potassium supply unless ammonium is present in the growth media (Amtmann et al., 2005). To assess if differences in root hair growth are associated with the QTL effect, the root tips were photographed under a microscope and the pictures of *Ler* and NIL3 compared to each other in both conditions. The root hairs did not show any obvious differences in length nor in density between the lines and the two conditions (Figure R9).

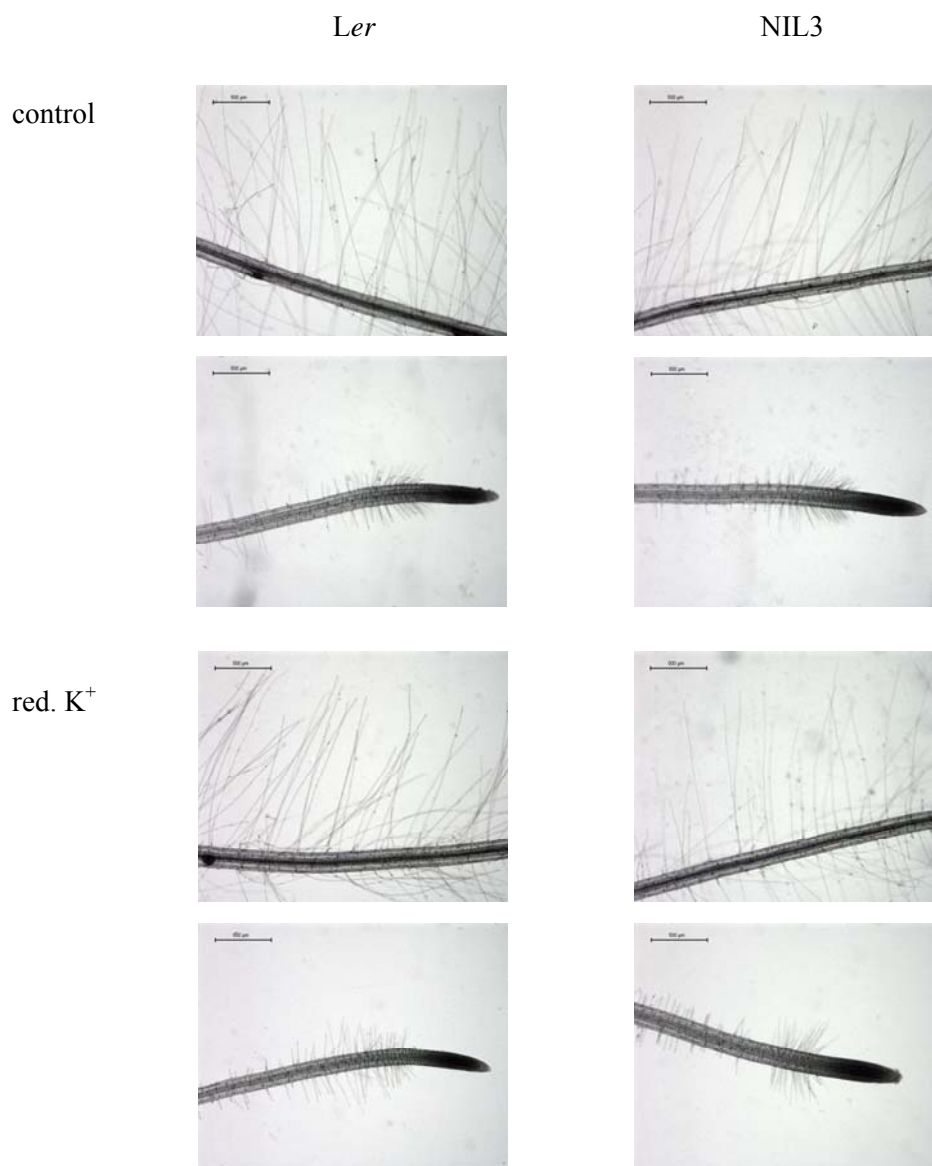


**Figure R9: Exemplary pictures of root hairs of *Ler* and the NIL3**

The pictures show the root tip and the root at the zones of maximal root hair length. Roots of *Ler* (on the left) and the NIL3 (on the right) are shown that were grown in the control and 20-fold reduced potassium supply (red. K<sup>+</sup>). The scale bars in the pictures represent a length of 500  $\mu\text{m}$ .

### 3.3.2.3 *Kas-2* alleles at the QTL are associated with a reduction of water loss

The water loss of *Ler* and the NIL3 was determined by assessing the weight loss of a detached leaf over time (Guo et al., 2003; Galpaz et al., 2008). The weight and thereby the water loss followed a logarithmic pattern for each leaf (Figure R10). The water loss of four to eight plants per genotype and condition was determined in four experiments. The slope of the logarithm of the weight loss over time (rate of water loss) was calculated for each leaf and an average per genotype, condition and experiment determined (bar chart in figure



R10). The change in the rate of water loss, the response, between the control and the reduced potassium supply was calculated with those values. There was no significant difference for this water loss response between *Ler* and the NIL3 (data not shown). However, the lines showed significant differences in the rate of water loss when grown in the control as well as 20-fold reduced potassium supply: The rate of water loss of *Ler* is always less than that of the NIL3 (bar chart in figure R10). The average water loss rate is less in the reduced potassium media for both lines, although, this difference is only significant for *Ler* (p-value=0.02).

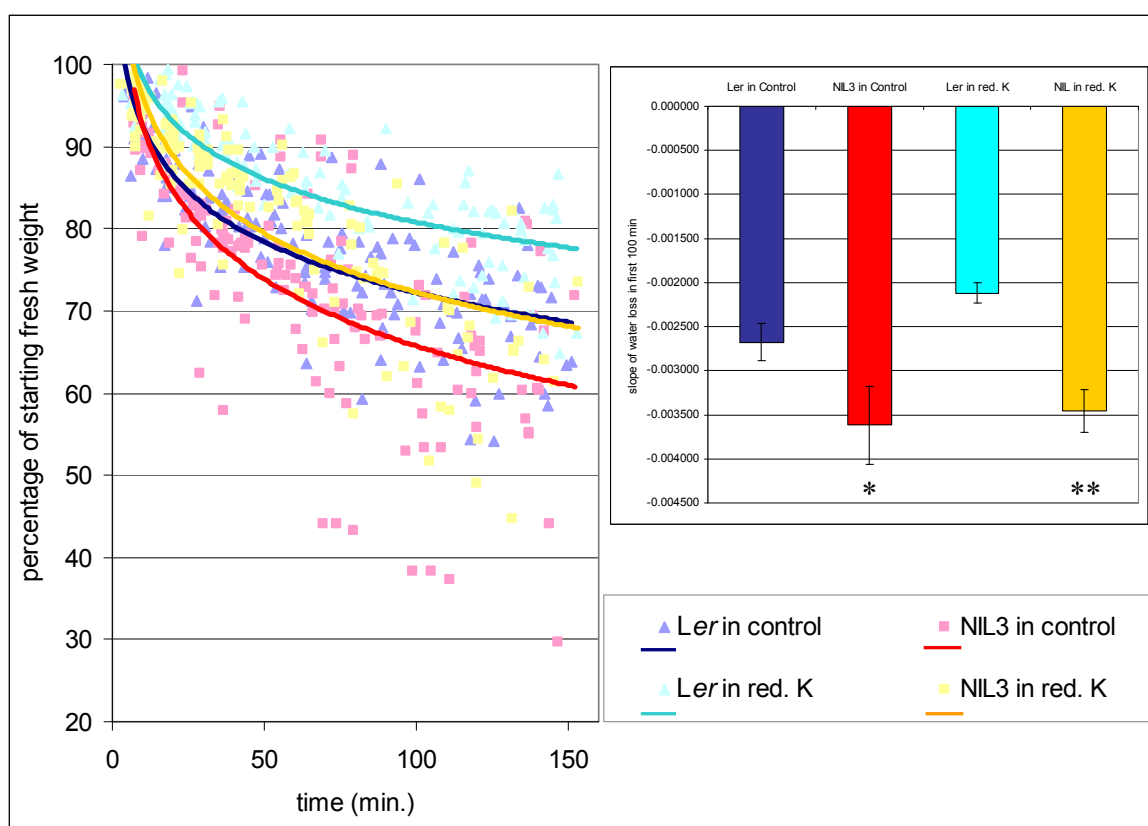


**Figure R10: Water loss of *Ler* and the NIL3 in the control and reduced potassium regime**

The figure contains data points for the weight loss of detached leaves over time of individual plants and four experiments. A logarithmic trend line was determined (with Excel) for each genotype in the control and reduced potassium supply (red. K). The very low values of the NIL3 in the control, around 40% of the original fresh weight, belong all to one plant that had a slightly higher water loss than the other plants but did not affect the average significantly. The bar chart shows the average rate of water loss for each genotype and condition and the asterisk indicate significant differences between *Ler* and the NIL3 in either the control or the reduced potassium supply (\*p-value below 0.05, \*\*below 0.005).

#### 3.3.2.4 No differences in stomata density coincide with the QTL effects

The difference in water loss can be attributed to a difference in stomatal aperture, movement or density. Pictures of prints of the abaxial leaf side were taken of the NIL3 and *Ler*. Those plants were either grown in the hydroponic system (in the control and in 20-fold reduced potassium media) or under regular greenhouse conditions on soil. The number of stomata on an area of 200  $\mu\text{m}$  by 200  $\mu\text{m}$  was scored per line and condition. *Ler* had on average  $10.7 \pm 3.9$  stomata in the control and  $8.7 \pm 1.6$  in the low potassium supply condition and the NIL3 had  $8.6 \pm 1.3$  and  $8.4 \pm 2.6$ , respectively. On soil, the average number of stomata on this area was  $4.5 \pm 1.2$  and  $5.3 \pm 1.2$  for *Ler* and the NIL3, respectively. No apparent differences in size or distribution of the stomata have been observed between *Ler* and the NIL3.

#### 3.3.3 Ionic differences between *Ler* and the NIL3

Several ion content response QTL co-locate with the rosette weight response QTL on the bottom of chromosome five (Figure R1). Although, there were differences in the response of some measured ion contents between *Ler* and the NIL3 (for sodium, magnesium and copper content response in the rosette and nickel concentration response in the root) none of the detected ion content response QTL (Figure R1) could be validated. However, in the region of the Kas-2 introgression of the NILs, are 29 QTL for ion content in either the control or the reduced potassium supply (Appendix Table A1). The rosette and root ionome of the NIL3 and *Ler* was compared and 14 of the QTL could be validated, one of those QTL was of opposite effect (*Mg\_rs*; Figure R11). The QTL for cadmium (Cd) content in the root could

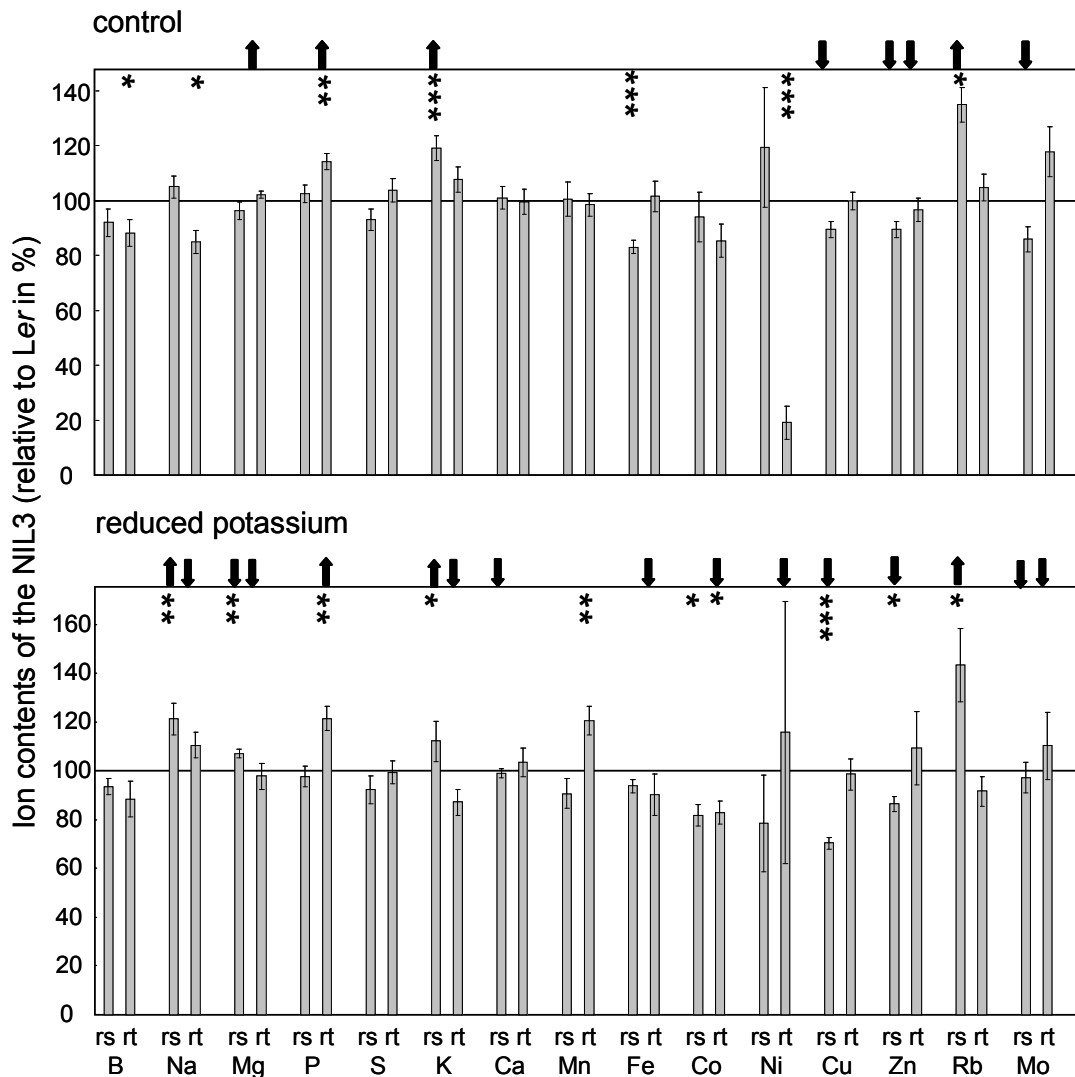


**Figure R11: Ionome of the NIL3 compared to *Ler***

The ion content (element abbreviations on the x-axis) of the NIL3 and *Ler* were determined in the rosette (rs) and in the root (rt) of plants grown in the control condition and the 20-fold reduced potassium supply. The relative ion content of the NIL3 compared to *Ler* is shown in percent, the asterisk indicate significant ion content differences (\*p<0.05, \*\*p<0.005, \*\*\*p<0.001). The arrows indicate the presence of ion content QTL according to the QTL mapping by Dr. Barbier and Dr. Reymond (arrows point upwards: Kas-2 allele confers higher ion content). In some cases, QTL for the same trait and with the same allelic effect co-located (in control: K\_rs, Zn\_rs, Rb\_rs; in reduced potassium supply: K\_rs), these QTL were indicated by only one arrow in the figure. These are combined data from four experiments for the rosette ion content and from two experiments for the root ion content.

not be tested, as the concentration of this ion was too low in *Ler* and NIL3. For the remaining 14 QTL, the ion content was not significantly different between the lines. However, in eleven of these cases, the ion content differences between *Ler* and the NIL3, were in tendency according to the QTL analysis. Furthermore, six significant ion content differences between *Ler* and the NIL3 were not predicted by the QTL analysis (B\_rt, Na\_rt, Fe\_rs, Ni\_rt in the control and Mn\_rt, Co\_rs in reduced potassium supply; Figure R11).

Among the validated ion content QTL were two rosette potassium content QTL for the control and two in the reduced potassium regime. All of them should confer higher potassium content if the genomic region is Kas-2. Indeed, the NIL3 had a  $19\% \pm 7\%$  higher rosette potassium content in the rosette than *Ler* if grown in the control condition and a  $12\% \pm 9\%$  higher potassium content if grown in the reduced potassium regime. A similar allelic effect can be seen for the rosette rubidium content (Rb\_rs), the NIL3 had a higher rubidium content than *Ler* ( $35\% \pm 9\%$  and  $43\% \pm 19\%$  in control and reduced potassium media, respectively). Furthermore, a root potassium content QTL was detected in the low potassium regime that was involved in a reduction of potassium content if the locus was of Kas-2 allelic value. The NIL3 had in fact a  $13\% \pm 7\%$  lower potassium content in the root than *Ler*.

### 3.3.4 Dominance of the *Ler* allele at the QTL position

All characterized lines so far (*Ler*, RIL138, the NILs) were homozygous for the QTL. To determine the dominance effect of the alleles, heterozygous plants for the QTL region were tested for their rosette weight response to reduced potassium supply. Seeds of the first generation (F1) of a cross between *Ler* and the NIL3 and *Ler* and a subNIL were used. The subNIL was shown to respond to the reduction of potassium like the other NILs and can therefore be recognized as another NIL in this experiment. The homozygous Kas-2 introgression of this subNIL was smaller than in the NILs. The subNIL was the parental line of the recombinant line R6 (Figure R13) and differed from this line only in a heterozygous introgression between the marker SO191 (15.02 Mbp) and lkbot5.8 (18.37 Mbp). *Ler*, the NIL, the subNIL and the heterozygote F1 were grown in control and 20-fold reduced potassium media and their rosette weight response was determined. The F1 plants were genotyped to confirm the heterozygosity in the QTL region after harvest (marker: lkbot5.1, lkbot5.8, K8A10). The response of the plants which are heterozygous at the QTL position was identical to the response of the *Ler* parent (Figure R12). The *Ler* allele is therefore dominant over the Kas-2 allele.

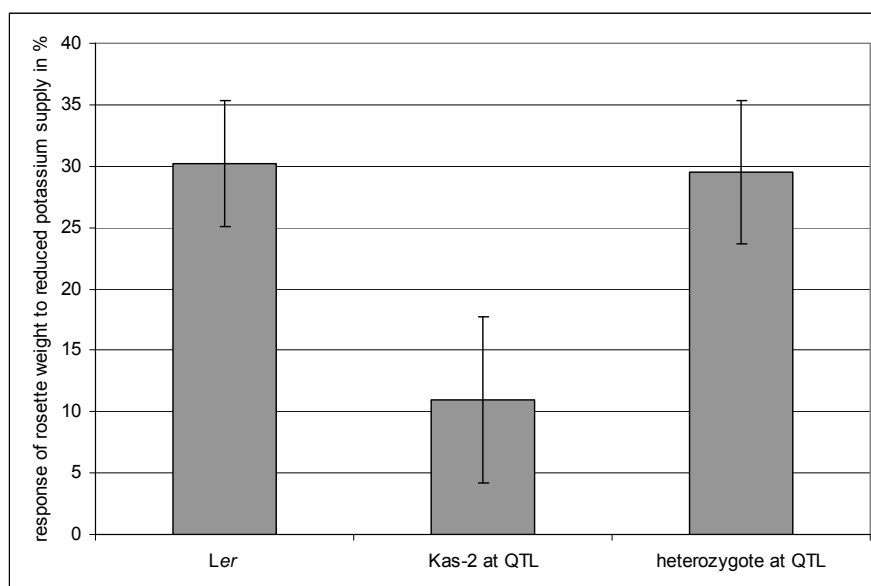


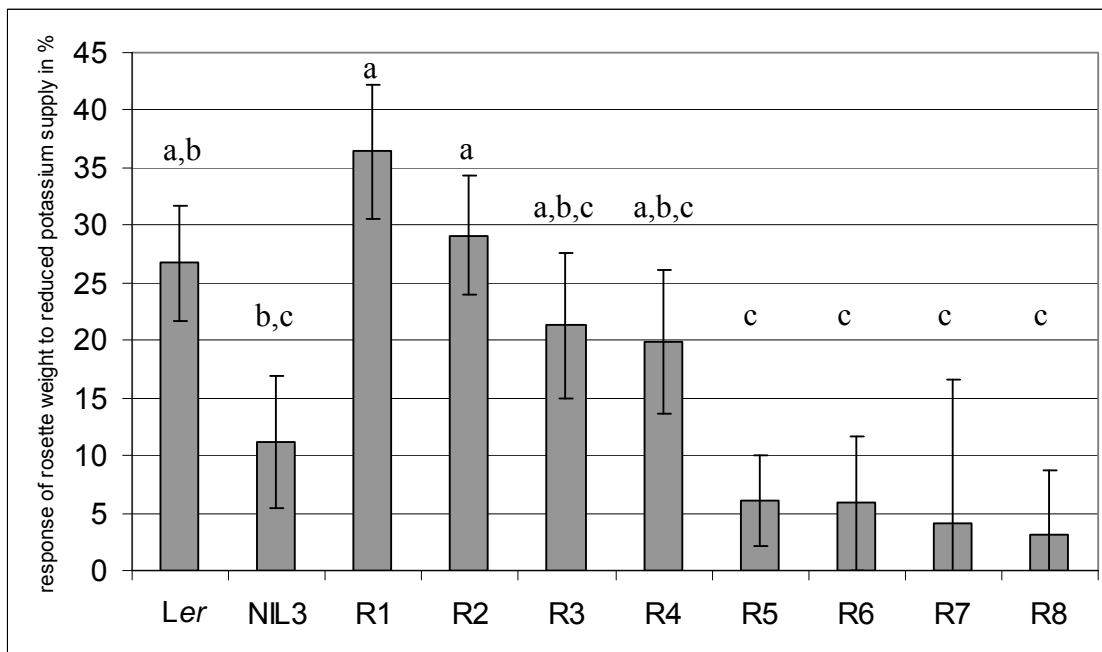
**Figure R12: Allelic dominance at the QTL position**

The figure shows the average rosette weight response to 20-fold reduced potassium supply for *Ler*, the NIL and subNIL (Kas-2 at QTL; see text) and the F1 of *Ler* x NIL3 and *Ler* x subNIL (heterozygous at QTL). The response values are averages from two independent experiments.

**3.4 Fine mapping of the rosette weight response QTL on chromosome five**

To elucidate which genes are underlying the QTL effects, lines carrying homozygous recombinant events in the QTL region were selected (in a *Ler* allelic background). These homozygous recombinants were selected in the fourth generation of the first backcross of the RIL 138 and *Ler* (BC1F4). *Ler*, the NIL3 and selected recombinant lines (Figure R13b) were grown in the control and the 20 times reduced potassium supply media and the response of the rosette weight was calculated (Figure R13a). When their response is compared to the response of *Ler* and the NIL3 it can be seen that the lines R1 and R2 responded like *Ler* and the lines R5 to R8 responded like the NIL3. The lines were tested by a Student-Newman-Keuls (SNK) test and could be distributed into three overlapping groups. Although, *Ler* and the NIL3 fell together in group b, the lines R1 and R2 were only in one group with *Ler* (a) while the lines R5 to R8 fell into one group with the NIL3 only (c). The Kas-2 introgression that caused the low response phenotype of the NIL can be reduced to a region common to the lines R5, R6, R7 and R8 which is between the marker CNGC4\_11 (22.03 Mbp) and the marker K8A10 (26.77 Mbp) at the very end of the chromosome five. The line R2 covers with its Kas-2 introgression a region from marker lkbot5.1 (which marks the upper end of the Kas-2 introgression of the NIL3; 10.1 Mbp) to lkbot5.6 (at 18.57 Mbp). The line R2 had a *Ler*-like response which proves that this region

a)



b)

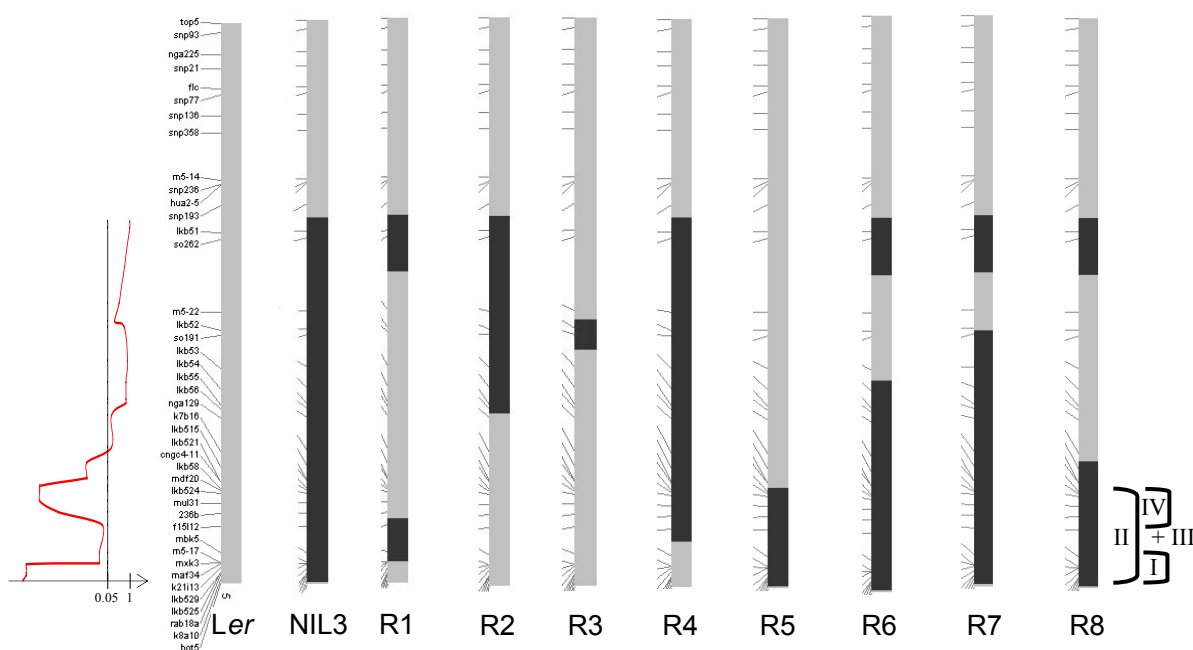


### Figure R13: Fine mapping I, the recombinant lines R1 to R8

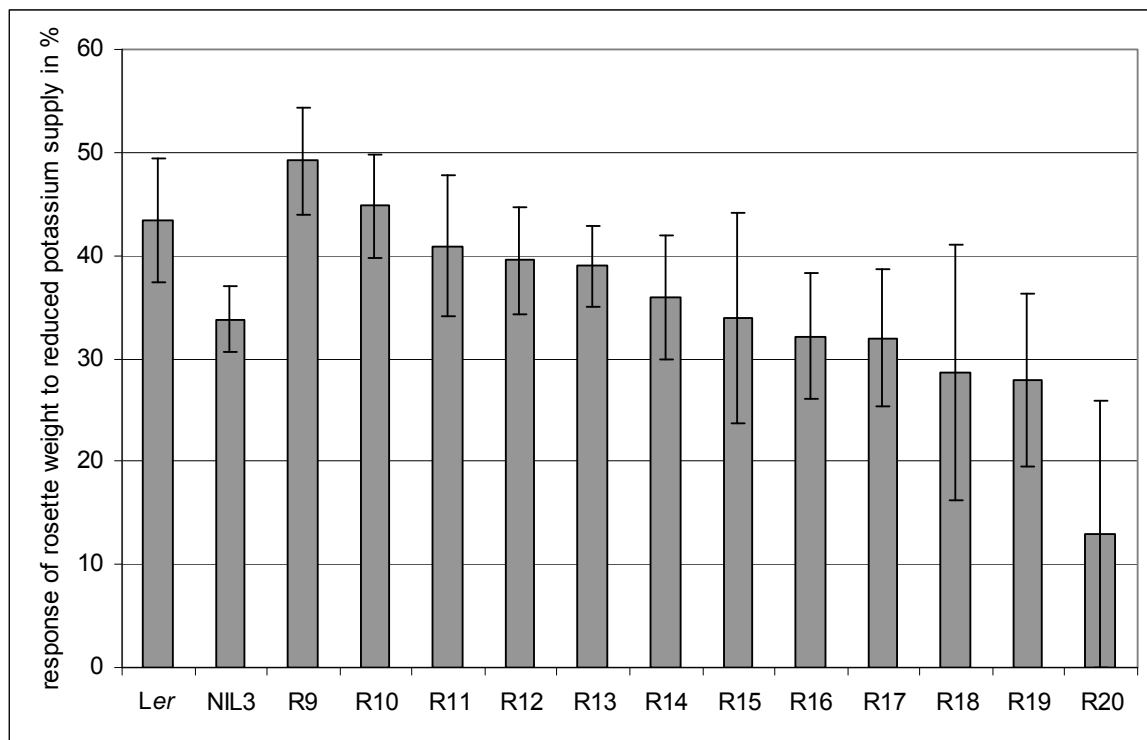
The rosette weight response to 20-fold reduced potassium supply (a) of *Ler*, NIL3 and the recombinant lines is presented (average from two or three experiments). The lines differ in their genotype on chromosome five which is schematically presented (b): grey represents *Ler* and black Kas-2. The lines can be divided into three overlapping groups, a, b and c, according to the Student-Newman-Keuls test (confidence interval of 95%). Possible fine mapped regions (according to the four proposed hypotheses I to IV, see text) are indicated by the clamps on the right side of the genotypic representation. The statistical implication of each marker in the response value was tested by an univariate ANOVA and the p-values were plotted (logarithmic scale) at the left side of the genotypes next to the corresponding marker positions.

(10.1 Mbp to 18.57 Mbp) is not involved in the QTL effect. It can be clearly deduced from these data that the region causal to the QTL effect is between the marker CNGC4\_11 and K8A10. If this region can be reduced further and how many genes are involved, depends on the interpretation of the other lines R1, R3 and R4. The line R1 responded like *Ler* and contained two small Kas-2 introgressions one at the markers lkb05.1/SO262 (which is not causal to the QTL effect) and one from the marker F15L12 (24.2 Mbp) to the marker mxk3-5 (25.99 Mbp). The lines R3 and R4 had an intermediate response between the response values of *Ler* and the NIL3 (the lines were present in all groups of the SNK test). However, with 21.3% and 19.8%, their responses were more similar to *Ler* (26.7%) than to the NIL (11.1%). Furthermore, the line R3 had only a very small Kas-2 introgression between the markers lkb05.2 and SO191. This region is also Kas-2 in the line R2 which responded like *Ler* and does not belong to the common region of the lines R5 to R8. Altogether, this indicates that the line R3 is an outlier that should not be taken into account. There are now four possible hypotheses (I-IV) where the causal introgression might be, depending mainly on the interpretation of the response of the line R4. If R4 can be evaluated as response similar to *Ler*, the genetic region conferring the NIL-response could be a single gene on the very bottom of chromosome five from the marker mxk3-5 (25.99 Mbp; last marker of the Kas-2 introgression of line R1) to the very end (hypothesis I). This region is common to the lines R5 to R8 and cannot be excluded by the lines R1 to R4. Or the phenotype is caused by regions with epistatic effect (which would need to be all present in order to produce the phenotype) in the region from 22.03 Mbp (CNGC4\_11) to the very bottom of the chromosome (hypothesis II). The lines R1 and R4 would not cover all of these regions with their Kas-2 introgressions and thus respond like *Ler*. If the line R4 would show a true intermediate response phenotype, there are two regions involved of which the line R4 covers only one. Those regions would be below and above the Kas-2 introgression of the line R1, as this line shows a clear *Ler*-like response and not an intermediate response: The upper region would be between the markers CNGC4\_11 (22.03Mbp) and F15L12 (24.2 Mbp) and the lower region would be below the marker mxk3-5 (25.99 Mbp) to the end of the chromosome (hypothesis III). Lines covering this lower region would also be expected to show an intermediate phenotype. The involvement of each marker in the response was tested with an univariate ANOVA and the p-value distribution (Figure R13b) confirms the hypothesis on the two additive regions. The last hypothesis could be: The line R4 behaves like the NILs and thereby the QTL would be located to a single region from 22.03 Mbp (CNGC4\_11) to 24.2 Mbp (F15L12) which is

common to the lines R4 to R8 and excluded by the line R1 (hypothesis IV). Additional recombinants (R9 to R20; Figure R14b) were selected in the F5 of the original backcross of RIL138 and *Ler* (BC1F5) and the third generation of the second backcross of a BC1F3 line with *Ler* (BC2F3). The lines R16 to R20 showed a response similar to the NIL (Figure R14a) and shared a *Kas-2* introgressions between the markers CNGC4\_11 and m5.17. The region of interest can therefore be reduced to this region from 22.03 Mbp (marker CNGC4\_11) to 25.95 Mbp (marker m5.17; Figure R14). How many genetic regions are involved in the phenotype cannot be clarified but the initial hypotheses can be refined: The lines R16 to R20 clearly exclude the bottom of the chromosome five (m5.17 to K8A10) from the region causal to the QTL effect. In addition, two lines that carried a *Kas-2* introgression at the very end of the chromosome five from 23.1 Mbp (R10) or 25.5Mbp (R9) showed a clear *Ler* response and thereby also excluded that region from the fine mapping area. The hypotheses including the bottom of the chromosome five (I and III) do not hold true any more and can be neglected. That means, the QTL is either caused by one gene or two or more genes with epistatic effect. If only one gene would be causal to the QTL effect, it would be in the region from 22.03 Mbp (marker CNGC4\_11) to now 23.1 Mbp the position of the marker MUL3-1. MUL3-1 marks the beginning of the *Kas-2* introgression covered by the line R10 that responded like *Ler*. This region would be in accordance with the marker per marker ANOVA test, performed on the recombinant lines R9 to R20 (Figure R14) which indicated a region from 19.1 Mbp to 22.63 Mbp to be significantly involved in the response. However, that would mean that the line R4 (Figure R13) would need to respond like the NIL, as R4 is *Kas-2* at the region from 22.03 Mbp to 23.1 Mbp. It was already stated that the response of the line R4 was more similar to *Ler* in the single experiments, which means that the hypothesis II is more likely and the QTL effect is caused by two or more genes with epistatic effect in the region from 22.03 Mbp (marker CNGC4\_11) to now 25.95 Mbp (marker m5.17).



a)



b)

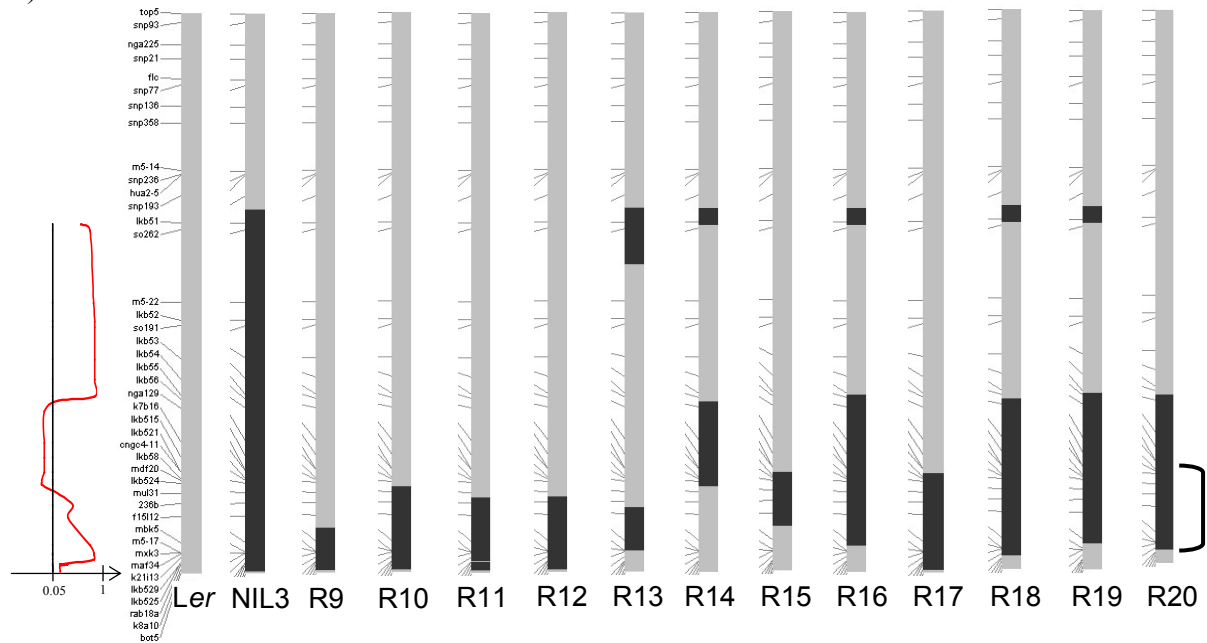


**Figure R14: Fine mapping II, the recombinant lines R9 to R20**

The rosette weight response to 20-fold reduced potassium supply (a) of *Ler*, NIL3 and the recombinant lines (average from two experiments). The lines differ in their genotype on chromosome five which is schematically presented (b) grey represents *Ler* and black *Kas-2* alleles. The clamp at the right side of the genotypes indicates the fine mapped region. The red line indicates the p-value at each marker position with which the marker contributes to the response phenotype (black line is the threshold of 0.05).

### 3.5 Candidate genes for the potassium dependent rosette weight response QTL

#### 3.5.1 Genes in the region between the markers CNGC4\_11 and m5.17

The ca 3.9 Mbp region between the markers CNGC4\_11 and m5.17 to which the QTL for rosette weight response to low potassium supply could be fine mapped (chapter 3.4), contains 1202 genes with 1484 transcripts in total. This estimation of the gene number is based on the Col-0 reference sequence and can differ for *Ler* or *Kas-2*. For an overview of the gene functions in this region, the transcripts were sorted according to their annotated function with the TAIR Go annotation function tool (<http://www.arabidopsis.org/tools/bulk/go>). Transcripts can be annotated to several biological processes: Protein metabolism, response to abiotic and biotic stimulus, developmental processes, response to stress, transport, cell organisation and biogenesis, transcription, signal transduction, DNA or RNA metabolism, electron transport or energy pathways and unknown biological processes. The TAIR Go annotation function assigned many transcripts to two or more categories. Especially the categories “other biological/metabolic/cellular processes” became in comparison to the functionally distinct categories very large due to putative annotations (according to eg. sequence homologies). For a better overview, genes that are involved in one of the above listed, distinct processes (“protein metabolism”, “transport” and others) were removed from the categories “other biological/metabolic/cellular processes” and only the remaining transcripts were placed into “other biological processes”. More than one quarter of the transcripts in the fine mapped region are of unknown biological function. The next biggest categories are “Protein metabolism” and “response to abiotic and biotic stimulus” followed by “developmental processes” and “response to stress” (Figure R15). Those four categories belong also to the biggest functional groups in a genome wide annotation that can be performed with the TAIR Go annotation function (unknown transcripts constitute for one quarter of all genomic transcripts of *A. thaliana*). The fine mapped region does not differ in its functional categorisation from the average genome.

According to their annotated function and map position in the Col-0 reference sequence some possible candidate genes can be highlighted (Figure R15): The fine mapped locus contains several genes that are responsive to jasmonic acid (e.g. AT5G64890, AT5G64930), ethylene (e.g. AT5G61890, AT5G61590), auxin (e.g. AT5G63310, AT5G57090) and calcium signalling (e.g. AT5G55990, AT5G54490) as well as a gene for

jasmonic acid synthesis (AT5G63380). All of these genes could be potentially involved in the signalling of the low potassium status (see chapter 1.5). RPD3-like histone acetylases (AT5G63110, AT5G61070) are also possible signalling factors. The *reduced potassium dependency* (*rpd*) mutants were identified in yeast to suppress the growth defects of the potassium transporter mutant *trk1* by increasing the transcript levels of another potassium transporter TPK2 (Vidal and Gaber, 1991). Members of the RPD3 histone acetylase family in *A. thaliana* were shown to mediate transcriptional changes in response to abiotic and biotic stresses (Zhou et al., 2005; Chinnusamy and Zhu, 2009). Several genes for plant defence and pathogen interaction are also in the region. Pathogen related responses are assumed to be affected by low potassium supply as the initial signalling mechanism is similar (JA, ethylene). The effect of low potassium on those genes is either a side effect of the overlapping pathways or a counteraction of the increased disease susceptibility of potassium starved plants (Amtmann et al., 2008). Furthermore, it has been shown that low

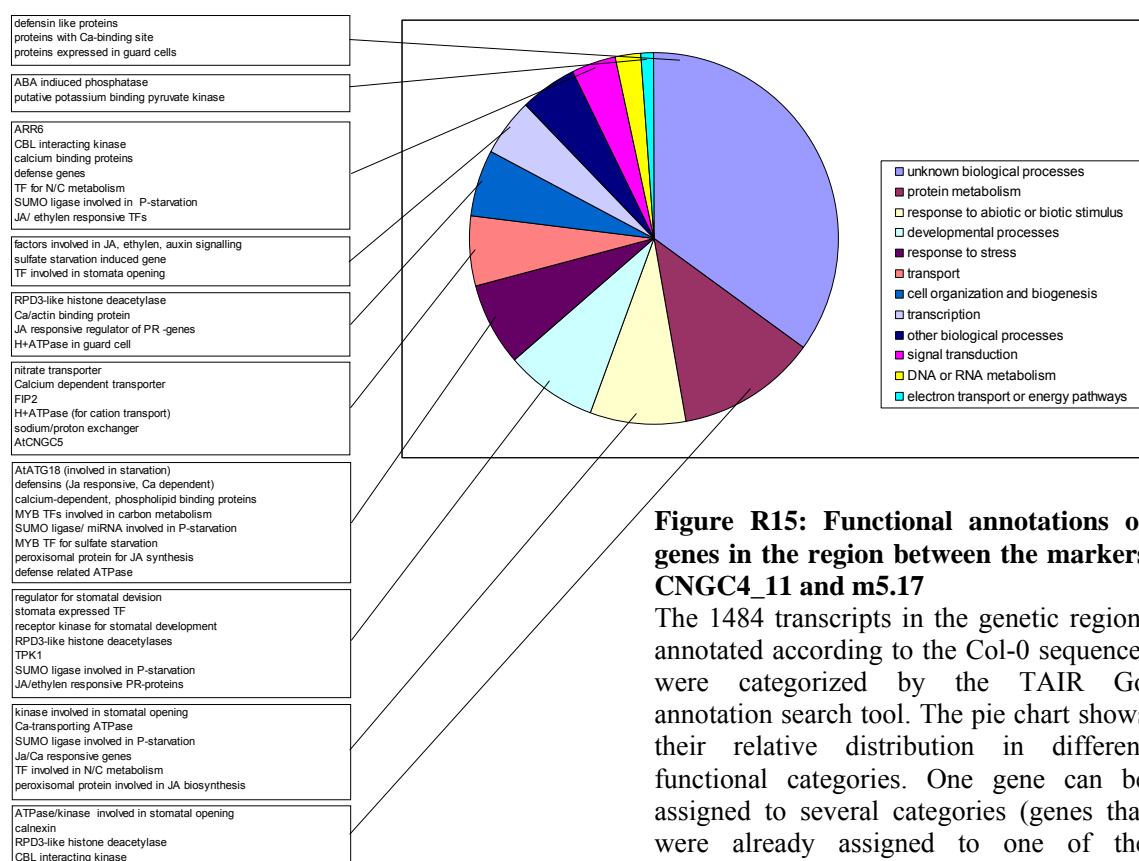


**Figure R15: Functional annotations of genes in the region between the markers CNGC4\_11 and m5.17**

The 1484 transcripts in the genetic region, annotated according to the Col-0 sequence, were categorized by the TAIR Go annotation search tool. The pie chart shows their relative distribution in different functional categories. One gene can be assigned to several categories (genes that were already assigned to one of the categories above were removed from "other processes", see text). Possible candidates that may be involved in potassium stress signaling, homeostasis or potassium related growth effects are indicated in the boxes on the left.

supply of different mineral nutrients shares overlapping signalling pathways (Amtmann et al., 2005; Schachtman and Shin, 2007). Therefore, the SUMO ligase (AT5G60410) and miRNA (AT5G62162) involved in phosphate starvation, AtATG18 which is involved in nitrogen starvation and genes induced by sulphur starvation (AT5G60890, AT5G61420) could potentially also be involved in the observed effects of the QTL in response to low potassium supply. Another group of candidates in the region are guard cell expressed proteins as well as H<sup>+</sup>ATPases and kinases involved in stomatal opening as the movement of the stomata depends on potassium fluxes. Photosynthesis, sugar transport and nitrogen assimilation are also negatively affected by potassium starvation (Amtmann et al., 2005) and in the fine mapped region are transcription factors for carbon and nitrate metabolism, a putative potassium binding pyruvate kinase (AT5G56350), and a putative nitrogen transporter (AT5G62730). Proton transport is necessary for the transport of potassium and the proton/sodium exchanger (AT5G55470) or the H<sup>+</sup>ATPase (AT5G62670) might therefore also be involved in potassium uptake or homeostasis. So far, the genetic candidates might be involved in a general stress signalling or potential downstream effects of low potassium supply but there are also genes that have a more specific or direct effect on potassium homeostasis: The region comprises the potassium channel TPK1 (AT5G55630) and two putative potassium channels FIP2 (AT5G55000) and CNGC5 (AT5G57940). In addition, a protein similar to a bacterial response regulator, ARR6 (AT5G62920), that was shown to be upregulated in phosphate, nitrogen and potassium starvation conditions (Coello and Polacco, 1999), is also in the fine mapped region.

### **3.5.2 Transcriptional differences between *Ler* and the recombinant line R5**

Genes can cause QTL effects, either through changes in their function, which would mainly be based on sequence polymorphisms in the coding region, or due to changes in their expression level or timing. Therefore, another way to identify possible candidates for the QTL effect is to identify genes with a differential expression between lines with different response-phenotypes. The transcriptome of *Ler* and the recombinant line R5 was analysed with an ATH1-expression chip (Affymetrix). The line R5 was chosen for the analysis as it contained the smallest Kas-2 introgression that was still causal to the QTL effect. RNA-samples from three experiments per line per condition were analysed, while each sample was consisting of pooled material from at least three plants. The array was analysed calculating rank products according to the publication of Breitling et al. (2004).

The analysis could only be performed between two different groups: the condition effect for one genotype or the genotype effect on gene expression in one condition. The percentage of false predictions was cut off at 5% ( $p_{fp} \leq 0.05$ ). Although the probes “AFFX-r2-Bs-dap-5\_at” and “AFFX-DapX-5\_at” (indicators for RNA degradation) showed significant differences between *Ler* and R5 in the control condition, the RNA quality control prior to chip hybridisation was satisfactory, as well as the quality control of the chip hybridisation. The supposed differential expression of these probes will therefore be due to random hybridisation effects. Altogether, 389 genes were differentially regulated in *Ler* and R5, between the control and in the 20 times reduced potassium supply. Of more interest of course were the genes that were differentially regulated between the lines, as those genes might be candidates for the QTL effect. In total, 34 genes were differentially regulated between *Ler* and the recombinant line R5, grown either in the control condition or the lowered potassium supply (two gene pairs with the same functional annotation bind to the same probe of the ATH1 chip and cannot be analysed distinctively; Table R1). Differentially regulated genes could be found on all chromosomes and also one gene of the chloroplast genome was affected. The genes with the highest expression difference were a gene involved in starch mobilisation (AT4G25000) which was 8-fold higher expressed in *Ler* than in the line R5 and a putative kinase (AT5G59670) which is nearly 11-fold higher in R5 than in *Ler*. The latter is located in the fine mapped region. Five other genes in the fine mapped region were differentially expressed between *Ler* and R5 but none of them was an obvious candidate. The fine mapped region contained the putative kinase, two genes of unknown function, a glycosyl hydrolase family protein and a beta-galactosidase (BGAL4) that were differentially regulated.

AGI	condition	fold change (Ler/R5)	pfp	locus (in Mbp)	functional annotation
AT1G14700	red. K	0.3308	0.035	5.06	phosphatase (PAP3)
AT1G33960	red. K	4.5735	0.03	12.35	induced by avirulence genes
AT1G52690	red. K	4.3655	0.0325	19.62	involved in embryogenesis
At1G61510/ AT4G22450	red. K	0.3596	0.0467	22.7/11.8	transposable element
AT1G73260	red. K	3.3784	0.05	27.55	trypsin inhibitor involved in pathogen interactions
AT1G74670	red. K	0.196	0	28.05	gibberellin/sucrose-responsive protein
AT2G29350	red. K	4.7738	0.0275	12.6	senescence-associated alcohol dehydrogenase
AT2G30600	control	0.4107	0.0233	13.04	involved in cell adhesion
AT2G40435	red. K	0.3316	0.035	16.89	putative TF involved in salt stress
AT3G22910	red. K	3.6999	0.0473	8.12	putative Ca(2+)-ATPase
AT3G44990	red. K	0.2921	0.03	16.45	transglycosylase involved in cell wall biogenesis
AT3G48360	red. K	0.2488	0.038	17.91	ABA responsive telomerase activator
AT4G10500	red. K	3.4069	0.032	6.49	oxidoreductase
AT4G23150	red. K	3.3425	0.0469	12.13	kinase
AT4G25000	red. K	7.9249	0	12.85	involved in starch mobilization (ABA response)
AT4G37610	red. K	0.3649	0.045	17.67	putative TF (response to auxin/chitin)
AT5G20250	control	0.418	0.014	6.83	glycosyl hydrolase (senescence, responds to sugars)
AT5G22580	control	2.9358	0.025	7.5	unknown
At5G24770/ At5G24780	red. K	3.5894	0.0257	8.5/8.5	phosphatase induced by wounding and jasmonic acid
AT5G42800	red. K	3.3194	0.031	17.16	biosynthesis of anthocyanins.
AT5G48490	red. K	0.2995	0.03	19.65	lipid transfer protein
AT5G49360	control	0.3678	0.025	20.01	required for pectic arabinan modification
AT5G55180	red. K	4.7232	0	<b>22.39</b>	glycosyl hydrolase
AT5G56870	red. K	2.7812	0.0333	<b>23</b>	beta-galactosidase
AT5G56980	control	0.4411	0.0312	<b>23.06</b>	unknown
AT5G59670	control	0.2034	0	<b>24.04</b>	putative kinase
AT5G59670	red. K	0.0938	0	<b>24.04</b>	putative kinase
AT5G62140	red. K	0.2581	0.0033	<b>24.95</b>	unknown
AT5G66040	control	3.7761	0	26.41	sulfurtransferase involved in aging
AT5G66040	red. K	3.7875	0	26.41	sulfurtransferase involved in aging
AT5G66060	control	0.4651	0.0444	26.42	oxidoreductase
ATCG00270	control	0.445	0.0183	0.03	PSII D2 protein

**Table R1: Expression differences between *Ler* and the recombinant line R5**

The table lists the genes (sorted by their AGI code) that were differentially transcribed between *Ler* and the recombinant line R5, when grown in the control (nine genes) and the reduced potassium media (“red. K”; 25 genes). For each significantly differential expressed gene the condition in which the gene differs in expression between the lines, the fold change of the expression, the percentage of false prediction (pfp; cut-off at 0.05), the genes position (in bold if the gene is in the fine mapped region) and a brief functional annotation according to TAIR is given. Two probes of the ATH1 chip corresponded to two genes with a similar functional annotation according to TAIR.

### 3.5.3 Polymorphisms between the *Ler* and *Kas-2* alleles of the candidate TPK1

One of the possible candidate genes that is located in the fine mapped region is the potassium channel TPK1. The locus of the TPK1 gene was sequenced and several polymorphisms were detected between the TPK1-locus of *Ler* and the RIL138. In the 5' untranslated region (5'UTR), there are nine single nucleotide polymorphisms (SNPs) and two deletions and insertions (Indels) between *Ler* and the RIL138, respectively and four SNPs and one Indel in the 3'UTR. The sequences of *Ler* and RIL138 differed further for one SNP and a single base pair deletion (in *Ler*) in the intron of the TPK1-gene (Figure A1, appendix). The TPK1-gene has two exons and in the first one are seven nucleotide polymorphisms of which two are non-synonymous and translate into amino acid changes in the predicted protein sequence (Figure R16). The first one is at the amino acid position 261 where a serine in *Ler* is changed to a threonine in the RIL138. The second predicted amino acid change is at position 295 and caused a change from asparagine to serine between *Ler* and the RIL138.

The first non-synonymous polymorphism resided in the predicted fourth transmembrane segments of the TPK1 channel (aa position 251 – 280; Czempinski et al., 1997). The second polymorphism resided in the first  $\alpha$ -helical structure of the putative EF-hand motif (aa position 290 to 357) adjacent to an diacidic motif that was shown to be involved in the ER export of the protein (Dunkel et al., 2008).

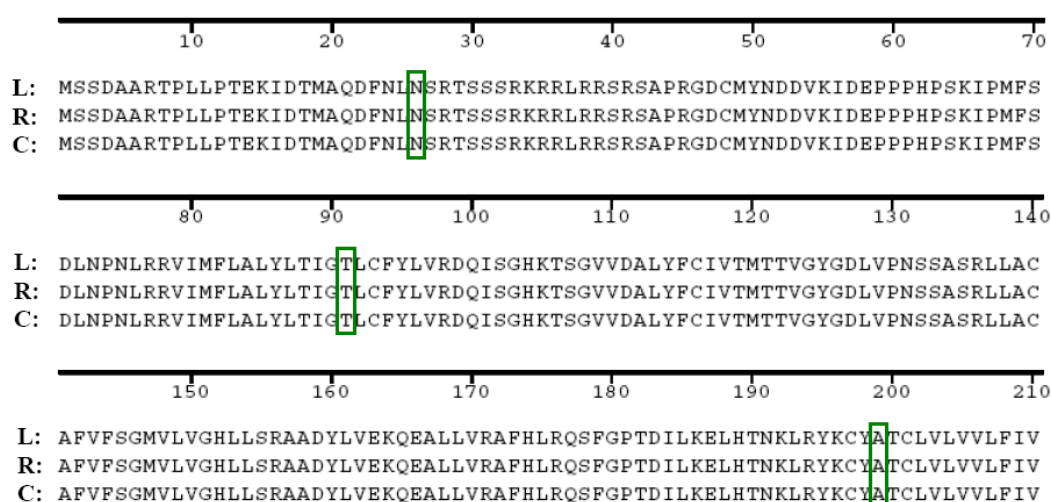


**Figure R16: Comparison of the predicted protein sequences of TPK1 from *Ler*, the RIL138 and Col-0**

The predicted amino acid sequence is shown for *Ler* (L), the RIL138 (R) and Col-0 (C). The synonymous polymorphisms between *Ler* and the RIL138 are highlighted by green boxes while the two non-synonymous polymorphisms are highlighted by red boxes.

```

      220      230      240      250      260      270      280
L: GTIFLVMVEKMPVISAFYCVCSVTTLGYGDKSSFNSEAGRLFAVFWILTSSICLAQFFLYVAELNTENKQ
R: GTIFLVMVEKMPVISAFYCVCSVTTLGYGDKSSFNSEAGRLFAVFWILTSSICLAQFFLYVAELNTENKQ
C: GTIFLVMVEKMPVISAFYCVCSVTTLGYGDKSSFNSEAGRLFAVFWILTSSICLAQFFLYVAELNTENKQ

      290      300      310      320      330      340      350
L: RALVKWVLTRRITNNOLEAADLDEDGVVGAAEFIVYKLEMGKIDEKDISGIMDEFEQLDYDESGTLTTS
R: RALVKWVLTRRITNSDOLEAADLDEDGVVGAAEFIVYKLEMGKIDEKDISGIMDEFEQLDYDESGTLTTS
C: RALVKWVLTRRITNNOLEAADLDEDGVVGAAEFIVYKLEMGKIDEKDISGIMDEFEQLDYDESGTLTTS

      360
L: DIVLAQTTSQIQR.
R: DIVLAQTTSQIQR.
C: DIVLAQTTSQIQR.

```

**Figure R16 (continued): Comparison of the predicted protein sequences of TPK1 from *Ler*, the RIL138 and Col-0**



## 4. Discussion

### 4.1 The validation of the potassium dependent rosette weight QTL

Response QTL are detected if changing environments cause a different effect on the genetics of a trait. In the QTL mapping of Dr. Barbier and Dr. Reymond a QTL was detected that was involved in the rosette weight change in response to reduced potassium supply. The genetic basis of the rosette weight response QTL will therefore be a gene that is differentially affected by the potassium status of the plant and might therefore be involved in the adaptation to the changing nutritional supply. The allelic diversity that was used for the QTL detection comes from the two accessions Landsberg *erecta* (*Ler*) and Kashmir-2 (*Kas-2*). Natural accessions are thought to have adapted to their local environment. Different environmental impacts are even more likely if their habitat is as far apart geographically as the one of *Ler*, which is from Poland and *Kas-2*, from Kashmir. The exact mineral supply of the region where the accessions were taken from is unknown but Kashmir has a largely mountainous landscape where erosion can cause low mineral supply (Abbasi and Rasool, 2005). It is no necessary prerequisite for the QTL mapping that the parental accessions differ in their studied phenotype, as RIL populations can show diverging phenotypes from their parental accessions (Keurentjes et al., 2006). This transgression effect can be due to an advantageous or disadvantageous combination of alleles that cause the trait value in the progenies. Nevertheless, it was assumed that the Mid-European and Asian accessions were different enough in their genome merely by the geographically distance to have a potential for a QTL mapping (Loudet et al., 2003). In fact this proved to be the case as many QTL were detected for growth related traits as well as for biochemical traits. Only three of the growth related trait QTL were involved in the response to the reduced nutritional supply, two for phosphate and one for potassium. The growth related traits, compared to the biochemical/ionomic traits, were of higher interest for further analysis as growth reduction is one of the first hallmarks of reduced nutrient supply (Marschner, 1995) and represents an agronomical interesting trait.

If the QTL are really causal to the growth related trait, lines which differ mainly at this genetic region should show a distinct growth phenotype. This was the reason to test the selected RILs (Figure R1) for their growth responses to the reduced potassium or phosphate supply compared to the respective parental line. Lines showing the expected growth effect are suitable starting material to construct NILs. The genetic position of the

response QTL for reduced potassium supply (on the bottom of chromosome five) differed in allelic value between the line RIL138 and *Ler*. Although not significantly, the rosette weight response difference between the lines was in accordance with the QTL mapping, as *Ler* had a more positive response than RIL138. The RIL135, which was chosen for validation of the RGR response QTL on chromosome one, did not differ from Kas-2 in relative growth rate (RGR) in response to phosphate reduction. It would be unlikely that the QTL effect could be validated with NILs derived from this line. The line RIL85 was *Ler* at the position of the root length response QTL on chromosome one and showed a significantly lower root length response to reduced phosphate supply than Kas-2. Anyway, this response QTL co-located with a previously described QTL for primary root growth arrest in response to reduced phosphate supply that was detected in a different mapping population (Reymond et al., 2006). The underlying gene was identified to be a multicopper oxidase, LPR1, which could either be involved in the phosphate perception in the root cap (Svistoonoff et al., 2007) or in iron toxicity caused by the increased availability of iron in phosphate starvation (Ward et al., 2008). The QTL of LPR1 was detected in a Bayreuth-0 (Bay-0)/ Shahdara (Sha) RIL population, with the dominant Sha allele causing increased primary root growth arrest (Reymond et al., 2006). Presumably, the difference between the alleles that cause the QTL are increased transcript levels of the Sha-LPR1 (Svistoonoff et al., 2007). Comparison of growth related trait QTL detections in a *Ler*/Kas-2 and a *Ler*/Sha line showed in several incidences similarities in the effect of the Kas-2 and Sha-alleles compared to *Ler* (Pieper, 2009). Therefore, it is likely that LPR1 is also underlying the rosette length response QTL detected in the *Ler*/Kas-2 population by Dr. Barbier and Dr. Reymond. It strengthens the reliability of the QTL mapping that such co-localizations between similar QTL can be found. Nevertheless, the validation and fine mapping of this QTL is of less interest, as it is likely to reveal an already identified gene for phosphate starvation response. The rosette weight response QTL on the bottom of chromosome five was followed up in fine mapping as the RIL138 showed the expected phenotypic difference to *Ler* and the QTL was never described before. Harada and Leigh (2006) detected co-localizing QTL for potassium content and for the relation between shoot dry and fresh weight also on bottom of chromosome five. Nevertheless, this is not a response QTL, it was only detected in standard growth conditions and Harada and Leigh didn't validate the QTL and the genetic basis is unknown. That the response difference between the RIL138 and *Ler* was not significant might on the one hand depend on the relatively low effect of the QTL ( $R^2 = 9.3\%$ ) and on the other hand on a genomic background effect on

the QTL. The genomic background of *Ler* and the RIL138 was not identical: The RIL138 possesses a 9.7 Mbp *Kas-2* introgression on the top of chromosome one and a heterozygous region on the very bottom of chromosome three (marker *nga6*). Neither of those two positions contained a QTL of rosette weight response or constitutive rosette weight QTL that might influence the QTL effect. However, the response difference between *Ler* and the RIL138 was not significant, while the response difference between *Ler* and the NILs was significant and the NILs have an identical background with *Ler*. There was only one QTL for rosette weight response detected for the whole genome, if there would be no background effect from other regions RILs with recombinant events in the QTL region should be theoretically usable for fine mapping. This however was not possible for this QTL, the comparison of the responses of RILs from the *Ler*/*Kas-2* population with different recombinant events in the QTL region did not allow to fine map the QTL (data not shown). The QTL is clearly background dependent. Kroymann and Mitchell-Olds (2005) also described a clear background dependency for a small-effect growth QTL. Keurentjes et al. (2007b) could show that mapping populations derived from NILs have a higher statistical power to identify low effect QTL than RIL populations. Anyway, the NILs derived from the RIL138 validated the rosette weight response QTL on chromosome five. The significance of the response differences between these lines was confirmed with the Student-Newman-Keuls test.

#### **4.2 The fine mapping of the potassium dependent rosette weight QTL**

The development of NILs with an exclusive *Ler* background, allowed the validation of the response QTL on bottom chromosome five and thus the further fine mapping. In the fine mapping approach, lines with recombinant events in the QTL region are phenotyped and the correlation of phenotype and genotype narrows down the region of interest, ideally to the underlying gene. In plants, most QTL that were cloned to date were major QTL, like the flowering time QTLs *FLC* and *FRI* (Alonso-Blanco et al., 2009). Those QTL have a high impact on the phenotype and cause high differences between genotypes, which facilitates the fine mapping process. The only publication to date, describing the cloning of a low effect QTL, was done by Kroymann and Mitchell-Olds (2005). They detected in an analysis of NILs for herbivore resistance, a 210 kbp region which contributed to biomass accumulation. They identified a putative serine/threonine kinase to underly the QTL effect. The allelic variation between *Ler* and *Col-0* at this locus caused a 15.1% or 5.1%

difference in biomass, depending on the genetic background. The validated rosette weight QTL is also of low effect and although, the identification of a low effect QTL is difficult (Salvi and Tuberosa, 2005), the underlying genetic determinism is far from being less important than of major QTL. It might be a redundant pathway or on the contrary a highly conserved pathway that does not allow too much allelic variation. Minor QTL contribute to most complex trait variations but often cannot be detected due to low marker density or high variation. However, in the end the trait variation depends on the overall genetic variation that is represented by these small effect QTL (Kroymann and Mitchell-Olds, 2005).

The potassium dependent rosette weight response QTL caused on average a response of  $34.3\% \pm 4.8\%$  and  $13\% \pm 3.1\%$  for *Ler* and the NILs, respectively. To pursue the fine mapping, a precise genotype and phenotypes with a low variation were required, to detect response differences between the lines. Therefore, only homozygous recombinants were used for the fine mapping. Homozygous lines have less trait variation, which can be caused by a segregating background and can be grown in a large number of replicates. The calculated response needed further to be confirmed in several independent experiments, to compensate for experimental effects that were detected. The experimental effect had a higher impact on the overall plant fresh weight than on the fresh weight response of one line. Nevertheless, by combining several experiments the response difference between lines became more distinct as the error reduced.

The fine mapping revealed a region of ca 3.9 Mbp between the marker CNGC4\_11 and m5.17 to be responsible for the rosette weight response. How many genes might be in this region that cause the response effect cannot be deduced from the data. If only one gene is responsible for the QTL effect, this gene would be located between the marker CNGC4\_11 and MUL3-1 (1.07 Mbp region). MUL3-1 is the upper end of the Kas-2 introgression of the line R10 (Figure R14) which shows a *Ler* response phenotype and if only one gene would cause the phenotype the region of this Kas-2 introgression can be excluded. In this case, the recombinant line R4 (Figure R13) would need to be responding like the NIL because Kas-2 alleles are present at this locus in the line R4. This cannot be excluded; the response of this line cannot be attributed to *Ler* or the NIL exclusively. However, the response of the line R4 was in each experiment more similar to *Ler* than to the NIL. The intermediate response could be due to unpredictable experimental variation or modifiers in the relatively large Kas-2 introgression above the fine mapped region. Furthermore, the rather continuous distribution of the response phenotype between the lines R11 to R15

(Figure R14) also suggests the presence of modifiers that cause additional variation in the rosette weight response. Taken together, the QTL effect is more likely to be caused by several genes in this region.

The fine mapped region (22.03 Mbp to 25.95 Mbp) is below the original QTL which is focused at the marker *snp97* (17.23 Mbp). This discrepancy in the map position can have several reasons: the accuracy of a QTL detection with a RIL population is lower than the detection of a single QTL effect within a NIL, as individual line effects, background interferences, other QTL effects and the cofactor selection will decrease the statistical power. The mapping resolution (marker density and number of recombinant events in the region) in this region may have been too low, to detect the exact position of the response QTL. Only two molecular markers were between the original QTL region and the fine mapped region, according to the map used for the QTL detection.

#### **4.3 Characterizing the potassium dependent rosette weight QTL**

The plants rosette weight response to the reduced potassium supply is a complex trait and other physiological parameters are likely to be influenced as well. The root weight response between *Ler* and the NIL3 was identical to the rosette weight response differences between the lines. In contrast, the root length did not change; the response is almost zero for both lines. Although, detailed root architectural changes of the NIL were never studied, these data suggest that the primary root growth was not affected but the lateral root system was differentially reduced in response to the low potassium media between *Ler* and the NIL. Generally, for phosphate starvation a different trend was observed, the primary root growth is inhibited and the lateral roots increase. Such a general trend was never observed for potassium starved plants. Roots architecture does not seem to change and if changes were observed they seem to be species and condition dependent (Hodge, 2004; Amtmann et al., 2005). However, in accordance with our data is the observation of Armengaud et al (2004), who showed a lateral root reduction of *Arabidopsis thaliana* without an effect on root length, when the plants are grown on agar plates without potassium. A reduced biomass production caused by the reduced potassium availability, seem to affect the root and the shoot biomass equally. There is no indication that the growth reduction of one organ, root or rosette, precedes the other (and thereby causing the growth reduction of the later affected organ).

Another root architectural factor that may change potassium uptake is the root hair development. Root hairs were shown to effect the potassium uptake significantly (Rengel and Damon, 2008) and root hair mutants showed a decrease in potassium uptake and biomass production (Ahn et al., 2004). Root hair length increases in response to low potassium supply in some crops (Hogh-Jensen and Pedersen, 2003; Rengel and Damon, 2008) but for *Arabidopsis thaliana* this was reported to be only the case if ammonium is present in the medium (Amtmann et al., 2005), which was not the case in this setup. Accordingly, no differences in root hairs were observed between the conditions. A considerable variety in root hair density and length was shown for natural variants of *Arabidopsis thaliana* (Narang et al., 2000). However, *Ler* and *Kas-2* were not compared in the respective publication and there were no apparent differences found in root hair development for *Ler* and the NIL3. Root hair growth did not seem to cause the QTL effect. Therefore, genes involved in root hair development, which are also present in the fine mapped region, are unlikely to underlie the QTL effect.

The near isogenic lines (mainly the NIL3) and the recombinant inbred line RIL138 from which the NILs were derived, were further characterized. They were phenotyped under changing environmental conditions that might influence the response to the reduced potassium supply and for different physiological traits that might contribute to the rosette weight response phenotype. This was done in order to learn more about the QTL effect and to have the possibility to select putative candidate genes.

The first environmental change that was observed, was the impact of different levels of potassium reduction. The RIL138 was grown in a variety of potassium reduced solutions, starting with the reduction used for the mapping experiment until a nearly complete depletion of potassium in the growth media. The latter functioned as a negative control to show that there are no potassium impurities in the system itself that would influence the potassium concentration chosen for the experiment. The plants in the complete deprivation died which proved that there was really no potassium in the system at least not enough to sustain plant growth ( $> 10 \mu\text{M}$ ; Maathuis and Sanders, 1996). The other levels of potassium concentrations cover a range of external potassium supply that can either be taken up by a low affinity uptake mechanism (reduced potassium media used for the QTL detection, 10-fold and 13-fold reduction) or by a high affinity uptake mechanism (20-fold and 40-fold reduction; around  $100 \mu\text{M}$  potassium and below; Kochian and Lucas, 1988; Maathuis and Sanders, 1996). No matter which external potassium concentration was used, the response of the RIL138 was always more negative than the response of *Ler* and

therefore always in accordance with the QTL detection. The mechanism responsible for the QTL effect is consequently involved in the growth response in low and in high affinity uptake conditions.

The availability of potassium and the respective response of the plant are of course primary dependent on the external concentration of potassium but it is also influenced by other environmental factors. For example, the concentration of other minerals in the soil, like ammonium, can affect the potassium uptake. Ammonium can block high affinity potassium uptake and there are ammonium sensitive and insensitive pathways (Hirsch et al., 1998; Santa-Maria et al., 2000). The nutrient solution for the QTL detection did not contain any ammonium. The addition of ammonium to the solution resulted in the abolishment of the QTL effect. The response of *Ler* to the low potassium supply slightly reduced in the presence of ammonium, while the NILs response increased. There was no more response difference between these lines. The QTL effect is therefore clearly ammonium sensitive. However, if this sensitivity is due to an effect of ammonium on a potassium uptake protein in the reduced potassium supply, is questionable. While the rosette weight of *Ler* seems hardly affected by the addition of ammonium, the NILs rosette weight changed predominantly in the control condition. The higher weight of the NILs in the control with ammonium caused the increase in response, their weight in the reduced potassium supply was similar with and without ammonium. If lower potassium uptake in the reduced potassium supply with ammonium would cause the effect of growth response, one would expect that the response difference would be due to a decrease of weight in this condition. As this is not the case, an alternative explanation for the ammonium sensitivity of the QTL could be that the NILs might be capable of a higher ammonium usage efficiency. This higher ammonium usage efficiency however seems to be dependent on the potassium status of the plant. The NILs have only an advantage in ammonium usage if they are fully supplied with potassium (in the control condition), in the reduced potassium supply the higher usage of ammonium is not possible any more. This would explain why their rosette weight only increased in the control if ammonium was added but remained unchanged if ammonium was added in the reduced potassium supply. Another factor might be involved in this trait that is independent of the genetic basis of the rosette weight response QTL. An additional mapping experiment was performed in all four conditions (control and reduced potassium with and without ammonium) to elucidate if other genomic regions were affected by the ammonium supply. However, no response QTL were detected, neither with nor without ammonium (data not shown). Maybe the mapping power was too low due to

the reduced replicate and line number (five replicates; 85 RILs) that needed to be used to conduct the four experiments in parallel.

The photosynthetic period should influence the need for potassium, as it changes the growth of the plant (Zeevaart, 1971; Cookson et al., 2007). The increase in photoperiod length, from eight hours (mapping condition) to 14 hours long day conditions, did not change the QTL effect. The NIL3 was still found to have a significant lower response of rosette weight to the reduced potassium supply than *Ler*. Because the response QTL is not affected by day length, photosynthetic processes are less likely to be involved in the QTL effect.

Apart from growth related changes also changes in ion content were detected in the QTL mapping in response to the changing nutrient supply. Although, the response QTL for potassium content could not be validated with the NIL3, the NIL3 had higher rosette potassium content than *Ler* in the control and in the reduced potassium supply. The response in potassium concentration may not have been detected due to the small effect of the QTL (only five percent) which is difficult to prove significantly. Apart from the higher potassium content, the ionomic analysis showed that also the rubidium content in the rosette (*Rb\_rs*) was significantly higher in the NIL3 than in *Ler*. This can be seen as an independent replicate of the potassium content analysis. Most potassium transport studies use the rubidium isotope  $^{86}\text{Rb}^+$  which has a longer half time than the potassium isotope  $^{42}\text{K}^+$ . Rubidium is thought to be transported like the potassium ion (Läuchli and Epstein, 1970; Kochian and Lucas, 1982). Although, it was questioned if potassium and rubidium uptake is comparable under all conditions, the study of potassium transport with  $^{86}\text{Rb}$  is still the most widely used methodology (Britto and Kronzucker, 2008). In the root, the NIL3 had a reduced potassium content compared to *Ler* when grown in the low external potassium concentration. It may be assumed that increased allocation of potassium from the root to the shoot may occur in the NIL in reduced potassium supply. Higher potassium concentrations in the rosette might sustain processes like the carbohydrate allocation, or alter signalling mechanisms and thereby the NIL could attain a growth advantage over *Ler*. The higher potassium concentration in the NILs may result in a higher osmotic pressure. The weight response difference could be due to a higher water content of the NILs in low potassium supply, therefore the dry weight response of the lines was determined. *Ler* had always a higher response of the rosette dry weight than the NIL3/ RIL138. This was not significant in all cases, because the dry weight is very low, as are the differences between the lines. The statistical power to detect differences is reduced. However, the correlation



between the fresh and the dry weight response over all tested levels of potassium was very high for the RIL138 and *Ler*. Rosette fresh and rosette dry weight response are similar. It can therefore be assumed that the QTL affects really the biomass production of the plant and not just the water content.

Altered potassium concentration in the rosette may also affect the potassium concentration in the stomata. Stomata opening depends on potassium uptake on day onset (in the mid day sucrose can take over the osmotic function) and for stomatal closure (Talbot and Zeiger, 1996; Blatt, 2000). A reduction in potassium tissue concentration is accompanied by a reduction in turgor which can lead to stomatal closure (Hsiao and Läuchli, 1986 cited in: Benlloch-Gonzalez et al., 2010). Stomatal closure would lead to a reduction in water loss via transpiration. To look for differences in stomatal opening, the transpiration was investigated by studying the water loss of detached leaves. Both genotypes *Ler* and NIL3 showed a reduction in water loss when grown in the low potassium regime, maybe as a consequence of a decreased turgor. However, this water loss reduction was only significant in *Ler*. Furthermore, the NIL3 had a significantly higher water loss compared to *Ler* in both conditions. In summary, the water loss of the NIL3 is higher and less affected by the condition than the water loss of *Ler*. This may indeed result from the higher potassium concentration in the NIL3 compared to *Ler*, which enables the NIL to build up a higher turgor. This theory is in agreement with the fact that the stomata density did not change between the lines, thus the water loss can only be attributed to changes in the opening time of the stomata and not their number. Prolonged opening (or higher number of open stomata per time period) in the NIL3 may favour gas exchange and intake of CO<sub>2</sub>. The higher gas exchange of this line may in turn favour an enhanced biomass production of the NIL3 in the reduced potassium supply and thereby explain the QTL effect.

The study of the F1 generations that were heterozygous at the QTL position showed that the *Kas-2* allele which confers the reduced response of rosette weight to the lower potassium regime, is recessive. As the *Kas-2* allele confers a higher potassium concentration in the rosette along with the growth advantage, it is straight forward to assume that a more efficient potassium transporter might underlie the QTL effect. However, such a transporter would be more prone to be the dominant allele, as it would be likely to confer a higher uptake of potassium also in a heterozygous disposition. Therefore, it would be more probable, that the recessive *Kas-2* allele constitutes a (maybe less functional) signalling component or regulatory domain of a gene involved in the potassium responsive pathway.

In conclusion, the genetic factor underlying the QTL affects rosette and root weight equally and has no effect on root hair development. It seems to have an effect on the water loss of the plants maybe by regulating the stomatal opening time. However, the QTL is not caused by water content changes in the cell but by a real difference in biomass accumulation. It is so far correlating with an increase in potassium content in the rosette and is implicated in the potassium response to low and high affinity uptake ranges of external potassium. For the response to the high affinity uptake range (20-fold potassium reduction) ammonium sensitivity could be demonstrated.

#### **4.4 The candidates, what is likely to cause the QTL effect?**

According to the functional annotation of the Col-0 genes in the fine mapped region (between 22.03 Mbp and 25.95 Mbp) a discussion of possible candidates can be done. The most likely candidates (Figure R15) in this region that might cause the QTL effect, are of course those genes that are known to be directly influenced by the potassium status of the plant or are involved in its translocation. To the first category belong the putative pyruvate kinase (AT5G56350) and the response regulator ARR6 (AT5G62920). Pyruvate kinases were shown to depend for their activity on potassium (Ramírez-Silva et al., 1993). Because the QTL effect was not altered in long day conditions, it was assumed that genes involved in photosynthesis and carbon fixation are, of course not excluded as candidates but less likely. Therefore, the putative pyruvate kinase (Andre et al., 2007) is less probable to be involved in the QTL effect. The response regulator ARR6 was identified in a screen for homologues of bacterial response regulators and it was shown to be upregulated in response to low potassium supply (Coello and Polacco, 1999). The transcription analysis performed in this work did neither demonstrate an upregulation of this gene in *Ler* or the recombinant line R5 nor a differential regulation between the lines. This reduces the possibility of the involvement of this gene in the QTL effect (at least at the expression level).

The putative potassium channels FIP2 (AT5G55000) and CNCG5 (AT5G57940) and the potassium channel TPK1 (AT5G55630) could directly act on the potassium status of the plant, by potassium allocation. There is not too much known about the two putative potassium channels. FIP2 is located at the position 22.3 Mbp on chromosome five (above the marker MDF20). It has sequence homology to animal K<sup>+</sup>ATPases (Banno and Chua, 2000) and has a BTB domain which has not been implicated into specific cellular functions

(80 proteins with a BTB-domain were found in Arabidopsis) but was associated with ethylene biosynthesis, hormonal perception and disease resistance (Gingerich et al., 2005). FIP2 transcript was shown to be enriched, among 290 other transcripts, in the quiescent center of the root compared to the surrounding tissue (Nawy et al., 2005). It was shown to interact with the protein AFH1 and supposed to form a complex in cell membranes that controls the actin cytoskeleton. The involvement in actin organisation was deduced from the domain homologies of AFH1 (Banno and Chua, 2000). CNGC5 (at 23.5 Mbp; below the marker MUL3-1) is a cyclic nucleotide-gated ion channel, a family with 20 members in Arabidopsis (Köhler et al., 1999; Mäser et al., 2001) that were so far implicated in cation homeostasis and play roles in development (Chan et al., 2003; Gobert et al., 2006) and in response to biotic stimuli (Balagué et al., 2003; Jurkowski et al., 2004). They are Shaker-like channels with six transmembrane domains and a single pore (Varnum and Zagotta, 1997; Mäser et al., 2001). They are generally unspecific for the transport of mono- and divalent cations and are believed to be activated by cyclic nucleotides and inhibited by calmodulin (Köhler et al., 1999; Kaplan et al., 2007). CNGC5 is a plasma membrane protein and its mRNA is equally expressed in roots and the rosette (Christopher et al., 2007). There are no publications to date that would have shown that FIP2 and CNGC5 perform potassium or general cation translocation. Therefore, their involvement in the effect of the response QTL to low potassium supply cannot be fully established.

The channel TPK1 (formerly KCO1) is located at the position 22.53 Mbp close to marker MDF20. It belongs to the two-pore  $K^+$  channel (TPK) family which has five members in Arabidopsis, of which it is the most abundantly expressed member (Becker et al., 2004; Gobert et al., 2007). Its opening is voltage independent but depends on pH and calcium. TPK1 is a vacuolar membrane protein with a strong selectivity for potassium over sodium (Bihler et al., 2005). Vacuolar proteins have a presumed house keeping function in ion homeostasis (Dunkel et al., 2008). Indeed, knock out mutants of TPK1 were shown to have a reduced fresh weight (of 14 days old plants) when grown in extremely low (10  $\mu$ M) or very high (80 mM) supply of potassium, while on the contrary overexpression lines of TPK1 performed better than the Col-0 wild type (Gobert et al., 2007). However, these plants showed no significant alterations in overall tissue concentration of potassium and therefore it was suggested that TPK1 has a role in inter- and intracellular distribution of potassium. Furthermore, TPK1 is important for the ABA induced potassium release from the vacuole during stomatal closure (Gobert et al., 2007). The channel TPK1 is the best candidate to explain the QTL effect. As it is involved in inter- and intracellular potassium

homeostasis it could play a role in both, low and high affinity uptake ranges of external potassium supply and mutations of the gene were already shown to affect plant fresh weight in potassium stress conditions. In potassium deficiency, the cytosolic concentration of potassium is maintained by allocation of potassium from the vacuole and K-efficient barley accessions were shown to have a better vacuolar/cytoplasmic allocation (Rengel and Damon, 2008). In addition, due to its predicted role in intercellular homeostasis it could function in the hypothesized increased allocation of potassium from the root to the rosette in the NIL3. This better allocation from non photosynthetic organs to photosynthetic organs is assumed to cause a better adaptation to potassium starvation (Rengel and Damon, 2008). Rice varieties with a better potassium usage efficiency were shown to allocate more potassium to younger leaves and maintained thereby a higher stomatal conductance and photosynthetic activity in the bolting phase (Yang et al., 2004). Moreover, its involvement in stomatal closure could explain the water loss phenotype that was observed in the NIL3. Allelic differences between *Ler* and *Kas-2* could cause a delay in potassium outward conductance and thereby increasing the opening time of the stomata. Sequencing the TPK1-loci revealed several polymorphisms between the *Ler* and the *Kas-2* alleles. For example, the predicted non-synonymous amino acid polymorphism in the EF-hand motif close to the ER-export signal might affect the posttranscriptional regulation of TPK1 by calcium or the channel density in the vacuolar membrane via ER retention (Zerangue et al., 1999; Dunkel et al., 2008). In addition, the polymorphisms in the URTs might cause subtle transcriptional changes which might not have been detected by the microarray experiment. Although, Gobert et al. (2007) showed no significant differences in potassium content in the *tpk1* mutant compared to the wild type, the mutant had a slightly lower potassium content. Maybe TPK1 also has a minor role in potassium uptake but it is redundant with other transport mechanism that outweigh the effect of TPK1 in the Col-0 background (but which becomes more relevant in the *Ler* background). Or other transport proteins in the NILs (maybe the channel CNGC5) work more efficiently and thereby cause the increased potassium content of the NILs and causing together with the TPK1 channel to the growth response effect. Unfortunately, there is no data available if TPK1 is sensitive to ammonium. However, as discussed before, the ammonium sensitivity of the QTL might depend rather on an additional factor located in the NILs *Kas-2* introgression that confers high ammonium usage efficiency, rather than an ammonium sensitive potassium transporting protein. So far, ammonium sensitivity was just demonstrated for the high affinity uptake which is mainly performed by transporter and rarely by channels (Hirsch et

al., 1998; Szczerba et al., 2006). This would furthermore argue for the involvement of another component in the QTL effect.

The transcription analysis revealed that 32 genes were differentially transcribed in the rosette between *Ler* and the recombinant line R5 (Figure R13) and 389 genes were differentially transcribed in response to the growth conditions (control vs. low K) in the two lines. A previous study (Armengaud et al., 2004) revealed 116 differentially regulated genes in the rosette due to potassium starvation of which three (At5G24150, At5G40780, At2G29350) were in common with the present study. The allelic differences (Col-0 and *Ler*/Kas-2, respectively) combined with drastically different growth conditions (Armengaud et al. grew the plants on agar plates with sucrose in a complete deprivation of potassium) and different plant age (14 days old plants vs. 32 days old plants), will cause huge transcriptional differences. These transcriptional changes might mask common differentially expressed genes in the statistical analysis of the present study and the study of Armengaud et al. (2004) and explain the expression discrepancies between the two studies. It would have been necessary to analyse both dataset together but this was not possible as different chip technologies were used. Expression changes after potassium starvation were already reported to depend highly on the accompanying environmental factors, even HAK5 expression, which is one of the most highly expressed root potassium transporter in potassium deficient conditions (Gierth et al., 2005; Gierth and Maser, 2007). However, the genes that were shown to be differentially regulated between *Ler* and the recombinant line R5 are generally genes that could be well involved in potassium responses. The expression differences affected genes involved in salt stress, senescence, hormone and calcium signalling, pathogen defence and a photosystem protein. Two genes for cell wall biogenesis and a gene involved in cell adhesion were also differentially regulated between the lines. The gene AFH1, that was shown to interact with the potential potassium channel FIP2, was implicated in actin cytoskeleton organisation. The actin skeleton is further thought to guide the cellulose synthesis complex that is required for cell wall synthesis (Buchanan et al., 2002). An indirect involvement of FIP2 in cell wall synthesis is thereby possible and the three differentially regulated genes for cell wall biogenesis/ adhesion may be involved in a downstream pathway of FIP2. They might act together to contribute to cell growth and to the QTL effect. Cell wall related proteins were already shown to be differentially transcribed in response to potassium deficiency and may play a role in growth adaptations, signalling and ROS detoxification (Armengaud et al., 2004; Amtmann et al., 2005). Another possibility to relate the differentially transcribed

genes to the QTL effect are the ABA responsive genes and the putative calcium ATPase that might play a role in an upstream signalling pathway for the calcium dependent channel TPK1 and thereby modulating its function.

#### **4.5 Conclusion and outlook**

A QTL for rosette weight in response to reduced potassium supply was validated and further phenotypically characterized, using developed near isogenic lines. The QTL effect was present over a wide range of external potassium supplies and in the high affinity uptake range, it was shown to be sensitive to ammonium. The NIL3 had an increased rosette potassium concentration and water loss, the latter is likely caused by altered opening periods of the stomata. With recombinant lines the QTL could be narrowed down to a region of ca 3.9 Mbp containing most likely several genes that contribute to the response QTL. The vacuolar channel TPK1 is a plausible candidate in this region, as it was shown to function in potassium homeostasis, growth and stomata closure. It could potentially exert its effect on the QTL by a differential regulation due to upstream ABA or calcium signalling components or in interplay with a putative potassium channel that might increase the potassium content in the plant while TPK1 is responsible for the subsequent usage efficiency.

The fine mapping of the QTL offered genetic candidates for plant responses to reduced potassium supply and a selection of potential upstream and downstream targets of those candidates. Complementation tests with one or several of those candidate genes in one transformant may elucidate their role in the observed potassium dependent growth effects. The TPK1-gene had polymorphisms in the coding region but, even more extensively, in the 5'UTR and 3'UTR, an effect on gene transcription cannot be ruled out and an rtPCR analysis would be a sensitive approach to test for this. For most growth QTL, as well as for the rosette weight response QTL, a polygenic basis was assumed (Kroymann and Mitchell-Olds, 2005) with a complex regulation that allows the plant to adapt to environmental changes. The identification of genes that cause the QTL effects will increase our knowledge of the complex pathways growth regulation to potassium deficiency is build upon. It is tempting to speculate that similar mechanism might underlie potassium efficiency in crop plants and that the elucidation of alleles that confer a higher fresh weight to plants in low potassium conditions might help in future breeding strategies.

## References

- Abbasi MK, Rasool G** (2005) Effects of different land-use types on soil quality in the hilly area of Rawalakot Azad Jammu and Kashmir. *Acta Agr Scand* **55**: 221-228
- Ahn SJ, Shin R, Schachtman DP** (2004) Expression of KT/KUP genes in Arabidopsis and the role of root hairs in K<sup>+</sup> uptake. *Plant Physiol* **134**: 1135-1145
- Alcázar R, García AV, Parker JE, Reymond M** (2009) Incremental steps toward incompatibility revealed by Arabidopsis epistatic interactions modulating salicylic acid pathway activation. *Proc Natl Acad Sci USA* **106**: 334-339
- Alonso-Blanco C, Aarts MG, Bentsink L, Keurentjes JJ, Reymond M, Vreugdenhil D, Koornneef M** (2009) What has natural variation taught us about plant development, physiology, and adaptation? *Plant Cell* **21**: 1877-1896
- Alonso-Blanco C, Koornneef M** (2000) Naturally occurring variation in Arabidopsis: an underexploited resource for plant genetics. *Trends Plant Sci* **5**: 22-29
- Amtmann A, Hammond JP, Armengaud P, White PJ, Callow JA** (2005) Nutrient sensing and signalling in plants: potassium and phosphorus. *In Advances in Botanical Research*, Vol 43. Academic Press, pp 209-257
- Amtmann A, Troufflard S, Armengaud P** (2008) The effect of potassium nutrition on pest and disease resistance in plants. *Physiol Plantarum* **133**: 682-691
- Anderson JA, Huprikar SS, Kochian LV, Lucas WJ, Gaber RF** (1992) Functional expression of a probable *Arabidopsis thaliana* potassium channel in *Saccharomyces cerevisiae*. *Proc Natl Acad Sci USA* **89**: 3736-3740
- Andre C, Froehlich JE, Moll MR, Benning C** (2007) A heteromeric plastidic pyruvate kinase complex involved in seed oil biosynthesis in Arabidopsis. *Plant Cell* **19**: 2006-2022
- Armengaud P, Breitling R, Amtmann A** (2004) The potassium-dependent transcriptome of Arabidopsis reveals a prominent role of jasmonic acid in nutrient signaling. *Plant Physiol* **136**: 2556-2576
- Ashley MK, Grant M, Grabov A** (2006) Plant responses to potassium deficiencies: a role for potassium transport proteins. *J Exp Bot* **57**: 425-436
- Balagué C, Lin B, Alcon C, Flottes G, Malmström S, Köhler C, Neuhaus G, Pelletier G, Gaymard F, Roby D** (2003) HLM1, an essential signalling component in the hypersensitive response, is a member of the cyclic nucleotide-gated channel ion channel family. *Plant Cell* **15**: 365-379
- Banno H, Chua NH** (2000) Characterization of the Arabidopsis formin-like protein AFH1 and its interacting protein. *Plant Cell Physiol* **41**: 617-626
- Basile B, Reidel EJ, Weinbaum SA, DeJong TM** (2003) Leaf potassium concentration, CO<sub>2</sub> exchange and light interception in almond trees (*Prunus dulcis* (Mill) D.A. Webb). *Scientia Horticulturae* **98**: 185-194
- Bates TR, Lynch JP** (1996) Simulation of root hair elongation in *Arabidopsis thaliana* by low phosphorus availability. *Plant Cell Environ* **19**: 529-538
- Becker D, Geiger D, Dunkel M, Roller A, Bertl A, Latz A, Carpaneto A, Dietrich P, Roelfsema MRG, Voelker C, Schmidt D, Mueller-Roeber B, Czempinski K, Hedrich R** (2004) AtTPK4, an Arabidopsis tandem-pore K<sup>+</sup> channel, poised to control the pollen membrane voltage in a pH- and Ca<sup>2+</sup>-dependent manner. *Proc Natl Acad Sci USA* **101**: 15621-15626
- Benloch-Gonzalez M, Romera J, Cristescu S, Harren F, Fournier JM, Benloch M** (2010) K<sup>+</sup> starvation inhibits water-stress-induced stomatal closure via ethylene synthesis in sunflower plants. *J Exp Bot* **61**: 1139-1145

- Bihler H, Eing C, Hebeisen S, Roller A, Czempinski K, Bertl A** (2005) TPK1 is a vacuolar ion channel different from the slow-vacuolar cation channel. *Plant Physiol* **139**: 417-424
- Blatt MR** (2000) Cellular signaling and volume control in stomatal movements in plants. *Annu Rev Cell Dev Biol* **16**: 221-241
- Breitling R, Armengaud P, Amtmann A, Herzyk P** (2004) Rank products: a simple, yet powerful, new method to detect differentially regulated genes in replicated microarray experiments. *FEBS Lett* **573**: 83-92
- Brinkmann R** (1967) *Lehrbuch der Allgemeinen Geologie*, Ed Bd.III. Enke-Verlag, Stuttgart; 630 pp.
- Britto DT, Kronzucker HJ** (2008) Cellular mechanisms of potassium transport in plants. *Physiol Plantarum* **133**: 637-650
- Britto DT, Siddiqi MY, Glass AD, Kronzucker HJ** (2001) Futile transmembrane  $\text{NH}_4^+$  cycling: a cellular hypothesis to explain ammonium toxicity in plants. *Proc Natl Acad Sci USA* **98**: 4255-4258
- Brownlee C** (2002) Plant  $\text{K}^+$  transport: not just an uphill struggle. *Curr Biol* **12**: R402-404
- Buch-Pedersen MJ, Rudashevskaya EL, Berner TS, Venema K, Palmgren MG** (2006) Potassium as an intrinsic uncoupler of the plasma membrane  $\text{H}^+$ -ATPase. *J Biol Chem* **281**: 38285-38292
- Buchanan BB, Grissem W, Jones RJ** (2002) *Biochemistry & molecular biology of plants*. John Wiley & Sons, Ltd., West Sussex, 1366 pp.
- Carden DE, Walker DJ, Flowers TJ, Miller AJ** (2003) Single-cell measurements of the contributions of cytosolic  $\text{Na}^+$  and  $\text{K}^+$  to salt tolerance. *Plant Physiol* **131**: 676-683
- Chan CW, Schorrak LM, Smith RK, Jr., Bent AF, Sussman MR** (2003) A cyclic nucleotide-gated ion channel, CNGC2, is crucial for plant development and adaptation to calcium stress. *Plant Physiol* **132**: 728-731
- Chen A, Baumann U, Fincher GB, Collins NC** (2009) Flt-2L, a locus in barley controlling flowering time, spike density, and plant height. *Funct Integr Genomics* **9**: 243-254
- Chen YF, Wang Y, Wu WH** (2008) Membrane transporters for nitrogen, phosphate and potassium uptake in plants. *J Integr Plant Biol* **50**: 835-848
- Chinnusamy V, Zhu JK** (2009) Epigenetic regulation of stress responses in plants. *Curr Opin Plant Biol* **12**: 133-139
- Christopher DA, Borsics T, Yuen CY, Ullmer W, Andeme-Ondzighi C, Andres MA, Kang BH, Staehelin LA** (2007) The cyclic nucleotide gated cation channel AtCNGC10 traffics from the ER via Golgi vesicles to the plasma membrane of Arabidopsis root and leaf cells. *BMC Plant Biol* **7**: 48
- Clarkson DT** (1980) The mineral nutrition of higher plants. *Ann. Rev. Plant Physiol.* **31**: 239-298
- Coello P, Polacco JC** (1999) ARR6, a response regulator from Arabidopsis, is differentially regulated by plant nutritional status. *Plant Science* **143**: 211-220
- Cookson SJ, Chenu K, Granier C** (2007) Day length affects the dynamics of leaf expansion and cellular development in *Arabidopsis thaliana* partially through floral transition timing. *Ann Bot* **99**: 703-711
- Czempinski K, Zimmermann S, Ehrhardt T, Muller-Rober B** (1997) New structure and function in plant  $\text{K}^+$  channels: KCO1, an outward rectifier with a steep  $\text{Ca}^{2+}$  dependency. *Embo J* **16**: 2565-2575
- Dean-Drummond CE, Glass ADM** (1983) Short term studies of nitrate uptake into barley plants using ion-specific electrodes and  $^{36}\text{ClO}_3^-$ . *Plant Physiol* **73**: 105-110



- Deeken R, Geiger D, Fromm J, Koroleva O, Ache P, Langenfeld-Heyser R, Norbert Sauer N, May ST, Rainer Hedrich R** (2002) Loss of the AKT2/3 potassium channel affects sugar loading into the phloem of *Arabidopsis*. *Planta* **216**: 334-344
- Deeken R, Sanders C, Ache P, Hedrich R** (2000) Developmental and light-dependent regulation of a phloem-localised K<sup>+</sup> channel of *Arabidopsis thaliana*. *Plant J* **23**: 285-290
- Dietrich P, Sanders C, Hedrich R** (2001) The role of ion channels in light-dependent stomatal opening. *J Exp Bot* **52**: 1959-1967
- Duby G, Hosy E, Fizames C, Alcon C, Costa A, Sentenac H, Thibaud JB** (2008) AtKC1, a conditionally targeted Shaker-type subunit, regulates the activity of plant K<sup>+</sup> channels. *Plant J* **53**: 115-123
- Dunkel M, Latz A, Schumacher K, Muller T, Becker D, Hedrich R** (2008) Targeting of vacuolar membrane localized members of the TPK channel family. *Mol Plant* **1**: 938-949
- El-Dessougi H, Claassen N, Steingrobe B** (2002) Potassium efficiency mechanisms of wheat, barley, and sugar beet grown on a K fixing soil under controlled conditions. *J Plant Nutr Soil Sc* **165**: 732-737
- El-Lithy ME, Bentsink L, Hanhart CJ, Ruys GJ, Rovito D, Broekhof JLM, van der Poel HJA, van Eijk MJT, Vreugdenhil D, Koornneef M** (2006) New *Arabidopsis* recombinant inbred line populations genotyped using SNPWave and their use for mapping flowering-time quantitative trait loci. *Genetics* **172**: 1867-1876
- Epstein E, Rains DW, Elzam OE** (1963) Resolution of dual mechanisms of potassium absorption by barley roots. *Proc Natl Acad Sci USA* **49**: 684-692
- Fu HH, Luan S** (1998) AtKup1: a dual-affinity K<sup>+</sup> transporter from *Arabidopsis*. *Plant Cell* **10**: 63-73
- Fuchs I, Philippar K, Hedrich R** (2006) Ion channels meet auxin action. *Plant Biol* **8**: 353-359
- Galpaz N, Wang Q, Menda N, Zamir D, Hirschberg J** (2008) Abscisic acid deficiency in the tomato mutant high-pigment 3 leading to increased plastid number and higher fruit lycopene content. *Plant J* **53**: 717-730
- Gautier L, Cope L, Bolstad BM, Irizarry RA** (2004) affy—analysis of Affymetrix GeneChip data at the probe level. *Bioinformatics* **20**: 307-315
- Gaymard F, Pilot G, Lacombe B, Bouchez D, Bruneau D, Boucherez J, Michaux-Ferriere N, Thibaud JB, Sentenac H** (1998) Identification and disruption of a plant shaker-like outward channel involved in K<sup>+</sup> release into the xylem sap. *Cell* **94**: 647-655
- Gierth M, Maser P** (2007) Potassium transporters in plants - involvement in K<sup>+</sup> acquisition, redistribution and homeostasis. *FEBS Lett* **581**: 2348-2356
- Gierth M, Maser P, Schroeder JI** (2005) The potassium transporter AtHAK5 functions in K<sup>+</sup> deprivation-induced high-affinity K<sup>+</sup> uptake and AKT1 K<sup>+</sup> channel contribution to K<sup>+</sup> uptake kinetics in *Arabidopsis* roots. *Plant Physiol* **137**: 1105-1114
- Gingerich DJ, Gagne JM, Salter DW, Hellmann H, Estelle M, Ma L, Vierstra RD** (2005) Cullins 3a and 3b assemble with members of the broad complex/tramtrack/bric-a-brac (BTB) protein family to form essential ubiquitin-protein ligases (E3s) in *Arabidopsis*. *J Biol Chem* **280**: 18810-18821
- Gobert A, Isayenkov S, Voelker C, Czempinski K, Maathuis FJ** (2007) The two-pore channel TPK1 gene encodes the vacuolar K<sup>+</sup> conductance and plays a role in K<sup>+</sup> homeostasis. *Proc Natl Acad Sci USA* **104**: 10726-10731

- Gobert A, Park G, Amtmann A, Sanders D, Maathuis FJM** (2006) *Arabidopsis thaliana* Cyclic Nucleotide Gated Channel 3 forms a nonselective ion transporter involved in germination and cation transport. *J Exp Bot* **57**: 791-800
- Guo F-Q, Young J, Crawford NM** (2003) The nitrate transporter AtNRT1.1 (CHL1) functions in stomatal opening and contributes to drought susceptibility in *Arabidopsis*. *Plant Cell* **15**: 107-117
- Haeder HE, Mengel K, Forster H** (1973) The effect of potassium on translocation of photosynthates and yield pattern of potato plants. *J Sci Food Agric* **24**: 1479-1487
- Harada H, Kuromori T, Hirayama T, Shinozaki K, Leigh RA** (2004) Quantitative trait loci analysis of nitrate storage in *Arabidopsis* leading to an investigation of the contribution of the anion channel gene, AtCLC-c, to variation in nitrate levels. *J Exp Bot* **55**: 2005-2014
- Harada H, Leigh RA** (2006) Genetic mapping of natural variation in potassium concentrations in shoots of *Arabidopsis thaliana*. *J Exp Bot* **57**: 953-960
- Hermans C, Hammond JP, White PJ, Verbruggen N** (2006) How do plants respond to nutrient shortage by biomass allocation? *Trends Plant Sci* **11**: 610-617
- Hirsch RE, Lewis BD, Spalding EP, Sussman MR** (1998) A role for the AKT1 potassium channel in plant nutrition. *Science* **280**: 918-921
- Hodge A** (2004) The plastic plant: root responses to heterogeneous supplies of nutrients. *New Phytol* **162**: 9-24
- Hogh-Jensen H, Pedersen MB** (2003) Morphological plasticity by crop plants and their potassium use efficiency. *J Plant Nutr* **26**: 969-984
- Hsiao TC, Läuchli A** (1986) A role of potassium in plant-water relations; In: Tinker B, Läuchli A "Advances in plant nutrition, Vol.2". Praeger Scientific, New York: pp. 281-311
- Imas M, Imas P** (2007) Evaluation of potassium compared to other osmolytes in relation to osmotic adjustment and drought tolerance of chickpea under water deficit environments. *J Plant Nutr* **30**: 517-535
- Irizarry R, Bolstad B, Collin F, Cope L, Hobbs B, Speed T** (2003) Summaries of Affymetrix GeneChip probe level data. *Nucleic Acids Res* **31**: e15
- Jansen RC, Nap JP** (2001) Genetical genomics: the added value from segregation. *Trends Genet* **17**: 388-391
- Jung JY, Shin R, Schachtman DP** (2009) Ethylene mediates response and tolerance to potassium deprivation in *Arabidopsis*. *Plant Cell* **21**: 607-621
- Jurkowski GI, Smith RK, Jr., Yu IC, Ham JH, Sharma SB, Klessig DF, Fengler KA, Bent AF** (2004) *Arabidopsis* DND2, a second cyclic nucleotide-gated ion channel gene for which mutation causes the "defense, no death" phenotype. *Mol Plant Microbe Interact* **17**: 511-520
- Kachmar JF, Boyer PD** (1953) Kinetic analysis of enzyme reactions:II. The potassium activation and calcium inhibition of pyruvic phosphoferase *J Biol Chem* **200**: 669-682
- Kaplan B, Sherman T, Fromm H** (2007) Cyclic nucleotide-gated channels in plants. *FEBS Letters* **581**: 2237-2246
- Keurentjes JJ, Fu J, de Vos CH, Lommen A, Hall RD, Bino RJ, van der Plas LH, Jansen RC, Vreugdenhil D, Koornneef M** (2006) The genetics of plant metabolism. *Nat Genet* **38**: 842-849
- Keurentjes JJ, Fu J, Terpstra IR, Garcia JM, van den Ackerveken G, Snoek LB, Peeters AJ, Vreugdenhil D, Koornneef M, Jansen RC** (2007a) Regulatory network construction in *Arabidopsis* by using genome-wide gene expression quantitative trait loci. *Proc Natl Acad Sci USA* **104**: 1708-1713

- Keurentjes JJB, Bentsink L, Alonso-Blanco C, Hanhart CJ, Blankestijn-De Vries H, Effgen S, Vreugdenhil D, Koornneef M** (2007b) Development of a near-isogenic line population of *Arabidopsis thaliana* and comparison of mapping power with a recombinant inbred line population. *Genetics* **175**: 891-905
- Kochian LV, Lucas WJ** (1982) Potassium transport in corn roots: I. Resolution of kinetics into a saturable and linear component. *Plant Physiol* **70**: 1723-1731
- Kochian LV, Lucas WJ** (1988) Potassium transport in roots. *Adv. Bot. Res.* **15**: 93-178
- Köhler C, Merkle T, Neuhaus G** (1999) Characterisation of a novel gene family of putative cyclic nucleotide- and calmodulin-regulated ion channels in *Arabidopsis thaliana*. *Plant J* **18**: 97-104
- Koornneef M, Alonso-Blanco C, Vreugdenhil D** (2004) Naturally occurring genetic variation in *Arabidopsis thaliana*. *Annu Rev Plant Biol* **55**: 141 - 172
- Kronzucker HJ, Szczerba MW, Schulze LM, Britto DT** (2008) Non-reciprocal interactions between  $K^+$  and  $Na^+$  ions in barley (*Hordeum vulgare* L.). *J Exp Bot* **59**: 2793-2801
- Kroymann J, Mitchell-Olds T** (2005) Epistasis and balanced polymorphism influencing complex trait variation. *Nature* **435**: 95-98
- Larsen JB** (1976) Untersuchungen über die Frostempfindlichkeit von Douglasienherkünften und über den Einfluss der Nährstoffversorgung auf die Frostresistenzen der Douglasie. *Forst- und Holzwirt.* **15**: 299-302
- Läuchli A, Epstein E** (1970) Transport of potassium and rubidium in plant roots: The significance of calcium. *Plant Physiol* **45**: 639-641
- Lea-Cox JD, Stutte GW, Berry WL, Wheeler RM** (1999) Nutrient dynamics and pH/charge-balance relationships in hydroponic solutions. *Acta Hort.* **481**: 241-249
- Lebaudy A, Very AA, Sentenac H** (2007)  $K^+$  channel activity in plants: genes, regulations and functions. *FEBS Lett* **581**: 2357-2366
- Lee SC, Lan WZ, Kim BG, Li L, Cheong YH, Pandey GK, Lu G, Buchanan BB, Luan S** (2007) A protein phosphorylation/dephosphorylation network regulates a plant potassium channel. *Proc Natl Acad Sci USA* **104**: 15959-15964
- Lehninger AL, Nelson DL, Cox MM** (1993) Principles of biochemistry, Ed 2nd. Worth Publishers, Inc., New York, 1013 pp.
- Leigh RA, Jones RGW** (1984) A hypothesis relating critical potassium concentrations for growth to the distribution and functions of this ion in the plant cell. *New Phytol* **97**: 1-13
- Li J, Lee YR, Assmann SM** (1998) Guard cells possess a calcium-dependent protein kinase that phosphorylates the KAT1 potassium channel. *Plant Physiol* **116**: 785-795
- Li L, Kim BG, Cheong YH, Pandey GK, Luan S** (2006) A  $Ca^{2+}$  signaling pathway regulates a  $K^{+}$  channel for low-K response in *Arabidopsis*. *Proc Natl Acad Sci USA* **103**: 12625-12630
- Liebersbach H, Bernd Steingrobe B, Norbert Claassen N** (2004) Roots regulate ion transport in the rhizosphere to counteract reduced mobility in dry soil. *Plant Soil* **260**: 79-88
- Loudet O, Chaillou S, Krapp A, Daniel-Vedele F** (2003) Quantitative trait loci analysis of water and anion contents in interaction with nitrogen availability in *Arabidopsis thaliana*. *Genetics* **163**: 711-722
- Maathuis FJ** (2009) Physiological functions of mineral macronutrients. *Curr Opin Plant Biol* **12**: 250-258
- Maathuis FJM, Ichida AM, Sanders D, Schroeder J** (1997) Roles of higher plant  $K^+$  channels. *Plant Physiol* **114**: 1141-1149

- Maathuis FJM, Sanders D** (1996) Mechanisms of potassium absorption by higher plant roots. *Physiol Plantarum* **96**: 158-168
- Maloof JN** (2003) Genomic approaches to analyzing natural variation in *Arabidopsis thaliana*. *Current Opinion in Genetics & Development* **13**: 576-582
- Marschner H** (1995) Mineral nutrition of higher plants, Ed 2nd. Academic Press Inc., London, 889 pp.
- Mäser P, Thomine S, Schroeder JI, Ward JM, Hirschi K, Sze H, Talke IN, Amtmann A, Maathuis FJ, Sanders D, Harper JF, Tchieu J, Gribskov M, Persans MW, Salt DE, Kim SA, Guerinot ML** (2001) Phylogenetic relationships within cation transporter families of *Arabidopsis*. *Plant Physiol* **126**: 1646-1667
- Mendez-Vigo B, Andres MT, Ramiro M, Martinez-Zapater JM, Alonso-Blanco C** (2010) Temporal analysis of natural variation for the rate of leaf production and its relationship with flowering initiation in *Arabidopsis thaliana*. *J Exp Bot* **61**: 1611-1623
- Moody PW, Bell MJ** (2006) Availability of soil potassium and diagnostic soil tests. *Aust. J. Soil Res.* **44**: 265-275
- Mouline K, Very AA, Gaymard F, Boucherez J, Pilot G, Devic M, Bouchez D, Thibaud JB, Sentenac H** (2002) Pollen tube development and competitive ability are impaired by disruption of a Shaker K(+) channel in *Arabidopsis*. *Genes Dev* **16**: 339-350
- Munson RD, Nelson WL** (1963) Movement of applied potassium in soils. *J Agr Food Chem* **11**: 193-201
- Murashige T, Skoog F** (1962) A revised medium for rapid growth and bio assay with tobacco tissue cultures. *Physiol Plantarum* **15**: 473-497
- Narang RA, Bruene A, Altmann T** (2000) Analysis of phosphate acquisition efficiency in different *Arabidopsis* accessions. *Plant Physiol* **124**: 1786-1799
- Nawy T, Lee JY, Colinas J, Wang JY, Thongrod SC, Malamy JE, Birnbaum K, Benfey PN** (2005) Transcriptional profile of the *Arabidopsis* root quiescent center. *Plant Cell* **17**: 1908-1925
- Nazoa P, Vidmar JJ, Tranbarger TJ, Mouline K, Damiani I, Tillard P, Zhuo D, Glass AD, Touraine B** (2003) Regulation of the nitrate transporter gene *AtNRT2.1* in *Arabidopsis thaliana*: responses to nitrate, amino acids and developmental stage. *Plant Mol Biol* **52**: 689-703
- Nitsos RE, Evans HJ** (1969) Effects of univalent cations on the activity of particulate starch synthetase. *Plant Physiol* **44**: 1260-1266
- Palmgren MG** (2001) Plant plasmamembrane H<sup>+</sup>-ATPases: powerhouses for nutrient uptake. *Annu Rev Plant Physiol Plant Mol Biol* **52**: 817-845
- Pandey S, Zhang W, Assmann SM** (2007) Roles of ion channels and transporters in guard cell signal transduction. *FEBS Lett* **581**: 2325-2336
- Peiter E, Maathuis FJ, Mills LN, Knight H, Pelloux J, Hetherington AM, Sanders D** (2005) The vacuolar Ca<sup>2+</sup>-activated channel TPC1 regulates germination and stomatal movement. *Nature* **434**: 404-408
- Peoples TR, Koch DW** (1979) Role of potassium in carbon dioxide assimilation in *Medicago sativa* L. *Plant Physiol* **63**: 878-881
- Pettigrew WT** (2008) Potassium influences on yield and quality production for maize, wheat, soybean and cotton. *Physiol Plantarum* **133**: 670-681
- Philippar K, Fuchs I, Luthen H, Hoth S, Bauer CS, Haga K, Thiel G, Ljung K, Sandberg G, Bottger M, Becker D, Hedrich R** (1999) Auxin-induced K<sup>+</sup> channel expression represents an essential step in coleoptile growth and gravitropism. *Proc Natl Acad Sci U S A* **96**: 12186-12191

- Pieper B** (2009) The genetic and molecular basis of natural variation for plant growth and related traits in *Arabidopsis thaliana*. Wageningen University, Wageningen, 131 pp.
- Pilot G, Gaymard F, Mouline K, Cherel I, Sentenac H** (2003) Regulated expression of *Arabidopsis* shaker K<sup>+</sup> channel genes involved in K<sup>+</sup> uptake and distribution in the plant. *Plant Mol Biol* **51**: 773-787
- Porra RJ** (2002) The chequered history of the development and use of simultaneous equations for the accurate determination of chlorophylls a and b. *Photosynth Res* **73**: 149-156
- Prinzenberg AE, Barbier H, Salt DE, Stich B, Reymond M** (2010) Relationships between growth, growth response to nutrient supply, and ion content using a recombinant inbred line population in *Arabidopsis*. *Plant Physiol* **154**: 1361-1371
- Pyo Y, Gierth M, Schroeder JI, Cho MH** (2010) High-affinity K<sup>+</sup> transport in *Arabidopsis*: AtHAK5 and AKT1 are vital for seedling establishment and post-germination growth under low K<sup>+</sup> conditions. *Plant Physiol* **153**: 863-875
- Ramírez-Silva L, de Gómez-Puyou MT, Gómez-Puyou A** (1993) Water-induced transitions in the K<sup>+</sup> requirements for the activity of pyruvate kinase entrapped in reverse micelles. *Biochemistry* **32**: 5332-5338
- Rengel Z, Damon PM** (2008) Crops and genotypes differ in efficiency of potassium uptake and use. *Physiol Plantarum* **133**: 624-636
- Rengel Z, Marschner P** (2005) Nutrient availability and management in the rhizosphere: exploiting genotypic differences. *New Phytol* **168**: 305-312
- Reymond M, Pieper B, Barbier H, Innatowicz A, El-Lithy M, Vreugdenhil D, Koornneef M** (2007) Genetic and molecular analysis of growth responses to environmental factors using *Arabidopsis thaliana* natural variation. In, Ed J.H.J. Spiertz, P.C. Struik and H.H. van Laar (eds.), *Scale and Complexity in Plant Systems Research: Gene-Plant-Crop Relations*. Springer, pp 3-13
- Reymond M, Svistoonoff S, Loudet O, Nussaume L, Desnos T** (2006) Identification of QTL controlling root growth response to phosphate starvation in *Arabidopsis thaliana*. *Plant Cell Environ* **29**: 115-125
- Roelfsema MR, Hedrich R** (2005) In the light of stomatal opening: new insights into 'the Watergate'. *New Phytol* **167**: 665-691
- Rubio F, Nieves-Cordones M, Aleman F, Martinez V** (2008) Relative contribution of AtHAK5 and AtAKT1 to K<sup>+</sup> uptake in the high-affinity range of concentrations. *Physiol Plantarum* **134**: 598-608
- Rufty TWJ, Jackson WA, Raper CDJ** (1982) Inhibition of nitrate assimilation in roots in the presence of ammonium: The moderating influence of potassium. *J Exp Bot* **33**: 1122-1137
- Rus A, Baxter I, Muthukumar B, Gustin J, Lahner B, Yakubova E, Salt DE** (2006) Natural variants of *AtHKT1* enhance Na<sup>+</sup> accumulation in two wild populations of *Arabidopsis*. *PLoS Genetics* **2**: e210
- Rus A, Lee B-h, Munoz-Mayor A, Sharkhuu A, Miura K, Zhu J-K, Bressan RA, Hasegawa PM** (2004) AtHKT1 facilitates Na<sup>+</sup> homeostasis and K<sup>+</sup> nutrition in planta. *Plant Physiol* **136**: 2500-2511
- Saalbach G, Schwerdel M, Natura G, Buschmann P, Christov V, Dahse I** (1997) Over-expression of plant 14-3-3 proteins in tobacco: enhancement of the plasmalemma K<sup>+</sup> conductance of mesophyll cells. *FEBS Lett* **413**: 294-298
- Salvi S, Tuberosa R** (2005) To clone or not to clone plant QTLs: present and future challenges. *Trends Plant Sci* **10**: 297-304

- Santa-Maria GE, Danna CH, Czibener C** (2000) High-affinity potassium transport in barley roots. Ammonium-sensitive and -insensitive pathways. *Plant Physiol* **123**: 297-306
- Schachtman DP, Shin R** (2007) Nutrient sensing and signaling: NPKS. *Annu Rev Plant Biol* **58**: 47-69
- Schroeder JI, Hedrich R** (1989) Involvement of ion channels and active transport in osmoregulation and signaling of higher plant cells. *Trends Biochem Sci* **14**: 187-192
- Sentenac H, Bonneaud N, Minet M, Lacroute F, Salmon JM, Gaynard F, Grignon C** (1992) Cloning and expression in yeast of a plant potassium ion transport system. *Science* **256**: 663-665
- Shin R, Schachtman DP** (2004) Hydrogen peroxide mediates plant root cell response to nutrient deprivation. *Proc Natl Acad Sci USA* **101**: 8827-8832
- Simon M, Loudet O, Durand S, Berard A, Brunel D, Sennesal FX, Durand-Tardif M, Pelletier G, Camilleri C** (2008) Quantitative trait loci mapping in five new large recombinant inbred line populations of *Arabidopsis thaliana* genotyped with consensus single-nucleotide polymorphism markers. *Genetics* **178**: 2253-2264
- Spalding EP, Hirsch RE, Lewis DR, Qi Z, Sussman MR, Lewis BD** (1999) Potassium uptake supporting plant growth in the absence of AKT1 channel activity: Inhibition by ammonium and stimulation by sodium. *J Gen Physiol* **113**: 909-918
- Svistoonoff S, Creff A, Reymond M, Sigoillot-Claude C, Ricaud L, Blanchet A, Nussaume L, Desnos T** (2007) Root tip contact with low-phosphate media reprograms plant root architecture. *Nat Genet* **39**: 792-796
- Szczerba MW, Britto DT, Balkos KD, Kronzucker HJ** (2008) Alleviation of rapid, futile ammonium cycling at the plasma membrane by potassium reveals K<sup>+</sup>-sensitive and -insensitive components of NH<sub>4</sub><sup>+</sup> transport. *J Exp Bot* **59**: 303-313
- Szczerba MW, Britto DT, Kronzucker HJ** (2006) Rapid, futile K<sup>+</sup> cycling and pool-size dynamics define low-affinity potassium transport in barley. *Plant Physiol* **141**: 1494-1507
- Talbott ID, Zeiger E** (1996) Central roles for potassium and sucrose in guard-cell osmoregulation. *Plant Physiol* **111**: 1051-1057
- Ten Hoopen F, Cuin TA, Pedas P, Hegelund JN, Shabala S, Schjoerring JK, Jahn TP** (2010) Competition between uptake of ammonium and potassium in barley and *Arabidopsis* roots: molecular mechanisms and physiological consequences. *J Exp Bot* **61**: 2303-2315
- Tester M, Blatt MR** (1989) Direct measurement of K<sup>+</sup> channels in thylakoid membranes by incorporation of vesicles into planar lipid bilayers. *Plant Physiol* **91**: 249-252
- Tipler PA, Mosca G** (2004) Physik für Wissenschaftler und Ingenieure, 2. deutsche Auflage. Spektrum Akadem. Verlag; Elsevier GmbH, München: pp.10-11
- Tocquin P, Corbesier L, Havelange A, Pieltain A, Kurtem E, Bernier G, Périlleux C** (2003) A novel high efficiency, low maintenance, hydroponic system for synchronous growth and flowering of *Arabidopsis thaliana*. *BMC Plant Biology* **3**: 2
- Tonsor SJ, Alonso-Blanco C, Koornneef M** (2005) Gene function beyond the single trait: natural variation, gene effects, and evolutionary ecology in *Arabidopsis thaliana*. *Plant Cell Environ* **28**: 2-20
- Trehan SP, Sharma RC** (2002) Potassium uptake efficiency of young plants of three potato cultivars as related to root and shoot parameters. *Commun Soil Sci Plan* **33**: 1813-1823

- Tuinstra MR, Ejeta G, Goldsbrough PB** (1997) Heterogeneous inbred family (HIF) analysis: a method for developing near-isogenic lines that differ at quantitative trait loci. *Theor. Appl. Genet.* **95**: 1005-1011
- Vale FR, Volk RJ, Jackson WA** (1988) Simultaneous influx of ammonium and potassium into maize roots: kinetics and interactions *Planta* **173**: 424-431
- Van den Wijngaard PWJ, Bunney TD, Roobeek I, Schönknecht G, De Boer AH** (2001) Slow vacuolar channels from barley mesophyll cells are regulated by 14-3-3 proteins. *FEBS Lett* **488**: 100-104
- Van Steveninck RFM** (1972) Inhibition of the development of a cation accumulatory system and of Tris-induced uptake in storage tissues by N6-benzyladenine and kinetin. *Physiol Plantarum* **27**: 43-47
- Varnum MD, Zagotta WN** (1997) Interdomain interactions underlying activation of cyclic nucleotide-gated channels. *Science* **278**: 110-113
- Very AA, Sentenac H** (2003) Molecular mechanisms and regulation of K<sup>+</sup> transport in higher plants. *Annu Rev Plant Biol* **54**: 575-603
- Vidal M, Gaber RF** (1991) RPD3 encodes a second factor required to achieve maximum positive and negative transcriptional states in *Saccharomyces cerevisiae*. *Mol Cell Biol* **11**: 6317-6327
- Vidmar JJ, Zhuo D, Siddiqi MY, Schjoerring JK, Touraine B, Glass AD** (2000) Regulation of high-affinity nitrate transporter genes and high-affinity nitrate influx by nitrogen pools in roots of barley. *Plant Physiol* **123**: 307-318
- Viola R, Davies HV** (1992) A microplate reader assay for rapid enzymatic quantification of sugars in potato tubers. *Potato Research* **35**: 55-58
- Voelker C, Schmidt D, Mueller-Roeber B, Czempinski K** (2006) Members of the Arabidopsis AtTPK/KCO family form homomeric vacuolar channels in planta. *Plant J* **48**: 296-306
- Walch-Liu P, Neumann G, Bangerth F, Engels C** (2000) Rapid effects of nitrogen form on leaf morphogenesis in tobacco. *J. Exp. Bot.* **51**: 227-237
- Walter BK, John EE, Julian IS** (1995) Effects of cytosolic calcium and limited, possible dual, effects of G protein modulators on guard cell inward potassium channels. *Plant J* **8**: 479-489
- Wang MY, Siddiqi MY, Glass ADM** (1996) Interactions between K<sup>+</sup> and NH<sub>4</sub><sup>+</sup>: effects on ion uptake by rice roots. *Plant Cell Environ* **19**: 1037-1046
- Wang Y, Wu W-H** (2010) Plant sensing and signaling in response to K<sup>+</sup>-deficiency. *Mol Plant* **3**: 280-287
- Ward JT, Lahner B, Yakubova E, Salt DE, Raghothama KG** (2008) The effect of iron on the primary root elongation of Arabidopsis during phosphate deficiency. *Plant Physiol* **147**: 1181-1191
- Xu J, Li HD, Chen LQ, Wang Y, Liu LL, He L, Wu WH** (2006) A protein kinase, interacting with two calcineurin B-like proteins, regulates K<sup>+</sup> transporter AKT1 in Arabidopsis. *Cell* **125**: 1347-1360
- Yang XE, Liu JX, Wang WM, Ye ZQ, Luo AC** (2004) Potassium internal use efficiency relative to growth vigor, potassium distribution, and carbohydrate allocation in rice genotypes. *J Plant Nutr* **27**: 837-852
- Yano M** (2001) Genetic and molecular dissection of naturally occurring variation. *Curr Opin Plant Biol* **4**: 130-135
- Zeevaart JAD** (1971) Effects of photoperiod on growth rate and endogenous gibberellins in the long-day rosette plant spinach. *Plant Physiol* **47**: 821-827

- Zerangue N, Schwappach B, Jan YN, Jan LY** (1999) A new ER trafficking signal regulates the subunit stoichiometry of plasma membrane K(ATP) channels. *Neuron* **22**: 537-548
- Zhao D, Oosterhuis DM, Bednarz CW** (2001) Influence of potassium deficiency on photosynthesis, chlorophyll content, and chloroplast ultrastructure of cotton plants. *Photosynthetica* **39**: 103-109
- Zhou C, Zhang L, Duan J, Miki B, Wu K** (2005) Histone Deacetylase 19 is involved in jasmonic acid and ethylene signaling of pathogen response in Arabidopsis. *Plant Cell* **17**: 1196-1204



Appendix

Trait	CONTROL						-K						-P								
	Chr	Chromosome	Marker	Position (cM)	LOD	% Expl.	Additive	Chr	Chromosome	Marker	Position (cM)	LOD	% Expl.	Additive	Chr	Chromosome	Marker	Position (cM)	LOD	% Expl.	Additive
Rosette Weight	0.988	1	snp177	89.54	2.42	4.3	0.17	0.986	2	Erecta	45.66	9.13	20.7	-0.28	0.930	1	snp110	96.91	6.05	9.4	-0.14
		1	snp110	98.90	4.90	9.0	-0.25		5	snp97	68.28	5.77	13.0	-0.24		2	Erecta	48.82	12.24	21.2	-0.21
		2	Erecta	46.86	9.47	19.1	-0.22		5	M5-17	94.31	4.89	10.3	-0.21		3	snp114	1.80	5.93	3.2	-0.14
		3	snp114	1.80	3.28	3.7	-0.16		5	K15162	63.02	5.13	9.3	-0.16		5	KGA10	101.81	2.58	3.9	-0.11
		5	snp101	85.19	10.98	22.3	-0.25		4	snp355	21.24	2.80	5.9	-0.07		5	KGA10	101.81	4.09	13.0	-0.01
RCR	0.818	1	snp251	17.27	3.01	3.0	-0.01	0.812	4	snp355	21.24	2.80	5.9	-0.07	0.915	5	KGA10	101.81	4.09	13.0	-0.01
		1	snp373	40.59	6.38	15.8	0.14		1	snp110	98.91	6.05	9.4	-0.14	0.924	1	snp373	38.87	5.41	7.9	0.07
		2	Erecta	46.82	4.84	6.1	-0.01		2	Erecta	45.66	10.81	18.1	-0.13		1	snp110	97.91	7.39	11.2	-0.08
		4	GAS	48.13	3.22	7.1	0.06		2	TK9	65.30	3.42	5.3	0.07		2	Erecta	45.66	10.29	16.3	-0.10
Root Length	0.946	1	snp157	95.18	2.72	6.0	-0.06	0.975	1	snp110	98.91	6.05	9.4	-0.14	0.945	1	snp110	97.91	7.39	11.2	-0.08
		2	PLS7	36.80	6.65	18.0	-0.09		2	CE7M19	53.63	5.75	13.2	-1.83		2	Erecta	48.82	2.83	6.8	-1.02
		3	F421	63.07	3.88	7.3	-1.23		4	snp295	34.68	3.00	5.5	1.20		4	GAS	44.13	7.20	19.3	1.83
		4	GAS	48.13	5.53	11.1	1.49		5	snp258	21.69	2.62	4.8	1.09		5	M5-17	96.91	3.32	8.0	1.16
		5	M5-17	96.31	3.60	7.1	1.21		5	K15122	71.88	4.81	8.4	1.40		5	M5-17	96.91	2.88	9.7	0.115448
Chia	0.688	1	SNP177	90.269	3.42	10.3	0.100	0.880	No QTL					0.882	5	M5-17	96.912	2.88	9.7	0.115448	
		5	KGA10	98.912	4.21	13.9	0.118		5	M5-17	96.912	4.12	13.4	0.037654		5	F421	63.07	4.89	16	0.047255
	0.537	5	KGA10	98.912	3.17	9.7	0.029	0.840	No QTL					0.845	5	M5-17	96.912	4.12	13.4	0.037654	
		3	NGAT2	0	2.74	8.8	8.443		2	SNP203	42.248	3.02	10.5	-1.768		5	SNP157	94.18	2.84	10	6.7164
	0.949	1	SNP110	97.906	2.95	10.4	0.997	0.907	1	SNP251	19.892	2.72	3.2	-0.813	0.985	No QTL					
Hosose	0.997	1	PLS7	36.80	4.9	11.2	-0.778	0.972	2	TK9	65.171	6.71	15.1	7.41	0.900	2	SNP203	45.662	7.18	20.3	12.784
		2	F12A24b	19.821	4.9	11.3	-0.514		4	GAS	48.486	11.35	28.9	-12.085		4	M4-9	50.466	3.56	9.7	-8.9507
		2	ERECTA	45.662	7.93	18.3	13.972		5	snp258	21.69	2.62	4.8	1.09		5	M5-17	96.91	3.32	8.0	1.16
		4	M4-3	5.921	2.89	6.1	7.997		5	K15122	71.88	4.81	8.4	1.40		5	M5-17	96.91	2.88	9.7	0.115448
		4	GAS	48.129	6.15	13.9	-11.503		5	M5-17	96.912	4.12	13.4	0.037654		5	M5-17	96.912	4.12	13.4	0.037654
B-R	0.589	No QTL					0.829	No QTL					0.829	No QTL							
	0.710	4	NGAT11T	28.378	13.06	38.3	0.023	0.829	5	M5-17	96.912	4.12	13.4	0.037654	0.916	4	SNP203	45.662	20.01	50.1	70.5122
		5	M5-17	96.912	2.4	7.2	-19.123		5	M5-17	96.912	4.12	13.4	0.037654		5	SNP183	39.833	3.07	5.9	23.9886
	0.728	No QTL					0.855	5	SNP203	45.662	7.18	20.3	12.784	0.855	5	SNP203	45.662	7.18	20.3	12.784	
	0.908	1	SNP142	98.906	5.79	17.3	-543.894	0.801	1	SNP142	97.906	5.54	11.9	-346.732	0.921	1	SNP110	96.151	7.08	17.1	-454.29
Mg-RS	0.908	2	F12A24b	22.084	3.78	10.7	425.780		2	SNP184	12.908	6.6	15.2	410.172		2	SNP184	17.821	3.12	7.4	336.494
		3	NGAT2	0	2.74	8.8	8.443		2	ERECTA	45.662	2.85	5.3	237.324		2	SNP203	45.662	3.41	7.6	330.446
		3	NGAT2	0	2.74	8.8	8.443		3	K15122	69.275	3.19	7	-219.914		3	K15122	70.275	5.16	12.3	410.35
		2	F12A24b	19.821	4.9	11.3	-0.514		2	SNP184	12.908	6.6	15.2	410.172		2	SNP184	17.821	3.12	7.4	336.494
		3	NGAT14	1	5.74	15.1	209.492		3	SNP233	51.618	4.05	8.5	32.888		3	SNP114	1.801	3.23	9.3	-1.96242
0.684	5	NGAT29	74.578	4.62	11.6	262.864		4	M4-35	30.378	2.61	5.3	251.560		4	M4-35	30.378	2.61	5.3	251.560	

**Table A1 (a): List of all QTL detected by Dr. Barbier and Dr. Raymond** (published in Prinzenberg et al., 2010 after thesis submission) The table summarizes mapping-data for rosette weight, root length and total chlorophyll (Chl a,b), protein, hexose-, ion-content in the rosette (-rs) and the root (-rt) and leaf number (L22, L32). QTL were detected for each trait in each nutritional regime (a) and in the response to reduced potassium and reduced phosphate (b). The heritability (h<sup>2</sup>), QTL position, LOD-score, explained variance (% Expl.; R<sup>2</sup>) and additive effect (Additive; 2a) is given (if the additive effect is positive, the *Ler* allele increases the trait value).

Trait	h <sup>2</sup>	Chromosome	Marker	Position (cM)	LOD	% Expl.	Additive	K	h <sup>2</sup>	Chromosome	Marker	Position (cM)	LOD	% Expl.	Additive	P	h <sup>2</sup>	Chromosome	Marker	Position (cM)	LOD	% Expl.	Additive		
P-rs	0.845	3	NGA172	0	12.66	38.4	-2379.800	0.946	0.846	3	NGA172	0	15.97	43.7	-2515.260	0.943	0.843	3	NGA172	0	3.27	11	-915.0184		
P-t	0.919	1	SNP32	30.865	2.42	4.6	-910.666	0.938	0.938	2	F12A24b	25.084	2.71	4.8	-988.056	0.934	No QTL								
		3	NGA172	0	12.48	28.7	-2275.320			2	NGA172	0	12.17	24.5	-2179.040										
		3	NGA6	7.83	2.91	5.7	-1028.158			3	NGA172	60.072	3.14	6.9	-1120.398										
		5	SNP204	55.389	4.21	9.1	-1397.950			5	SNP204	59.329	2.87	5.2	-1154.970										
S-rs	0.864	1	SNP107	11.424	3.59	12	-354.536	0.887	0.887	1	SNP32	34.865	4.59	12	-1055.315	0.881	0.881	1	SNP65	28.26	5.75	15	-1513.248		
		1	SNP172	11.424	3.59	12	-354.536			2	SNP233	52.472	4.86	12.2	-1377.602										
		2	SNP214	63.302	2.66	6.4	-997.944			5	F1C	11.109	7.01	18.4	-1640.872										
		3	SNP35	25.686	6.58	17.1	-1209.988			5	K15B22	72.578	2.33	8.8	-940.822										
S-t	0.914	No QTL						0.880	0.880	No QTL						0.885	No QTL								
K-rs	0.924	1	NGA126	48.535	4.14	9.5	-757.745	0.930	0.930	2	NGA1145	34.908	2.82	6.8	-1055.315	0.930	0.930	1	M1-13	87.684	4.32	11.3	-1124.16		
		3	M3-19	29.75	4.45	11	-7659.420			2	F12A24b	22.084	3.9	7.2	-7483.180										
		5	K15B22	70.275	2.91	7	-6415.880			2	M2-22	80.44	3.03	6.6	-7685.950										
		5	M5-17	98.912	2.83	6.5	-6189.480			2	M2-22	80.44	3.03	6.6	-7685.950										
		5	M5-17	98.912	2.83	6.5	-6189.480			5	K15B22	71.578	4.39	8.2	-6898.400										
K-t	0.777	2	SNP19	61.72	5.82	15.2	-15814.640	0.850	0.850	2	SNP177	80.538	3.88	8.1	-649.850	0.811	0.811	5	ERECTA	46.662	3.41	10.3	-3886.62		
		3	SNP208	30.08	5.21	13.6	-6892.140			2	NGA18	60.72	3.93	7.3	-1076.920										
		4	SNP298	30.08	5.21	13.6	-6892.140			3	SNP288	11.3	3.58	7.7	-6284.620										
		5	SNP97	68.275	4.12	8.8	-6888.460			5	SNP97	68.275	4.12	8.8	-6888.460										
C-rs	0.822	1	SNP32	34.865	2.7	6.1	-5130.940	0.865	0.865	1	M1-13	88.538	6.87	21.4	-9687.700	0.831	0.831	1	SNP32	30.153	4.2	8.4	-5465.22		
		1	M1-13	87.684	11.28	27.6	-10737.300			4	M4-9	54.806	2.24	5	-4820.780										
		3	SNP35	23.202	4.89	10.9	-6823.520			5	M5-14	29.889	3.06	7.5	-6182.840										
C-t	0.885	No QTL						0.844	0.844	No QTL						0.872	No QTL								
M-rs	0.674	1	M1-13	88.538	8.68	19.7	-1057.700	0.815	0.815	1	SNP5	4.495	2.42	6.6	-4.685	0.833	0.833	1	SNP32	30.885	4.36	8.4	-617.36		
		2	ERECTA	46.662	4.41	9.3	-75.781			1	M1-13	89.538	5.67	17	-70.122										
		3	M3-20	35.959	4.29	9.4	-79.180			2	ERECTA	46.816	5.61	11	-73.2648										
		4	GA5	50.466	3.28	7.6	-70.247			3	SNP35	25.686	5.17	10.1	-69.2868										
M-t	0.893	1	SNP19	61.72	5.82	15.2	-15814.640	0.916	0.916	3	M1204	32.3	3.59	7.7	-707.575	0.823	0.823	4	NGA1139	57.938	2.86	10.6	-1610.884		
		3	NGA172	71.023	2.84	6.9	-18.678			3	M3-18	71.808	7.07	14.3	-40.112										
		4	F8D20	59.938	2.64	7.7	-18.382			4	M4-9	50.466	4.12	8.7	-32.159										
P-rs	0.766	1	SNP177	88.538	4.49	15	-12.618	0.505	0.505	1	SNP5	2	2.43	6.6	-17.281	0.847	0.847	2	F1C	46.248	3.77	10.8	-22.382		
		2	ERECTA	46.662	7.07	19.5	-23.288			2	ERECTA	46.662	7.07	19.5	-23.288										
		3	M3-20	31.75	2.54	6.8	-9.61546			3	M3-20	31.75	2.54	6.8	-9.61546										
		5	NGA129	78.021	6.15	16.8	-147.6246			5	NGA129	78.021	6.15	16.8	-147.6246										
P-t	0.866	1	ERECTA	46.662	7.07	19.5	-23.288	0.969	0.969	1	SNP279	60.24	2.86	5.3	-388.582	0.976	0.976	1	ERECTA	46.662	7.07	19.5	-23.288		
		1	ERECTA	46.662	7.07	19.5	-23.288			1	SNP177	80.269	2.81	5.3	-388.582										
		1	ERECTA	46.662	7.07	19.5	-23.288			2	SNP177	80.269	2.81	5.3	-388.582										
		2	T2N18	60.72	6.7	14.2	-590.528			2	SNP177	80.269	2.81	5.3	-388.582										
		2	T2N18	60.72	6.7	14.2	-590.528			3	SNP197	73.53	2.72	5.4	-351.944										
		3	SNP197	73.53	2.72	5.4	-351.944			5	M5-17	94.306	3.43	7.2	-404.134										
		5	M5-17	94.306	3.43	7.2	-404.134			No QTL						0.487	No QTL								
Co-rs	0.638	No QTL						0.879	0.879	No QTL						0.882	No QTL								
Co-t	0.686	3	SNP268	6.801	2.76	8.4	0.147	0.888	0.888	1	SNP107	74.895	3.17	6.4	0.084	0.892	0.892	5	SNP193	36.358	2.95	9.2	0.114074		
		5	SNP358	31.969	2.88	9.1	0.142			2	ERECTA	46.662	7.07	19.5	-23.288										
		5	SNP358	31.969	2.88	9.1	0.142			2	ERECTA	46.662	7.07	19.5	-23.288										
		5	SNP358	31.969	2.88	9.1	0.142			5	SNP101	87.09	3.06	6	0.081										
		5	SNP101	87.09	3.06	6	0.081			1	SNP261	16.862	2.43	7.7	-1.285										
N-rs	0.649	1	SNP32	33.865	2.31	6.6	0.694	0.842	0.842	1	SNP110	96.151	2.45	7.9	-1.280	0.848	0.848	1	SNP32	30.153	2.92	8.1	0.616396		
		1	M1-13	89.538	7.39	22.2	-1.245			1	SNP110	96.151	2.45	7.9	-1.280										
		1	M1-13	89.538	7.39	22.2	-1.245			5	NGA129	78.021	2.88	9.8	-3.748										
N-t	0.756	No QTL						0.901	0.901	No QTL						0.843	No QTL								

Table A1 (a; continued): List of all QTL detected by Dr. Barbier and Dr. Reymond

Trait	CONTROL										-K										-P												
	h <sup>2</sup>	Chromosome	Marker	Position (cM)	LOD	% Expl.	Additive	h <sup>2</sup>	Chromosome	Marker	Position (cM)	LOD	% Expl.	Additive	h <sup>2</sup>	Chromosome	Marker	Position (cM)	LOD	% Expl.	Additive												
Cu-rs	0.870	2	SNP184	14.821	2.49	4.9	-0.552	0.895	3	SNP114	5.801	2.58	9	1.447	0.910	1	SNP107	9.495	3.13	6.8	0.720462												
			ERECTA	45.662	5.34	10.8	0.822		5	K1922	66.275	5.45	17.6	2.003		2	SNP164	14.821	4.28	9.3	-0.83677												
			NT204	15.202	2.47	4.6	0.517									2	NGA1126	51.618	3.62	7.7	0.76289												
			SNP136	17.894	8.06	16.7	0.985									3	NT204	15.202	3.34	6.8	0.696688												
			K1522	71.275	7.8	16.2	0.985									5	SNP136	17.894	3.63	7.5	0.74151												
Cu-r	0.827	No QTL										0.925	No QTL										0.893	No QTL									
	Zn-rs	0.830	1	MT-13	88.538	3.21	7.7	-22.272	0.927	1	SNP107	8.495	2.8	5.8	16.831	0.927	2	NGA1126	47.618	3.39	6.5	19.76384											
			4	GA5	45.129	4.49	11.5	28.381		3	SNP268	6.801	7.19	15.7	27.490		3	SNP114	2.801	5.13	10.8	26.4986											
			5	NGA76	47.758	2.34	5.6	19.52		3	CFM19	49.626	3.89	7.3	-18.684		4	SNP20	33.75	7.43	16.2	-33.1874											
				SNP101	86.194	5.24	13.5	30.739		4	GA5	45.129	3.81	7.8	19.126		4	SNP136	17.894	3.93	8.4	23.5326											
			SNP22	71.275	7.8	16.2	0.985		5	K1922	71.1578	7.82	15.9	27.179		5	JV6162	85.184	9.01	19.2	34.9286												
Zn-r	0.903	1	SNP22	71.275	7.8	16.2	0.985	0.926	1	SNP110	96.151	7.15	16.4	19.465	0.924	1	MT-10	21.156	5.57	8.8	13.3456												
		2	SNP110	96.151	7.15	16.4	19.465		2	MT-5	1.801	3.34	7.3	66.283		1	SNP65	28.226	6	16.8	-177.178												
		3	SNP114	1.801	2.91	6.1	64.594		3	SNP268	7.801	8.25	23	139.6362		3	SNP268	7.801	8.25	23	139.6362												
		4	SNP35	21.202	6.03	9.1	117.652																										
		5	NGA1139	55.938	3.74	5	75.543																										
RB-rs	0.860	1	GENEA	71.029	2.76	5.9	-0.149	0.931	1	MT-13	87.654	4.51	12.2	0.210	0.882	1	MT-13	88.538	5.61	15.4	0.358196												
		2	NGA1126	48.618	4.16	9.2	-0.189		5	SNP304	88.888	7.4	21.3	-0.278		5	SNP304	87.888	5.97	16.5	-0.281284												
		3	SNP114	6.801	2.39	5.7	-0.232																										
		4	NT204	18.202	6.19	15.7	0.301																										
		5	K1522	73.578	2.94	6.6	-0.171																										
RB-r	0.708	2	SNP214	64.302	2.54	5.9	0.200	0.795	1	MT-13	86.684	3.18	11.3	0.235	0.933	No QTL																	
		1	GENEA	71.029	2.76	5.9	-0.149																										
		1	SNP22	71.275	7.8	16.2	0.985																										
		1	ERECTA	45.662	5.34	10.8	0.822																										
		2	ERECTA	45.662	5.34	10.8	0.822																										
Mo-rs	0.906	1	SNP22	71.275	7.8	16.2	0.985	0.954	2	ERECTA	46.662	11.92	29.8	-11.564	0.973	2	ERECTA	46.662	15.73	43.9	-19.8929												
		2	ERECTA	46.662	11.92	29.8	-11.564																										
		3	SNP114	1.801	2.91	6.1	64.594																										
		4	NT204	18.202	6.19	15.7	0.301																										
		5	K1522	73.578	2.94	6.6	-0.171																										
Mo-r	0.966	2	ERECTA	46.662	28.85	62.1	-17.692	0.966	2	ERECTA	46.662	11.92	29.8	-11.564	0.973	2	ERECTA	46.662	15.73	43.9	-19.8929												
		4	SNP53	66.312	2.66	3.7	4.475																										
		5	SNP204	16.419	4.25	8.1	-0.940																										
		5	SNP21	8.304	5.14	6.4	-0.932																										
		5	JV6162	81.021	9.08	12.5	1.439																										
Cd-rs	0.660	No QTL										0.448	No QTL										0.461	No QTL									
	Cd-r	0.487	2	SNP203	44.662	2.66	10	-0.037	0.612	2	SNP233	52.472	4.19	12.7	-0.048	0.740	2	NGA1126	48.618	4.34	14.7	-0.0870642											
			1	SNP373	35.865	6.78	18.8	-0.774		1	SNP65	30.183	4.81	15.2	-0.852	0.671	1	SNP251	16.424	2.65	5.5	-0.425278											
			2	ERECTA	46.816	3.44	8.7	-0.508		3	SNP35	20.202	3.82	12.3	-0.543		1	SNP373	35.865	4.89	10.7	-0.644728											
			3	SNP114	1.801	2.91	6.1	64.594									1	ERECTA	46.816	3.44	8.7	-0.508											
		5	SNP17	96.912	4.38	8.6	0.903									3	SNP35	20.202	3.82	12.3	-0.543												
L22	0.929	1	SNP373	35.865	9.01	18.5	-1.325	0.935	1	SNP65	28.226	6.35	14.9	-1.152	0.938	1	SNP373	35.865	4.72	9.5	-1.32674												
		2	ERECTA	46.816	5.73	11	-0.987		3	SNP35	24.202	5.25	12.3	-1.050		3	SNP35	24.202	3.13	6.2	-1.082202												
		3	SNP114	1.801	2.91	6.1	64.594		4	FR1	0	6.02	13.6	1.231		4	FR1	0	5.7	11.4	1.585372												
		4	FR1	0	4.05	7.6	-0.819		5	SNP395	18.061	2.85	5.9	0.912		5	SNP236	33.439	3.39	6.3	-1.05632												
		5	SNP17	96.912	4.38	8.6	0.903		5	MT-17	96.912	4.49	10.3	0.992		5	MT-17	96.912	6.96	14.3	1.624186												

Table A1 (a; continued): List of all QTL detected by Dr. Barbier and Dr. Reymond

Trait	K response						P response					
	Chromosome	Marker	Position (cM)	LOD	% Expl.	Additive	Chromosome	Marker	Position (cM)	LOD	% Expl.	Additive
Rosette Weigth	5	snp97	68.28	2.57	9.3	0.14	No QTL					
RGR	No QTL						1	snp177	89.54	4.41	14.6	0.05
Root Weight	No QTL						No QTL					
Root Length	No QTL						1	M1-10	23.20	4.57	15.6	0.08
Chla	No QTL						No QTL					
Chl-b	No QTL						No QTL					
Proteins	No QTL						No QTL					
Hexose	No QTL						No QTL					
B-rs	2	ERECTA	46.816	2.33	8	0.0576936	No QTL					
B-rt	No QTL						No QTL					
Na-rs	2	M2-22	80.44	2.75	7.6	0.072404	No QTL					
	3	M3-18	70.908	4.65	13.4	-0.0969934						
	4	NGA1111	27.378	5.06	14.7	0.1012434						
Na-rt	No QTL						No QTL					
Mg-rs	No QTL						No QTL					
Mg-rt	3	SNP268	12.3	2.4	8.7	0.087033	No QTL					
P-rs	No QTL						5	K8A10	100.912	4.07	14.7	-0.0477336
P-rt	1	SNP177	89.538	2.46	8.5	-0.0344696	1	M1-10	23.196	2.06	6.8	-0.0305026
							3	NGA172	0	2.42	7.8	-0.0316384
S-rs	No QTL						5	FLC	11.132	4.38	13.6	0.0893632
							5	K15122	68.275	2.62	8.1	-0.0708612
S-rt	No QTL						No QTL					
K-rs	1	SNP373	39.594	2.91	8	0.0427042	No QTL					
	3	M3-18	69.307	2.89	8.4	-0.0445888						
	5	K15122	71.578	4.06	11.4	0.0505602						
K-rt	2	SNP203	42.248	2.95	10.6	-0.0450804	4	GA5	44.129	2.43	9	0.0651406
Ca-rs	1	SNP157	93.289	3.33	9.9	-0.083502	No QTL					
	3	NT204	20.202	4.88	15.8	-0.107442						
	5	K15122	71.578	2.34	6.6	-0.0667656						
Ca-rt	2	F12A24b	24.084	2.92	10.3	-0.0986978	No QTL					
	4	SNP53	64.312	2.35	8.2	-0.0767498						
Mn-rs	No QTL						No QTL					
Mn-rt	2	T2N18	60.304	3.72	8.6	0.0960884	1	F6D8-94	63.477	2.33	8	-0.067075
	3	NT204	13.3	8.69	22.1	0.1551324						
	3	SNP197	71.908	3.56	8	0.0932226						
	4	CIW7	41.129	2.73	6.1	0.081017						
Fe-rs	No QTL						2	T2N18	60.72	2.71	9.3	-0.0438406
Fe-rt	5	SNP97	65.275	2.67	8.2	-0.0566152	5	SNP136	17.894	3.25	11	-0.0521724
	5	M5-17	95.306	3.25	9.6	-0.0631346						
Co-rs	No QTL						No QTL					
Co-rt	No QTL						No QTL					
Ni-rs	No QTL						No QTL					
Ni-rt	No QTL						No QTL					
Cu-rs	No QTL						No QTL					
Cu-rt	1	SNP110	96.151	3.28	11.7	0.696094	No QTL					
Zn-rs	No QTL						No QTL					
Zn-rt	1	SNP32	31.885	3.48	11.4	-0.0692202	No QTL					
	5	K15122	68.275	2.67	9	0.0619086						
Rb-rs	1	SNP373	39.594	3.33	8.4	0.0482326	No QTL					
	1	M1-13	85.684	3.54	9.8	-0.054422						
	3	SNP114	1.801	3.37	8.5	0.0483878						
	5	SNP101	87.09	3	7.5	0.0454412						
Rb-rt	No QTL						No QTL					
Mo-rs	2	ERECTA	46.816	5.45	14.8	-0.0813972	1	SNP107	10.495	7.88	13.1	-0.1267128
	3	F8J2	63.072	4.18	11.8	-0.0748506	2	ERECTA	46.862	20	40.9	0.223794
							5	FLC	11.132	6.19	9.7	0.107858
Mo-rt	2	ERECTA	46.862	7.78	21.9	-0.1349304	No QTL					
	5	SNP193	37.63	2.72	7	-0.0759724						
	5	NGA129	75.578	2.43	6.3	-0.0724856						
Cd-rs	No QTL						No QTL					
Cd-rt	No QTL						No QTL					
L22	No QTL						No QTL					
L32	No QTL						No QTL					

Table A1 (b; continued): List of all QTL detected by Dr. Barbier and Dr. Reymond

L:	gaattggccaactgtgagaacatcatcaatgaagaccaattgtgagatccgacaacacccgcttcttttgatttgcattactttctctgggt	92
R:	gaattggccaactgtgagaacatcatcaatgaagaccaattgtgagatccgacaacacccgcttcttttgatttgcattacttctctgggt	92
C:	<u>gaattggccaactgtgagaacatcatcaatgaagaccaattgtgagatccgacaacacccgcttcttttgatttgcattactttctctgggt</u>	92
L:	atgtctcaattct-----tcttctccttcagttcgtgtctgtgtctgattgattactctcacaaaactcatcttttcattgtctaaagg	184
R:	atgtctcaattct-----tcttctccttcagttcgtgtctgtgtctgattgattactctcacaaaactcatcttttcattgtctaaagg	184
C:	<u>atgtctcaattct-----tcttctccttcagttcgtgtctgtgtctgattgattactctcacaaaactcatcttttcattgtctaaagg</u>	184
L:	tctaactcttagctataaactcaaaatctgtatctaagttctgacaagtttctgttacgaaattcaattttttttatatacatatgttcatttct	276
R:	tctaactcttagctataaactcaaaatctgttctcaagttctgacaagtttctgaaacgaaattcaagttttttgatacatatgttcatttct	276
C:	<u>tctaactcttagctataaactcaaaatctgtatctaagttctgacaagtttctgttacgaaattcaattttttgatacatatgttcatttct</u>	276
L:	cagaacag-----gagatgtcaattttggcgatggttttctgtaacataaacatgagatttgattgttctgtgcagatctcat	368
R:	cagaacaggtttaaattaaacaagagatgtcaattttggcgatggttttctgtaacataaacatgagatttgattgttctgtgcagatctcat	368
C:	<u>cagaacag-----gagatgtcaattttggcgatggttttctgtaacataaacatgagatttgattgttctgtgcagatctcat</u>	368
L:	agttaactctggtttgagcttagaaATGTCGAGTGTATGCAGCTCGTACGCCATTGTTACCCACTGAGAAGATAGATACCATGGCTCAAGATTT	460
R:	agttaactctggtttgagcttagaaATGTCGAGTGTATGCAGCTCGTACGCCATTGTTACCCACTGAGAAGATAGATACCATGGCTCAAGATTT	460
C:	<u>agttaactctggtttgagcttagaaATGTCGAGTGTATGCAGCTCGTACGCCATTGTTACCCACTGAGAAGATAGATACCATGGCTCAAGATTT</u>	460
L:	CAACCTGAACCTCAAGAACTCTTCTTCAAGAAAAOAGAAGATTGOGTGCCTCTAGAAGTGCCTCTGTTGGTGTATGTATGACAATGATGATG	552
R:	CAACCTGAACCTCAAGAACTCTTCTTCAAGAAAAOAGAAGATTGOGTGCCTCTAGAAGTGCCTCTGTTGGTGTATGTATGACAATGATGATG	552
C:	<u>CAACCTGAACCTCAAGAACTCTTCTTCAAGAAAAOAGAAGATTGOGTGCCTCTAGAAGTGCCTCTGTTGGTGTATGTATGACAATGATGATG</u>	552
L:	TCAAAATOGAOGAACCCACTCCTCATCOGAGTAAATCCCAATGTTTCAGTGTACTAAAACCGAATCTCAGGOGAGTGATCATGTTCTTGGCT	644
R:	TCAAAATOGAOGAACCCACTCCTCATCOGAGTAAATCCCAATGTTTCAGTGTACTAAAACCGAATCTCAGGOGAGTGATCATGTTCTTGGCT	644
C:	<u>TCAAAATOGAOGAACCCACTCCTCATCOGAGTAAATCCCAATGTTTCAGTGTACTAAAACCGAATCTCAGGOGAGTGATCATGTTCTTGGCT</u>	644
L:	TTATATCTTACCATTGTAACGCTCTGTTTCTAACCCTGAGAGACCAGATCTCOGGTCATAAAAACAGTGGTGTGGTAGATGCTCTCTATTT	736
R:	TTATATCTTACCATTGTAACGCTCTGTTTCTAACCCTGAGAGACCAGATCTCOGGTCATAAAAACAGTGGTGTGGTAGATGCTCTCTATTT	736
C:	<u>TTATATCTTACCATTGTAACGCTCTGTTTCTAACCCTGAGAGACCAGATCTCOGGTCATAAAAACAGTGGTGTGGTAGATGCTCTCTATTT</u>	736
L:	CTGTATAGTAAOGATGACAACCTGTTGGATAOAGTACCTTGTCCCTAAATAGTTCOCCCTCAAGGCTACTTGCCTTGTGCTTGTCTCTCTCGG	828
R:	CTGTATAGTAAOGATGACAACCTGTTGGATAOAGTACCTTGTCCCTAAATAGTTCOCCCTCAAGGCTACTTGCCTTGTGCTTGTCTCTCTCGG	828
C:	<u>CTGTATAGTAAOGATGACAACCTGTTGGATAOAGTACCTTGTCCCTAAATAGTTCOCCCTCAAGGCTACTTGCCTTGTGCTTGTCTCTCTCGG</u>	828
L:	GAATGGTCCCTGTTGGTCACTCTTAAAGTGCAGGCGGGATTATCTAGTGGAGAAACAAGAGGCTTTGCTCGTTAGGGCTTTCCAITTGGGT	920
R:	GAATGGTCCCTGTTGGTCACTCTTAAAGTGCAGGCGGGATTATCTAGTGGAGAAACAAGAGGCTTTGCTCGTTAGGGCTTTCCAITTGGGT	920
C:	<u>GAATGGTCCCTGTTGGTCACTCTTAAAGTGCAGGCGGGATTATCTAGTGGAGAAACAAGAGGCTTTGCTCGTTAGGGCTTTCCAITTGGGT</u>	920
L:	CAAAGCTTTGGTCCAACAGACATTCTCAAGGAGTTGCATACTAACAAGTTGAGATACAAAATGCTATGCATACATGCTTTGCTCTGTAGTCTCT	1012
R:	CAAAGCTTTGGTCCAACAGACATTCTCAAGGAGTTGCATACTAACAAGTTGAGATACAAAATGCTATGCATACATGCTTTGCTCTGTAGTCTCT	1012
C:	<u>CAAAGCTTTGGTCCAACAGACATTCTCAAGGAGTTGCATACTAACAAGTTGAGATACAAAATGCTATGCATACATGCTTTGCTCTGTAGTCTCT</u>	1012
L:	CTTCATTGTTGGCACGATTTTCCTTGTAAATGTTGAGAAAAATGCOGGTTATCTCAGCTTTCTACTGCGTCTGCTCCAAGGTTACAACATTGG	1104
R:	CTTCATTGTTGGCACGATTTTCCTTGTAAATGTTGAGAAAAATGCOGGTTATCTCAGCTTTCTACTGCGTCTGCTCCAAGGTTACAACATTGG	1104
C:	<u>CTTCATTGTTGGCACGATTTTCCTTGTAAATGTTGAGAAAAATGCOGGTTATCTCAGCTTTCTACTGCGTCTGCTCCAAGGTTACAACATTGG</u>	1104
L:	GTTATGGAGATAAGAGCTTTAACTGCGAAGCGGACGCTTTTGTCTGTGTTTGGATCTTGAOGAGCAGCATATGTTGGCTCAGTTTTTC	1196
R:	GTTATGGAGATAAGAGCTTTAACTGCGAAGCGGACGCTTTTGTCTGTGTTTGGATCTTGAOGAGCAGCATATGTTGGCTCAGTTTTTC	1196
C:	<u>GTTATGGAGATAAGAGCTTTAACTGCGAAGCGGACGCTTTTGTCTGTGTTTGGATCTTGAOGAGCAGCATATGTTGGCTCAGTTTTTC</u>	1196
L:	CTTTATGTAGCTGAGCTAAATACAGAAAACAACAGAGGGCGTTGGTGAATGGGTTTAAACGGGAAGAAATCACAAACATGATCTOGAAGC	1288
R:	CTTTATGTAGCTGAGCTAAATACAGAAAACAACAGAGGGCGTTGGTGAATGGGTTTAAACGGGAAGAAATCACAAACATGATCTOGAAGC	1288
C:	<u>CTTTATGTAGCTGAGCTAAATACAGAAAACAACAGAGGGCGTTGGTGAATGGGTTTAAACGGGAAGAAATCACAAACATGATCTOGAAGC</u>	1288
L:	AGCTGATCTOGATGAAGATGGAGTTGTTGGgtaaagaaagacatcagacattctatctctctgttctcttcttctctctcttcttcttcttcttcttctt	1380
R:	AGCTGATCTOGATGAAGATGGAGTTGTTGGgtaaagaaagacatcagacatattctatctctctgttctcttcttctctctctcttcttcttcttcttcttctt	1380
C:	<u>AGCTGATCTOGATGAAGATGGAGTTGTTGGgtaaagaaagacatcagacatattctatctctctgttctcttcttctctctctcttcttcttcttcttcttctt</u>	1380

**Figure A1: Sequence alignment of the TPK1-loci of *Ler*, *RIL138* and *Col-0***

The alignment shows the sequences of *Ler* (L), *RIL138* (R) and the *Col-0* (C) reference sequence from TAIR. Polymorphisms between the sequences are highlighted in red (\*SNPs). The start and the stop codon of the TPK1-gene are highlighted by blue boxes. The different annotated sequence parts of the TPK1 loci are indicated by differentially colored highlights: UTRs in blue, the exons (capital letters) in green, the intron in yellow. The primer position is indicated by underlining the consensus sequence in green for the forward and in orange for the reverse primers. The number of base pairs of the aligned amplicons is given on the right side of each line.

```

L: tt-ttgtctattgtgtgttgcaacAGCTGCAGAGTTTATTGTGTATAAACTGAAAGAAATGGGTAAGATTGATGAGAAAGATATTTCTGGGAT 1472
R: ttattgtctattgtgtgttgcaacAGCTGCAGAGTTTATTGTGTATAAACTGAAAGAAATGGGTAAGATTGATGAGAAAGATATTTCTGGGAT 1472
C: tt-ttgtctattgtgtgttgcaacAGCTGCAGAGTTTATTGTGTATAAACTGAAAGAAATGGGTAAGATTGATGAGAAAGATATTTCTGGGAT 1472

L: AATGGATGAGTTGAGCAACTTGATTACGATGAATCAGGAACCTCTCAGACTTCTGACATCGTTTTAGCTCAGACCAAGTCTCAGATTCAA 1564
R: AATGGATGAGTTGAGCAACTTGATTACGATGAATCAGGAACCTCTCAGACTTCTGACATCGTTTTAGCTCAGACCAAGTCTCAGATTCAA 1564
C: AATGGATGAGTTGAGCAACTTGATTACGATGAATCAGGAACCTCTCAGACTTCTGACATCGTTTTAGCTCAGACCAAGTCTCAGATTCAA 1564

L: GGTAAGcctcat-----catcatcatcatcttgogaagacgaatcagaatcttggtttagttataccttcacacaacaaaaagccgaagag 1656
R: GGTAAGcctcattatcatcatcatcatcttgogaagacgaatcagaatcttggtttagttataccttcacacaacaaaaagccgaagag 1656
C: GGTAAGcctcat-----catcatcatcatcttgogaagacgaatcagaatcttggtttagttataccttcacacaacaaaaagccgaagag 1656

L: agtgaacagtttttc-gaaatgtttgttttttctgtttgtttgtaatgtaatgccacacttaactctttgatcgtttcttgatgc 1748
R: agtgaacagtttttc-gaaatgtttgttttttctgtttgtttgtaatgtaatgccacagtcctaaactctttgatcgtttcttgatgc 1748
C: agtgaacagtttttc-gaaatgtttgttttttctgtttgtttgtaatgtaatgccacacttaactctttgatcgtttcttgatgc 1748

L: taagtgtataaatttacatcacatctatacatatgaagctctctagtgttatgctccatgaccaagaattcatggatgattctctcaaaggac 1840
R: tgagtgtataaatttacatcacatctatacatatgaagctctctagtgttatgctccatgaccaagaattcatggatgattctctcaaaggac 1840
C: tgagtgtataaatttacatcacatctatacatatgaagctctctagtgttatgctccatgaccaagaattcatggatgattctctcaaaggac 1840

L: agggatgaagactgttttattgctttaaacttttttggtattttgattgatacaaaacattttcaaaagatagcgggtttctcgcgTTATGG 1932
R: atggtatgaagactgttttattgctttaaacttttttggtattttgattgatacaaaacattttcaaaagatagcgggtttctcgcgTTATGG 1932
C: agggatgaagactgttttattgctttaaacttttttggtattttgattgatacaaaacattttcaaaagatagcgggtttctcgcgTTATGG 1932

L: AAGTOGTCGTTTCTCG 1948
R: AAGTOGTCGTTTCTCG 1948
C: AAGTOGTCGTTTCTCG 1948

```

**Figure A1 (continued): Sequence alignment of the TPK1-loci of *Ler*, RIL138 and Col-0**

## Acknowledgements

I would like to thank Dr. Matthieu Reymond for the supervision and his positive attitude that makes working with him so pleasant.

Many thanks to Prof. Maarten Koornneef for the opportunity to work in the department and helpful discussions.

Many thanks to Prof. Bucher for taking his time to be examiner of this thesis.

Thanks to the head of the committee Prof. Werr.

Thanks to Prof. Klaus Pillen and Dr. Benjamin Stich for being my second supervisors in the IMPRS program.

I am thankful the technical support of Barbara Eilts, Nele Kaul and Jens Maintz in the lab. Thanks to Ute Tartler and Anja Hoerold for sharing their experience in methodical matters. Many thanks to Regina Gentges for her great help in the green house. I also like to thank the people in the mechanical and climate workshop, especially Renate Michalowski for help and suggestions concerning the climate chambers. I'd like to thank Maret-Linda Kalda for beautiful mutant pictures (that were unfortunately not used in this work) and her help with the cover picture. Also many thanks to Birgit Thron for help in administrative issues, Britta Hoffmann for the library support, Bruno Hüttel for the microarray work and discussions in the planning of the experiment and to Ulrike Göbel for her help with the analysis.

I also want to thank my colleagues, for a great working atmosphere and support. Many thanks to Dr. Hugues Barbier for his help in the starting phase of the project.

I am grateful for the support of my parents and my boyfriend.

Thanks to the IMPRS and Prof. Maarten Koornneef for the funding of the project.



## **Erklärung**

Ich versichere, dass ich die von mir vorgelegte Dissertation selbständig angefertigt, die benutzten Quellen und Hilfsmittel vollständig angegeben und die Stellen der Arbeit – einschließlich Tabellen, Karten und Abbildungen –, die anderen Werken im Wortlaut oder dem Sinn nach entnommen sind, in jedem Einzelfall als Entlehnung kenntlich gemacht habe; dass diese Dissertation noch keiner anderen Fakultät oder Universität zur Prüfung vorgelegen hat; dass sie abgesehen von unten angegebenen Teilpublikationen noch nicht veröffentlicht worden ist sowie, dass ich eine solche Veröffentlichung vor Abschluss des Promotionsverfahrens nicht vornehmen werde.

Die Bestimmungen der Promotionsordnung sind mir bekannt. Die von mir vorgelegte Dissertation ist von Prof. Dr. Maarten Koornneef betreut worden.

Teilpublikation:

Prinzenberg AE, Barbier H, Salt DE, Stich B, Reymond M (2010) Relationships between growth, growth response to nutrient supply, and ion content using a recombinant inbred line population in Arabidopsis. *Plant Physiol* 154: 1361-1371

---

Aina Prinzenberg

Köln, März 2011



## Lebenslauf

### Persönliche Daten

- Name: Aina Elisabet Prinzenberg
- Geburtsdatum: 11.03.1982
- Geburtsort: Köln
- Familienstand: ledig

### Ausbildung

- 30.05.2001 Allgemeine Hochschulreife (Durchschnittsnote: 1.8) am Hildegard-von-Bingen-Gymnasium, Köln  
Während der Schulzeit Ausbildung zum Schulsanitäter und ehrenamtliche Mitarbeit beim Bund für Umwelt und Naturschutz (BUND)
- Okt 2001 – Dez 2006 Diplomstudiengang Biologie an der Universität zu Köln
- 2003/2004 Auslandssemester im Rahmen des ERASMUS Programms an der University of Manchester (60 credit points; Assessments: 4A, 3B, 5C)
- Aug 2004 Praktikum „Transformation von Kulturpflanzen“ bei Prof. Dr. Hans-Henning Steinbiß, Max-Planck-Institut für Pflanzenzüchtungsforschung, Köln
- Sept 2004 Laborpraktikum „Molekulare Charakterisierung von transgenen Pflanzen, die Malat-Synthase überexprimieren“ bei PD Dr. Veronica Maurino, Universität zu Köln
- Dez 2005 Diplomprüfungen in den Fächern Botanik, Genetik, und Biochemie
- 2006 Diplomarbeit „Homologe Rekombination in RAD51- und SRS2- Mutanten von *Arabidopsis thaliana*“ in der Abteilung „Entwicklungsbiologie der Pflanzen“ von Prof. Dr. George Coupland in der Arbeitsgruppe von Dr. Bernd Reiß, Max-Planck-Institut für Pflanzenzüchtungsforschung, Köln
- 19.12.2006 Diplom in Biologie (Gesamtnote: sehr gut) an der Universität zu Köln
- Seit Januar 2007 Doktorarbeit “Characterization and fine mapping of a potassium dependent growth QTL in *Arabidopsis*“ in der Abteilung „Genetik und Pflanzenzüchtung“ von Prof. Dr. Maarten Koornneef, in der Arbeitsgruppe von Dr. Matthieu Reymond, Max-Planck-Institut für Pflanzenzüchtungsforschung, Köln

Präsentationen auf internationalen Konferenzen

- Feb 2008 Poster „Genetic and molecular basis of QTL involved in the variation to growth responses to potassium-starvation in *Arabidopsis thaliana*“, Crossroads in Biology, Köln
- Okt 2008 Vortrag „Validation and fine mapping of ‘response-QTL’ for potassium ( $K^+$ ) starvation“ im Rahmen des “First international PhD-retreat”, Wageningen
- Feb 2009 Poster „Genetic basis of a  $[K^+]$ -dependent growth-QTL in *Arabidopsis thaliana*“ auf der Konferenz “Plant abiotic Stress Tolerance”, Wien
- Juni/Juli 2009 Poster „Mapping genes involved in growth response to potassium starvation“ auf der Konferenz “20th International Conference on Arabidopsis Research”, Edinburgh